



**Politecnico
di Torino**



POLITECNICO DI TORINO

MSc Environmental and Land Engineering

Programme: Climate Change

a.y. 2024/2025

MSc Thesis

“Experimental analysis of cellulose behavior in aqueous streams”

TUTOR

Professor Tiziana Anna Elisabetta Tosco

MENTOR

Doctor Milica Velimirovic

CO-MENTOR

Xiaoyu Zhang

STUDENT

Caterina Massola

Matr. 316997

March 2025

A special thank you to my supervisor, Prof. Tiziana Tosco, for her invaluable guidance, continuous availability, and insightful advice. Her support has been instrumental in shaping this work.

I also want to sincerely thank Dr. Milica Velimirovic and Xiaoyu Zhang from the VITO research center for their expertise, encouragement, and unwavering support throughout this experience.

Finally, I am deeply grateful to my family and everyone who has been part of this journey.



Abstract

The rising environmental awareness is leading scientists to find more sustainable technologies and materials to substitute the ones that have negative impacts on the ecosystems. Particularly, natural and sustainable polymers, such as cellulose, are under investigation to find out whether they can be substitutes for petroleum-based polymers in numerous applications (e.g. packaging, cosmetics industry).

In this work, the behaviors of nano fibrils and nanocrystalline cellulose materials, derived from plant and food grade, were analyzed in test media mimicking many environmental waters' conditions. Size and stability of NC particles, which were extracted from primary source using chemical and physical pre-treatment, were determined by Dynamic Light Scattering (DLS) and Nanoparticle Tracking Analysis (NTA). Particles' size was found to be ranging from 100 to 150 nanometers; NC pre-treated with chemical methods were found to be more stable than those pre-treated with mechanical fibrillation. Nanoparticles' characterization was followed by an experiment aimed to determine the colloidal stability of the materials. The Organization for Economic Co-operation and Development (OECD) test n°318 guidelines were followed; and for a better mimic of European natural waters some modifications of the test mediums were performed. Test media containing fixed amount of particles and two different sources of carbon (Sodium bicarbonate and Natural Organic Matter (NOM)) were prepared. Also varying concentrations of electrolytes were added. Different methods, such as Total Organic Carbon (TOC) and Pyrolysis-gas chromatography-mass spectrometry (Py-GC-MS) were chosen to monitor the variations of NC particles along the experimental time. However, many issues were faced due to low carbon concentration in the samples and due to the difficulty to separate the carbon coming from the nanocellulose and the one derived from the test mediums. Alternatively, the attachment or collision efficiency was determined for these materials, which were prepared with the same method described by the OECD guidelines but with a higher NC concentration. The DLS was used to monitor the variation of nanoparticles' size along the experimental time span. NC particles were found to have low attachment efficiency, that got lower when particles were dispersed in test mediums which contained natural organic matter, this was due to biofilm formation and particles' surface modification. So, particles were found to be stable in natural water. The fate and transport of NC particles in a generic natural river was modeled using the Full Multi framework, developed by Domercq et al. (2022). The



mechanisms that had bigger impacts on the fate of these particles were advection, settling and degradation, which are able to half the NC's concentration in very short time.

Despite NC samples being characterized by particles of different shapes, sizes and surface functional groups, their behaviors and potential fate in natural waterbodies resulted similar. In general, nanocellulose particles were mainly found in two states, namely aggregated and free. Mostly, the behavior of nanoparticles was influenced by the presence of NOM. Due to its properties and high degradation rate, nanocellulose can be an optimal substitute to microplastic and petroleum-based polymers, and its use in different fields (e.g. in cosmetic industry as rheological regulator in face masks and creams) can be promoted to develop more sustainable technologies and products.



Table of contents

1. Introduction	7
1.1. Nanocellulose: definition and classification	7
1.1.1. Nanocellulose characteristics and properties	9
1.2. Nanocellulose production	10
1.2.1. Substrate pre-treatment	11
1.2.2. Treatment for nanocellulose extraction	12
1.3. Nanocellulose: applications	14
1.4. Objectives of the study	14
2. Materials and Methods	16
2.1. Nanocellulose samples	16
2.2. Materials, chemicals and standards	18
2.2.1. Chemicals and standards for DLS	18
2.2.2. Chemicals and standards for NTA	18
2.2.3. Chemicals and materials for the dispersion test	19
2.3. Measurements and instrumentation	20
2.3.1. Dynamic Light Scattering (DLS)	20
2.3.2. Nanoparticles Tracking Analysis (NTA)	33
2.3.3. Dispersion test	37
2.3.4. Attachment efficiency determination	51
2.4. Nanocellulose suspensions preparation	53
2.4.1. Samples preparation for DLS	53
2.4.2. Samples preparation for NTA	54
2.4.3. Samples selection and preparation for the dispersion test	55
2.4.4. Samples preparation to determine the attachment efficiency	58
2.5. The Full Multi	58
2.5.1. Framework and configuration and parametrization	60
3. Results	61
3.1. Cellulose characterization	61
3.1.1. DLS results	61
3.1.2. NTA Results	66



3.2.	<i>Dispersion test – NC concentration measurement</i>	71
3.3.	<i>Attachment efficiency determination</i>	79
3.4.	<i>Full Multi model results</i>	84
4.	Discussion	93
4.1.	<i>Particles characterization</i>	93
4.2.	<i>Attachment efficiency</i>	94
4.3.	<i>Fate and transport of NC particles – Full multi model</i>	95
5.	Conclusion	96
6.	Acknowledgement	99
7.	Bibliography	100
8.	Appendix	104

1. Introduction

1.1. Nanocellulose: definition and classification

The use of synthetic polymers, such as plastic, has contributed, especially in the last two decades, to a strong increase in pollution of the natural ecosystem. The rising environmental awareness is nowadays leading scientists to move forward seeking for more sustainable materials and polymers, which can substitute those derived from petroleum. The cellulose represents a valid alternative as environmental-friendly material due to its abundance in the nature and renewability. This polymer can be obtained from different sources, the extraction from plants is the most viable while the one from other sources, such as bacteria, is less feasible since less cellulose is contained in those species.

The cellulose is a linear polysaccharide with high molecular weight, composed by thousands cellobioses, β -D-glucopyranose molecules (*Figure 1*) (1) (2). The presence of hydroxyl groups allows the creation of intramolecular hydrogen bonds, that give to the cellulose its main physical properties (2) (3).

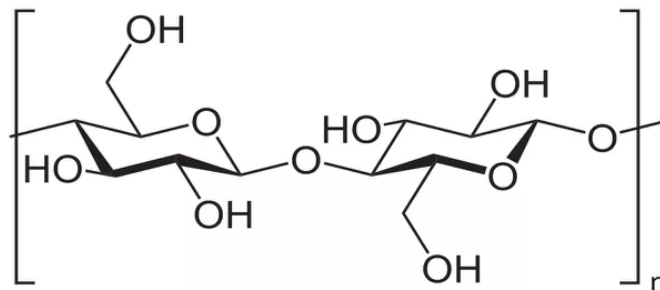


Figure 1: Cellulose molecular structure (4)

In plants, cellulose is located inside cells. In detail, the cellulose is a microfibril placed in the secondary walls of the cells, this structure is formed by crystalline microfibrils of cellulose, an amorphous region – made of lignin and hemicellulose – and other non-structural components. To enhance cellulose's physical qualities, it is reduced to nano particles, with characteristic size smaller than hundreds of nanometers. The main properties of nano cellulose are large surface area, high mechanical strength, hydrophobicity and ability to act as a liquid crystal (2).



To extract cellulose from plant substrates, it is necessary to pre-treat vegetal material and solubilize the non-cellulosic components. Different nanocellulose content, crystallinity and properties are derived from different sources.

The nano cellulose is obtained from the elementary fibrils (*Figure 2*) and it can be classified in:

- Nano crystalline cellulose (CNC): short rod-shaped particles, which are obtained from the crystalline region of the elementary fibrils. The CNC derived from plants has characteristic diameter of 5-70 nm and length of 100-250 nm.
- Cellulose nano fibrils (CNF): long fibrils that contain both crystalline and disordered domain. CNF particles are longer than CNC particles, their characteristic diameter is 5-60 nm and length can reach micrometric dimension.

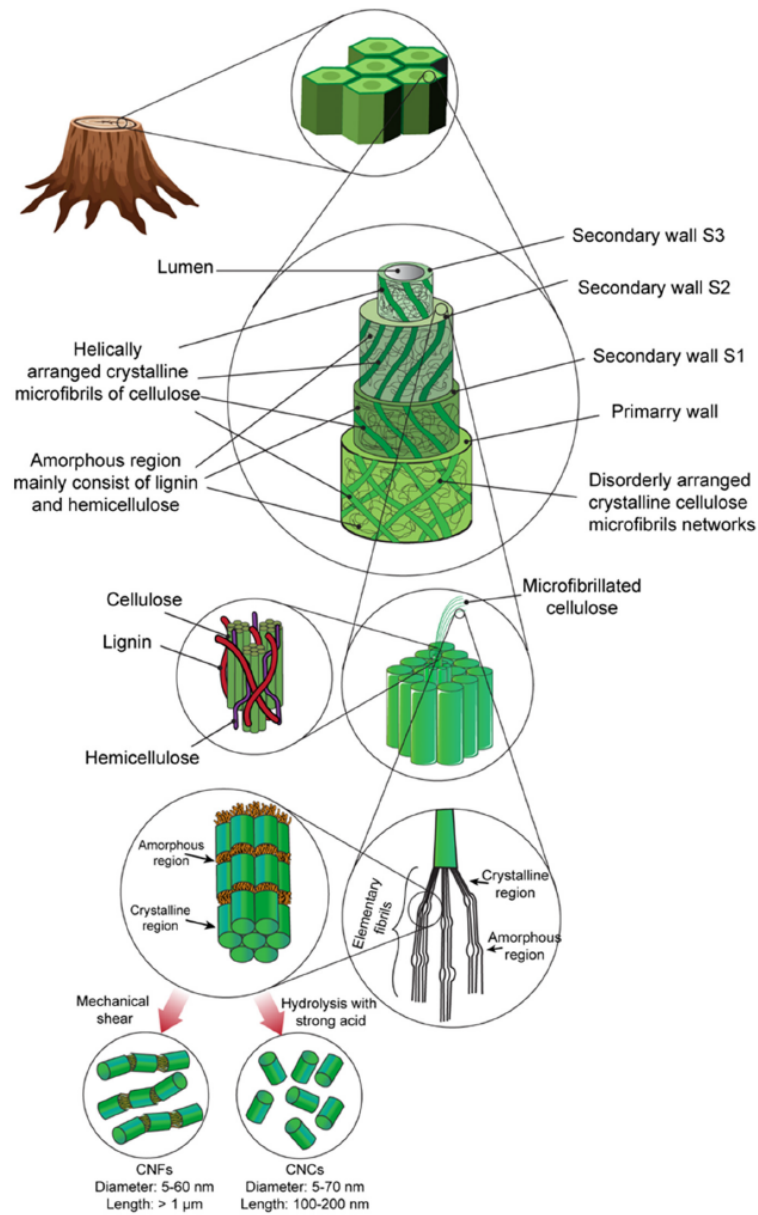


Figure 2: Schematic of a plant cell (1)

Other sources of nano cellulose are microalgae, which do not provide constant properties, and bacteria. The bacterial nano cellulose (BNC) has characteristic size of 20-100 nm, and its characteristics are dependent on the strain selection, temperature and pH of the culture.

1.1.1. Nanocellulose characteristics and properties

Nanocellulose properties are enhanced respect to native cellulose; higher strength and stiffness are given by the molecular structure of these nanoparticles. The presence of hydroxyl groups



(-OH) on the surface allows the modification and the enhancing of nanocellulose's qualities, therefore it can be adapted to many uses (1) (3).

Nanocellulose presents many physical characteristics, which are:

- Shape and size: different NC types are associated to unique shapes and aspect ratios. Low aspect ratio is associated to spherical NC, while both crystalline and fibrils nanocellulose present high aspect ratio and elongated shapes.
- High crystallinity: the crystallinity of nanocellulose varies according to the source and method of extraction. Nanocellulose derived from plants material has a crystallinity between 45-95% if extracted from softwood, while it is 90-95% if it is extracted from hardwood (1).
- Surface chemistry: due to the presence of hydroxyl groups (-OH) on the surface, it is possible to actuate chemical modifications that can be done during the isolation process, through physical adsorption – interaction with electrical charges – or formation of covalent bond. These modifications give to enhanced nanocellulose higher stability than native NC (3) (5).
- High viscosity and shear thinning behavior: nanocellulose's viscosity is high at zero shear. As a consequence of this characteristic, NC can be used as a rheological regulator, since it can modify the dripping and the shear-thinning effect, it can also facilitate the formation of thick and homogeneous layers.
- High water-holding and retention capacity: the water content in nanocellulose is up to 80% and being a non-soluble and non-adsorbent material, it preserves the moisture over time.
- Purity and biocompatibility: nanocellulose composition and purity vary according to the pre-treatment and treatment used for its extraction. High purity NC presents a neutral color. The presence of impurities can lead to lower stability over time, especially when NC is combined with other agents (3).

1.2. Nanocellulose production

The production of nanocellulose is a two steps process. First stage is the pre-treatment of the substrate to isolate the cellulose fiber from lignin and hemicellulose, then the fibers are broken down to nanoparticles (6).

1.2.1. Substrate pre-treatment

To reduce costs and energy consumption of nanocellulose extraction pre-treatments are required. The aim of these processes is to remove cementitious materials – such as hemicellulose and lignin – from the cell, thus increasing extraction efficiency and reducing the time needed for extraction. Preliminary processes facilitate the fibrillation, loosening the cell walls, treatments vary according to cellulose's source, purity of cellulosic raw material and nano particles that need to be obtained. Many pre-treatment methods can be chosen – such as alkali, bleaching, enzymatic, tempo mediated oxidation and other processes (1) – their use varies according to cellulose source and purity of raw plant material.

Chemical pre-treatments, which include alkali and bleaching, involve the use of chemical solvent to make cellulose component easier to be extracted.

The aim of alkali or mercerization pre-treatment is the depolymerization of lignin and the hydrolysis of hemicellulose, in doing so the accessibility to cellulose is increased. The mercerization is conducted at elevated temperature (70-90 °C), the chemicals typically used are strong bases, such as sodium hydroxide and ammonium hydroxide.

This process is not completely effective in lignin and hemicellulose removal; the most effective chemical used for this purpose is the sodium hydroxide, which can remove the impurities and make cellulose more accessible even though it is associated to rising cost and environmental impacts.

Bleaching pre-treatment can be used as complementary process to mercerization for lignin and hemicellulose components removal. In this process cellulose fibers are boiled with common bleaching agents under mildly acidic conditions. The chemical bleaching agents typically used are chlorine dioxide and sodium chlorite. As well as the alkali process, also bleaching pre-treatment produces toxic pollutant.

Avoiding the use of chlorine and its derivatives, environmentally safer methods can be implemented such as elemental chlorine free (ECF) and total chlorine free (TCF) bleaching (5).

An alternative to chemical pre-treatments is the enzymatic hydrolysis, which facilitates the refining and disintegration of fibers by selectively hydrolyzing cellulose. In this process enzyme complexes are used to break internal bonds in the disordered domain of cellulose.



Respectively to chemical processes, enzymatic one presents higher efficiency in separation, but it results less time efficient.

Tempo-mediated oxidation is a process that target the primary hydroxyl groups in cellulose's glucose units and converts them into carboxyl derivatives under mild conditions. Hydrogen bonds between fibers are weakened, allowing the reduction of required energy for mechanical fibrillation of lignin cellulosic component (5).

Other pre-treatment methods include the use of ionic-liquids, eutectic and organic solvents. In details, ionic-liquids (ILs) can serve as green solvents for removing lignin and hemicellulose, but they are associated with high toxicity concerns. A valid alternative to ILs is represented by eutectic solvents, which can be used to remove lignin and preserve cellulose and hemicellulose. Lastly, organosolv processes allow solvent recycling but involve challenges related to solvent flammability and costs.

Depending on the substrate that has to be treated, and the cellulose extraction requirements different pre-treatment processes are used. Consequently, nanocellulose is extracted from pre-treated substrate.

1.2.2. Treatment for nanocellulose extraction

The extraction of nanocellulose, CNC or CNF, from pre-treated material is done using various methods. Acid hydrolysis processes are preferred for crystalline nanocellulose extraction, while mechanical fibrillation is commonly used for CNF, as shown in *Figure 3*.

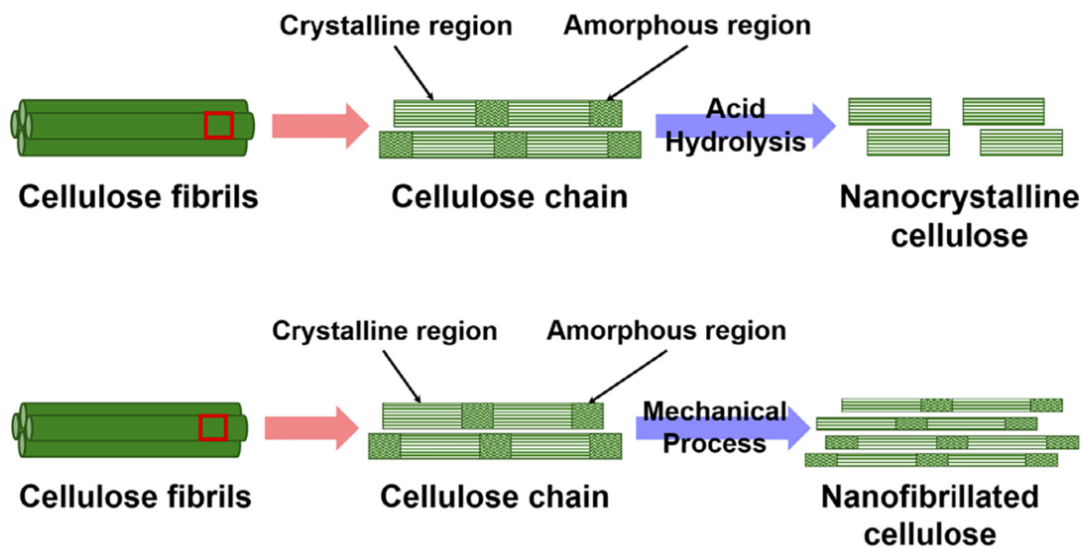


Figure 3: Schematic representation of CNC and CNF extraction with acid hydrolysis and mechanical process, respectively (5)

Acid-hydrolysis, pioneered by Nickerson and Habrle in 1947 (1), is used for CNCs extraction, can separate the crystalline components from the native cellulose (5). Acid conditions should be carefully chosen to hydrolyze just the disordered domain of cellulose – and not the crystalline (1). The hydrolysis of the amorphous domain is performed using acids like sulfuric or hydrochloric acid, which allows the production of crystalline rod-shaped particles. Acid hydrolysis conditions, necessary to separate CNCs, vary depending on the composition of the initial substrate and the required properties of final crystals.

To improve the quality of extracted crystals, also mechanical disintegration of the amorphous components is needed.

CNFs' isolation is mainly done through mechanical fibrillation of pre-treated substrate; other mechanical treatments, such as homogenization, micro fluidization, and micro grinding, should follow to delaminate the cellulosic fibers and separate them along the longitudinal direction, creating the nanofibers. The mechanical fibrillation involves high energy consumption; however, the use of pre-processed plant material grants less energy and time consumption and higher CNFs' quality (1) (5).



1.3. Nanocellulose: applications

Nanocellulose, due to its biodegradability and physic-chemical characteristics, is suitable for a wide range of applications; it is mainly used as a substitute for micro-plastics. The use of NC instead of petroleum-based polymers aims to develop new environmentally friendly technologies and materials.

In packaging industry plastic-based material are being substituted by biodegradable and biocompatible material, NC results as a good candidate for this purpose. In this field, nanocellulose is used as reinforcing additive in polymeric composite, with the aim of improving packages' mechanical and functional properties – such as hydrophobicity.

In energy and electronic field, due to its surface conductivity, NC can be used in displays, sensors, transducers and as enhancer of performance for energy storage units. Nanocellulose is considered suitable for most of the applications in energy sector (1) (7).

NC, thanks to its rheological features and skin compatibility, resulted a good ingredient for cosmetic, skincare and healthcare formulations (3). Because of hydroxyl groups presence, and so possible surface modifications, it is used as nanocarrier of bioactive ingredients and as gelling and moisturizer agent.

In cosmetic field, nanocellulose can be used as support material for sheet facial masks that carry moisturizers and other active substances (7); it can also be implied as anti-wrinkles due to its tissue healing process (2).

Other emerging applications can be found in biomedical field, in which NC is used for engineered tissues, bioactive implants and drug delivery.

1.4. Objectives of the study

Nanocellulose can be used as a replacement of petroleum-based polymers in broad range of applications, as previously stated (*Paragraph 1.3*).

Prior the employment of NC in new commercial fields, development of new technologies and materials, it is necessary to evaluate the fate of these particles in the environment.

The main objective of this study is reaching assessment of the coagulation, sedimentation and transport of nanocellulose particles in water bodies, and further predict behavior of NC in water environment.

To achieve this, several objectives can be determined as:



Objective 1 – Selection of suitable nanocellulose sample for experimental study:

- a) Characterize different nanocellulose materials to select suitable nanocellulose for experimental studies. It consists of determining particle sizes, zeta potential, and particles concentration. The experimental phase which is necessary to determine the fate and the transport in environmental water, is performed by adapting the OECD test n°318 (8) guidelines to NC particles.

Objective 2 – Prediction of nanocellulose's behaviors in water environments:

- a) Determine attachment efficiency of nanocellulose particles by using different test mediums which could mimic the European environmental waters.
- b) Apply Full Multi model: Implement the Full Multi model, developed by Domercq et al. (9), which can determine the fate and the transport of nanoparticles in waterbodies.

2. Materials and Methods

2.1. Nanocellulose samples

The analyzed sample set was composed of seven different nanocellulose materials, four of them were cellulose nano crystals (CNC), while the remaining were cellulose nano fibrils (CNF).

The analyzed NC particles were obtained from different sources, for instance food and industrial grade. Many pre-treatments were used to extract nanoparticles. Because of this, they possess distinct characteristics, such as size, appearance, aspect ratio – ratio between the two primary particle sizes – and functional surface groups.

The materials analyzed were categorized into four groups according to their properties and characteristics.

The samples 1 and 2 are hydrophilic sodium-neutralized sulphated cellulose nanocrystals (CNC), the aspect ratio of the particles is respectively 22:1 and 13:1, they present the highest nanocellulose weight composition among all the samples, which is 3.98%.

The samples 3 and 4, present the lowest CNC weight composition within the entire set of materials, it is equal to 1.00%; aspect ratio of 13:1 and, the surface functional groups are quaternary ammonium hydroxyl for sample 3 and carboxyl hydroxy for the 4.

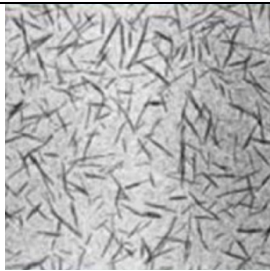
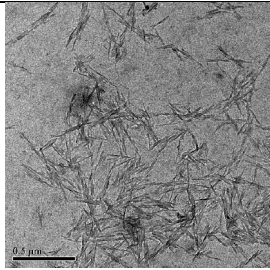
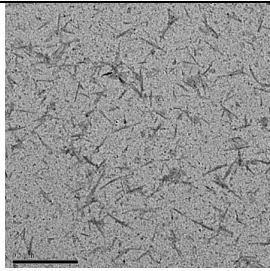
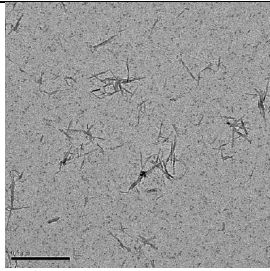
The CNF samples 5 and 6 have non-modified surfaces and mechanical fibrillation treatment is applied, for these materials no chemical surface modification is performed. The CNF sample 5 presents short fibrils (as specified by producer) and it is derived from food grade cellulose; whereas the CNF sample 6 has extra-short fibrils (as specified by producer) and it derives from industrial-grade cellulose; for both samples the CNF weight composition is 1.99%.

Differently from the sample others CNF samples, the sample 7 is pre-treated with mechanical force and high-pressure chemical modification, the functional group on the surface is oxalate ester, the aspect ratio of these particles is high (88:1), the NC weight composition is 2.09%.

It is worth to notice that all the materials present negative charged surfaces, exception made for the CNC sample 3, which presents positive charged surface.

Transmission Electron Microscopy (TEM) images of the samples 1,2,3 and 4, provided by the SDS (Safety Data Sheet) of the materials, together with other supplied data, are reported in *Table 1*.

Table 1: Samples CNC 1,2,3,4 and CNF 5,6,7 characteristics (pre-treatments; surface functional group, aspect ratio) and TEM images. Provided by materials suppliers.

Sample name	Pre-treatment	Functional group	Aspect ratio (L:W)	TEM images
CNC 1	Unknown	Sulfonic gr.	(22:1)	
CNC 2	Unknown	Sulfonic gr. (high content) Hydrophilic	(13:1)	
CNC 3	Unknown	Quaternary ammonium, hydroxyl gr. Hydrophilic	(13:1)	
CNC 4	Unknown	Carboxyl, hydroxyl gr. Hydrophilic	(13:1)	
CNF 5	Mechanical force	Non-modified	Short	-
CNF 6	Mechanical force	Non-modified	Extra short	-
CNF 7	Mechanical force and high-pressure chemical modification	Oxalate ester	High ratio (88:1)	-

Other information about the samples, including their compositions by weight (%wt), are reported in *Appendix: Table 1*.

2.2. Materials, chemicals and standards

2.2.1. Chemicals and standards for DLS

Nanocellulose solutions were prepared to adapt the suspensions to DLS instrument's requirements – particularly concerning the particles concentration.

The following solvents were used for this purpose:

- Milli-Q water (MQ): Ultrapure water (18.2 M Ω cm) was obtained from a Milli-Q system (Millipore, Burlington, Massachusetts, USA)
- Sodium dodecyl sulphate (SDS): a solution 1mM SDS (Fluka, Germany, CAS 151-21-3) was used to stabilize NC particles. The solvent presents a pH in the range 5-6.
- NovaChem (POSTNOVA, surfactant 100) and NaCl solution: another stabilizing solvent used to perform DLS analysis on nanocellulose particles is a solution 0.05% NovaChem and 3mM NaCl; the resulting pH is in the interval 6-7.

To check the reliability of the instrument, two standards were tested. The Polystyrene (PS) standard with 92 nm beads (Thermo scientific), and the Zeta Potential Transfer Standard - 40 \pm 5.8 mV (ZTS1240), produced by Malvern Panalytical.

2.2.2. Chemicals and standards for NTA

The nanocellulose dispersions, for the Nanoparticles Tracking Analysis, were prepared solely using MQ as solvent.

As for the DLS, the tested standard, to assess the quality of the results, was the PS. In this case the Polystyrene beads had characteristic dimension of 100 nm. To test the PS standard, prepare and calibrate the NTA instrument a specific procedure was followed.

Before starting the experiment, the cell was rinsed and its quality was checked; eventually, if the cell resulted not clean, more MQ was flushed through the chamber. Afterward, the standard was tested to prepare the instrument for the following measurements. The standard, according to the instrument's guidelines, must be diluted 250000 times and injected – without introducing air bubbles – as requested by the software. Subsequently to auto alignment, focus optimization

processes and checking of particles' concentration and drift, the daily performance measurement were performed.

2.2.3. Chemicals and materials for the dispersion test

Different test media were prepared to assess the dispersion stability of nanocellulose.

The chemicals used in the test media were Calcium Nitrate Tetrahydrate ($\text{Ca}(\text{NO}_3)_2$, AnalaR NORMAPUR by VWR, Italy CAS 13477-34-4), Magnesium Sulfate (Sigma-Aldric, Germany, CAS 7487-88-9) which aimed to adjust the ionic strength. As source of inorganic carbon Sodium Bicarbonate (Honeywell Fluka, Italy, CAS 144-55-8) was utilized. While for pH regulations NaOH (Sigma-Aldric, Germany, CAS 1310-73-2), and HNO_3 (CAS 7697-37-2) were added. Also, a source of organic carbon, Natural Organic Matter (NOM) was used for the preparation of the test media. Since the NOM represents a broad range of organic carbon sources, to perform this experiment and guarantee its repeatability, the use of a specific and well characterized NOM was necessary. The Suwannee River NOM (2R101N), purchased from the International Humic Substances Society (HISS), was used since it presents a well-defined composition. The chemical composition, weight percentage (%wt), of the Suwannee River NOM is reported in the following table (*Table 2*) (10).

Table 2: Chemical composition of Suwannee River NOM (11)

Aquatic NOM	Cat. No.	H ₂ O	Ash	C	H	O	N	S	P	$\delta^{13}\text{C}$	$\delta^{15}\text{N}$
Suwannee River NOM	2R101N	5.69	4.01	50.7	3.97	41.48	1.27	1.78	nd	nd	nd

*All the value represents the weight percentage %wt

Stock solutions were prepared diluting the chemicals with pure MQ, particularly:

- 0.1 M solution of NaHCO_3 .
- 80 mM $\text{Ca}(\text{NO}_3)_2$ solution and 80 mM of MgSO_4 solution; that were used to vary electrolytes concentrations.
- For pH adjustment a solution of 5 times dilution of HNO_3 was used together with a 0.1 M solution of NaOH.



- SRNOM was added to the test media to reach a Dissolved Organic Carbon (DOC) concentration of 10 g DOC/l in the final sample.

2.3. Measurements and instrumentation

The characterization of nanoparticles, so the determination of their size and stability inside a colloidal dispersion, was a crucial step for the study of the behavior of nanocellulose in aqueous streams.

Two complementary techniques were used to characterize the dimension of nanocellulose particles inside the samples: the Dynamic Light Scattering (DLS) and the Nanoparticle Tracking Analysis (NTA). Both the used technologies allowed the determination of particles' size; particularly, the first one allowed the determination of the hydraulic diameter while the second the diameter of the particles.

2.3.1. Dynamic Light Scattering (DLS)

The Dynamic Light Scattering technique was chosen to determine both the size and the stability of nanocellulose samples. These two measurements were performed using the DLS instrument in two modalities: size and zeta mode.

Size mode: theoretical principles

The DLS instrument, when used in size mode, can measure the hydrodynamic diameter of suspended particles, which undergo a Brownian motion. The device performs the measurement through a correlation function that relates the fluctuation of the intensity of the light scattered by the particles over time.

The size obtained is the hydrodynamic diameter, which is larger than the actual one since it is dependent on the electrical double layer (*Figure 4*).

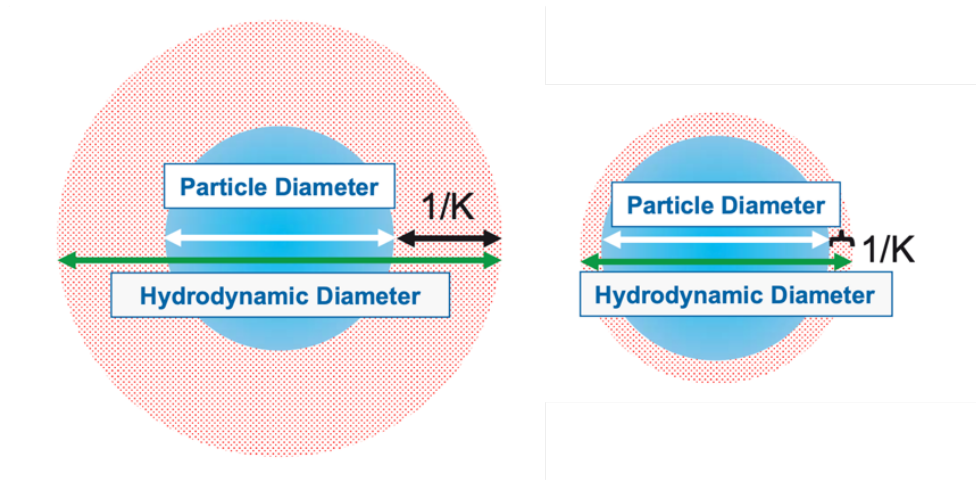


Figure 4: Hydrodynamic diameter and Debye length ($1/K$) (12)

The thickness of the electrical double layer – also called Debye length ($1/K$) – is conditioned by the ionic strength of the media. The width of the electrical double layer increases with lower ionic strength, contrary it is reduced or almost repressed when the ionic strength is higher (12). The random motion to which particles are subjected, is called Brownian motion and is due to the interaction between particles the surrounding solvent (13). When a light beam encounters particles, subjected to this motion, it is scattered with different intensities. The intensity fluctuations of the scattered light can be detected by a sensor. Is therefore possible to determine the diffusion coefficient (D) of the suspended particles (14).

The diffusion coefficient of nanoparticles is inversely proportional to their hydrodynamic diameter and the viscosity of the medium – as stated by Stokes-Einstein equation (*Equation 1*).

$$D = \frac{kT}{3\pi\eta d_h}$$

Equation 1: Stokes-Einstein eq.

Where:

- D is the diffusion coefficient proportional to the velocity of the particles – it is measured in m^2/s .
- d_h [m] is the hydrodynamic diameter.
- $k = 1.3806452 \times 10^{-23} J/K$ is the Boltzmann constant.
- T [K] the absolute temperature.

- η [kg/m s] the medium viscosity.

The relative movement between the suspended particles that scatter the light beam and the sensor, which detects it, generates the so-called Doppler effect. The interferences between scattered light waves can generate constructive and destructive phases.

The intensity fluctuations over time (ns- μ s) of the scattered light is related to the diffusion coefficient of the particles through an autocorrelation function.

It can be stated that the diffusion of small particles generates high frequency variations of scattered light, while larger particles diffusion gives lower frequencies of intensity fluctuations (*Figure 5*).

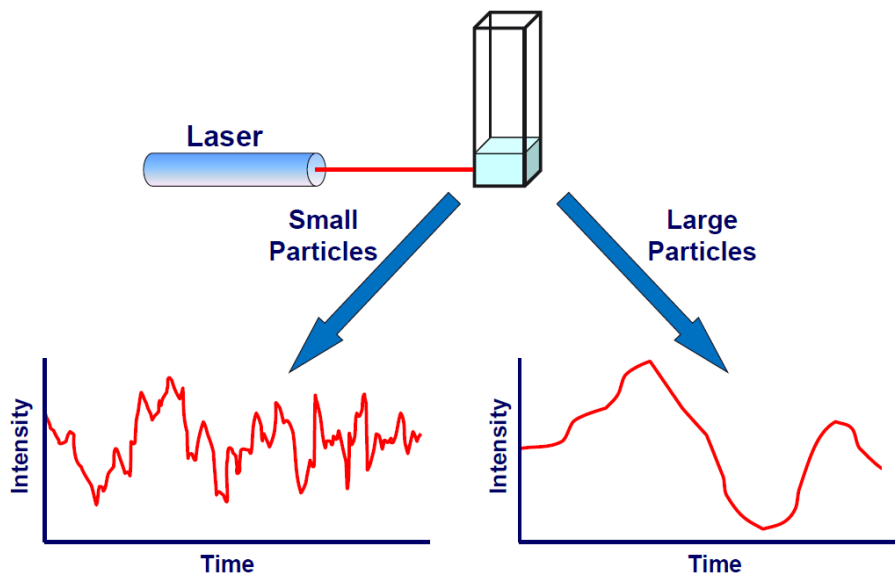


Figure 5: Scattered light intensity fluctuations for small and large particles (12)

The second order correlation function $g^{(2)}(\tau)$, Equation 2, is built shifting the intensity function by a delay time (τ), and the autocorrelation function is then computed.

$$g^{(2)}(\tau) = \frac{\langle I(t) \cdot I(t + \tau) \rangle}{\langle I(t) \rangle^2}$$

Equation 2: Intensity second order correlation function.

Where $I(t)$ is the intensity of scattered light at time t , τ is the time delay (very small value, usually nanoseconds). In *Figure 6* is reported the definition of the Correlogram, starting from the shifting of intensity fluctuations over time. For each time delay τ the correlation coefficient is determined.

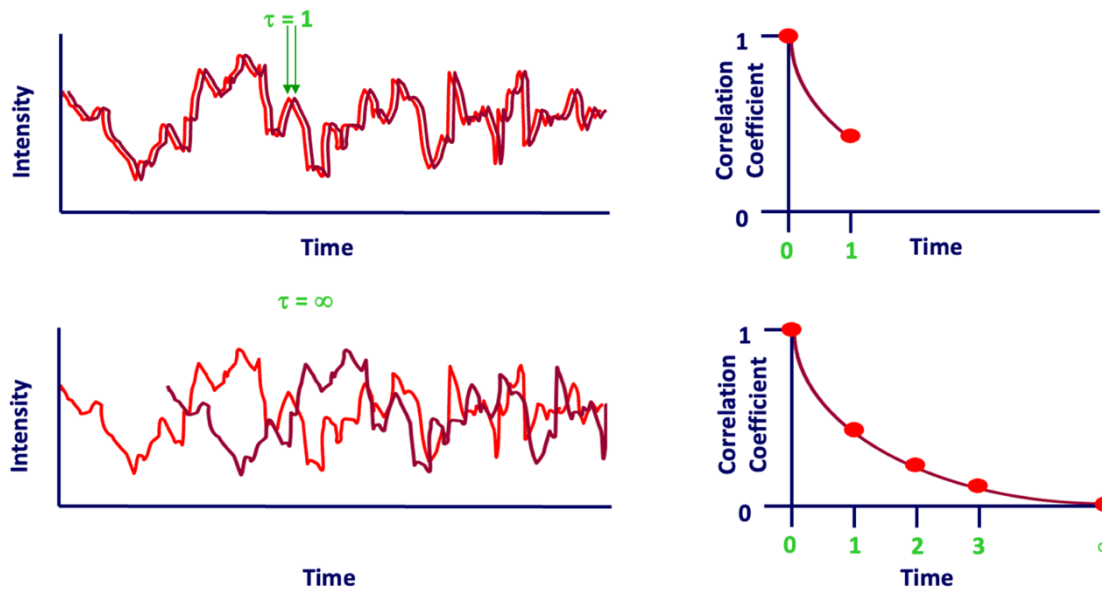


Figure 6: Correlogram definition starting from the autocorrelation function (12)

The correlation coefficient decay over time, determined from the autocorrelation function is reported in the Correlogram (*Figure 7*), which can be used to establish different parameters, such as particles' size and polydispersity index (PDI).

In details:

- The mean size of particles is given by the time in which the correlation coefficient starts to decay.
- The sample polydispersity Index (PDI) can be obtained by the gradient of the curve. The PDI indicates the degree of non-uniformity of a dispersion. In the DLS result analysis higher PDI values (> 0.4) are related to polydisperse solutions, while values in the interval $(0-0.4]$ are linked to monodisperse or moderately polydisperse solutions (15).
- The vertical axis intercept indicates whether the particle concentration within the sample is correct for performing the test obtaining reliable results. The presence of larger particles or aggregates imply high intercept (> 1) and not flat baseline.

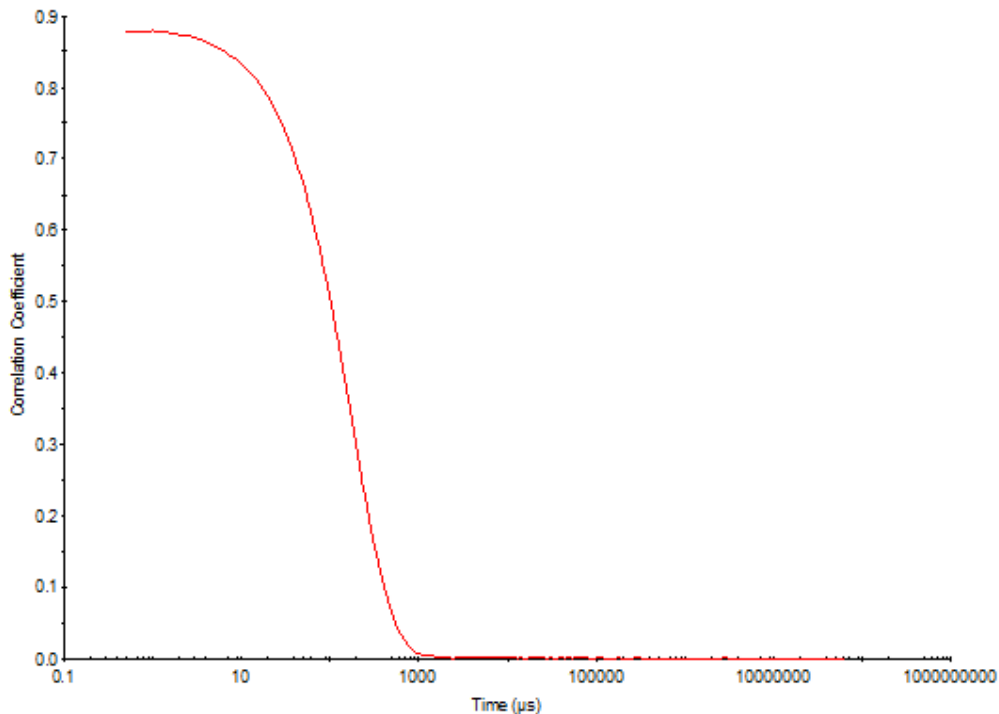


Figure 7: Correlogram (Correlation coefficient decay over time (μs))

Zeta potential mode: theoretical principles

The Zeta potential (ZP) is a physical property of dispersed particles, it is used to assess the long-term stability of a solution. The Zeta potential can be measured by the DLS instrument when used in Zeta mode.

In a dispersion, the suspended particles – due to attractive and gravity forces – can at first adhere, aggregate and the flocculate; if this process is irreversible is then called coagulation.

The particles' tendency of staying in suspension, either flocculate, is determined by many factors: their dimension, relative density with respect to the solvent density and surface charge.

The colloidal stability is supported by the DVLO theory, which was developed by Derjaguin, Verwey, Landau and Overbeek in the 1940s (16).

DVLO theory states that the total potential of a particle in solution, V_T , is the balance three contributions: solvent, attractive and repulsive potentials.



$$V_T = V_S + V_R + V_A$$

Equation 3: Total potential given by the three contributions (solvent, attractive and repulsive potentials)

Extensively, the three potentials, which have different competences and contribution to the balance, are defined as follow:

- Potential energy due to the solvent (V_S) – just a marginal contribution to the balance is given by this component.
- Repulsive and attractive potentials, respectively V_R and V_A , which mostly compete in the balance.

The electrical double layer repulsive forces contribute to V_R , those forces avoid the adhesion of two particles together.

On the other hand, the main contribute of V_A are the van der Waals attractive forces, which act on suspended particles and contribute to particles' adhesion, when sufficient energy is provided, so when the repulsive energy barrier is overcome.

The repulsive potential is proportional to the square of the Zeta potential, the solvent permeability, the distance between particle D_p (m) and other parameters, as shown in *Equation 4*.

$$V_R = 2\pi\epsilon a ZP^2 \exp(-\kappa D_p)$$

Equation 4: Repulsive potential

Where a is the particle radius (m), ϵ is the dielectric constant (F/m), κ the inverse Debye length (1/m) is function of the ionic composition and ZP is the zeta potential (mV).

Furthermore, the attractive potential, *Equation 5*, is proportional to the Hamaker constant (A) and it is inversely proportional to square of the particle separation (D_p).

$$V_A = -\frac{A}{12\pi D_p^2}$$

Equation 5: Attractive potential

The colloidal system is defined as “stable” when the particles have enough repulsive energy; therefore, when adhesion, flocculation and coagulation are avoided.

An increase in zeta potential can lead to decrease in repulsive forces, consequently to solution instability; for this reason, ZP is used as indicator of the stability of a colloidal dispersion.

The stability of colloidal systems can be achieved enhancing two different mechanisms: steric repulsion and electrostatic stabilization (16).

The factors that affect the Zeta potential are pH, conductivity – related to the thickness of the double layer – and concentration of dispersed particles.

Variations of ZP are strongly related to pH; unstable condition can be found at certain range of pH adding acids or alkali to the solution, as shown in *Figure 8*.

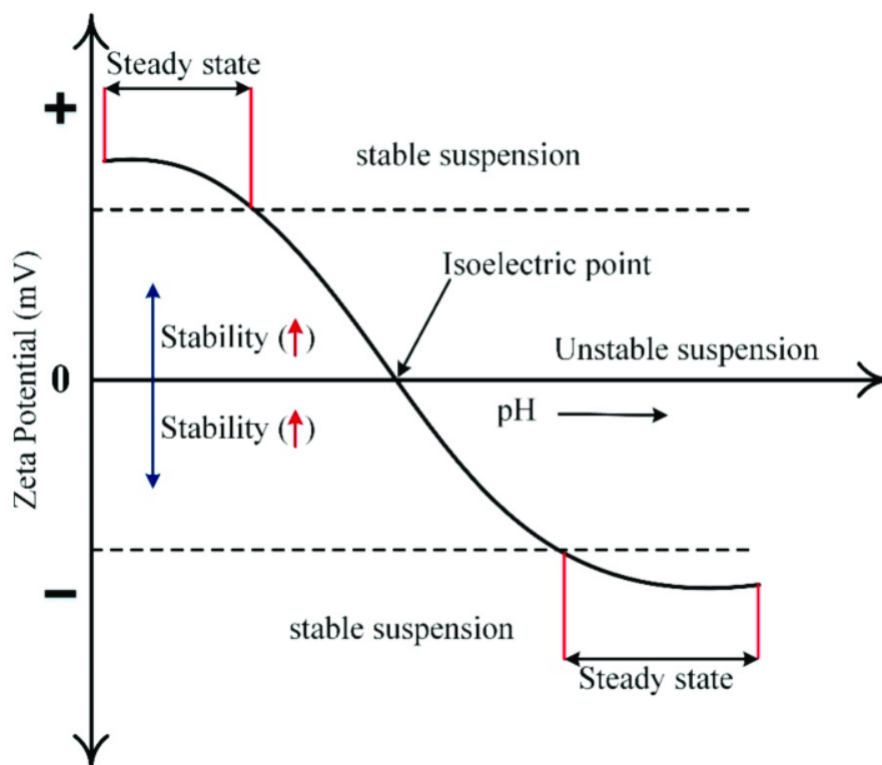


Figure 8: Schematic illustration of ZP vs pH curve (17)

It is worthwhile to define the isoelectric point – which is relevant from a practical point of view – as the pH value at which the positive and negative charge are balanced, so the surface is neutrally charged.



The ZP is also related to the electrophoresis mobility which is the movement of a charged particle – related to the suspension liquid – when an electric field is applied. As stated by the Henry equation (12), the electrophoretic mobility is directly proportional to Zeta potential, *Equation 6*.

$$U_E = \frac{2\varepsilon ZP}{3\eta} F(\kappa a)$$

Equation 6: Henry equation – electrophoresis mobility

Where:

- U_E (J) is the electrostatic potential energy or electrophoresis mobility; it can be measured using a cell with electrodes, in which a potential is applied. The velocity of particles can be evaluated in the electrical field.
- $F(\kappa a)$ [-] is the Henry's function; κa is the ratio of particle radius to the double layer thickness. This function can be approximated as follows: for a non-polar media $F(\kappa a)$ is 1.0, Huckel approximation; for a polar media, Smoluchowski approximation is used, $F(\kappa a) = 1.5$.

The electrophoresis mobility can also be defined as the ratio between the velocity of particles and the electric field which generates it, *Equation 7*.

$$U_E = \frac{V}{E}$$

Equation 7: Electrophoresis Mobility(J)

The velocity of particles (V) is expressed in $\mu\text{m/s}$, while the electric field (E) in V/cm .

The DLS applies an electric field to the dispersion, hence the electrophoresis mobility is measured and the zetapotential defined.

A laser beam incident on moving particles, subjected to electrophoresis mobility, is scattered and the Doppler shift is determined (18). Particles' velocity is obtained by the intensity of light scattered by them, which is detected by the sensor. Being the electric field applied by the instrument, on the dispersion, known, the electrophoresis mobility can be determined and consequently the zetapotential can be measured.

Testing phase/instrumentation

The instrument used for the determination of the size and stability of nanocellulose particles is the Zetasizer Nano ZSP (by Malvern Panalytical), shown in *Figure 9*, which was used in Size and Zeta modes.



Figure 9: Zetasizer Nano ZSP (by Malvern Panalytical) (19)

The Zetasizer Nano ZSP operates with the NIBS (Non-Invasive Back Scatter) technique, which determines automatically the attenuator setting and the optimal position. Thanks to the back scatter detection system at 173° (14), this instrument can accurately determine the size of particles in more concentrated sample.

The characterization of nanocellulose samples with Dynamic Light Scattering was performed in two steps: at first the size of particles was determined, then the stability, so the zeta potential was measured.

Size mode

The size mode allows the definition of the characteristic dimension, or rather the hydrodynamic diameter, of suspended particles. The parameters that are obtained from this test mode are Z-



average, Polydispersity Index (PdI), Attenuator and Derive Count rate. Accurately, the parameters that come out from the DLS size measurement are:

- Z-average, which define the diameter of the particles, it is expressed in nanometers (nm).
- Polydispersity Index (PdI) is referred to the degree of non-uniformity of a distribution, higher values of PdI are synonyms of non-good measurement. In this test, the measurements which show PdI > 0.7 are not considered in the final analysis.
- The Attenuator gives the correctness of the concentration of nanoparticles in the analyzed sample, both too high and too low concentrations would not lead to reliable results. Size measurements associated with attenuator factors < 10, or rather in the range 7-9, symbolize a correct particle concentration inside the sample and therefore a good measurement.
- The Derive Count Rate provides a direct measurement of the intensity of light scattered by the suspended particles. High values of Derived Count rate (>1,000 kpcs) can be associated to a saturated sensor, while low values of this parameter (< 100 kpcs) can be related to a weak signal that reach the sensor.

The Attenuator along with the Derived Count Rate (kpcs), which is a calculated parameter, can be used to assess the quality of the results.

The main parameters determined by the DLS software are reported in *Table 3*.

Table 3: Parameters determined by the DLS software (size mode)

Z-average (nm)	PdI (-)	Attenuator (-)	Derived Count Rate (kpcs)
Defines the average hydrodynamic diameter of suspended particles	Polydispersity index, define the degree of non-uniformity of a solution	Control mechanism that adjusts the intensity of the incident laser beam before it reaches the sample	Reflects the intensity of the scattered light from the sample
-	0 - 1	<10	-



To determine the size of the particles, disposable polystyrene cuvettes, DTS0012 Cell (*Figure 10*), were used. The sample volume injected in the cell, using an Eppendorf pipette, is 1 ml.



Figure 10: DTS0012 Cell for Zetasizer Nano ZSP (by Malvern Panalytical) (13)

The DLS sizing of nanoparticles was performed with the NIBS, so automatic attenuator setting backscatter and movable focal point were set to avoid multiple scatters and to determine automatically, the optimal relative position between laser and detector (12).

To evaluate the goodness and reliability of the DLS measurements, a blank sample of Milli-Q Water (MQ) and a Polystyrene (PS) Standard were tested.

Zeta mode

The evaluation of the stability of the tested colloidal suspensions is done through the outcomes of the zeta potential mode, which are the ZP and its standard deviation.

Particles in suspension are defined as highly stable when its ZP is in the ranges < -30 mV or $> +30$ mV, values of ZP in the ranges -30 mV to -20 mV or $+20$ mV to $+30$ mV are considered as moderately stable, other values of ZP are associated to unstable solutions, *Table 4*.

The ZP standard deviation states the width of the dispersion curve around its mean, high ZP standard deviation values cannot be associated to a precise Zeta Potential definition, so the stability of the sample is not assessed correctly.

Table 4: ZP stability ranges.

Zeta Potential (mV)	Stability
0 to +20 or 0 to - 20	Unstable
+ 20 to +30 or -30 to -20	Moderately stable
> +30 or < -30	Stable

In the final analysis, just results associated to ZP > + 30 or < - 30 were taken into account.

The cuvettes used to execute the Zeta mode, are the DTS1070 folded capillary Cell (*Figure 11*). Even if these cuvettes are disposable, the test was performed re-using the same cell, that was rinsed – at least three times with MQ – before and after testing each sample.

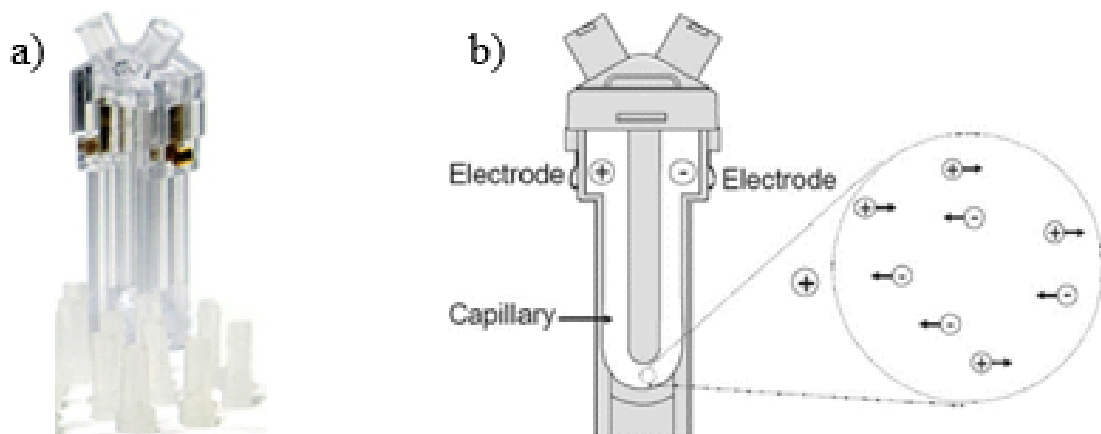


Figure 11: a) DTS1070 Cell for Zetasizer Nano ZSP (by Malvern Panalytical (13) b) Schematic representation of a folded capillary cell (20)

The dispersion is injected in the cell, with a disposable glass pipette, up to the indicated level; all air bubbles, that may have formed during filling, were removed before the test was carried out.

Measurements

As previously stated, the concentration of particles inside analyzed samples has high influence in the goodness of DLS test results. To obtain trustable dimension measurements, it was



necessary to find the concentration associated to lower Pdl, Attenuator in the range 7-9 and ZP in the stability intervals (*Table 5*).

Table 5: Parameters for a trustable characterization with DLS instrument

Size mode		Zeta mode
Pdl (-)	Attenuator (-)	ZP (mV)
< 0.7	7-9	< -30 or > +30

To have a correct size measurement of the suspended particles, before performing the actual DLS test, all the samples have undergone a sonication process necessary to avoid aggregation or flocculation of the particles inside the solution. To achieve better results, the sonication which took place inside a sonicator bath must be for ten minutes – since the test results were not as good when it was set to lower time.

The tested samples were first diluted, with MQ, at low concentration; the samples 1,2 at 4ppm, while the others (3,4,5,6,7) at 10 ppm. For all the samples, these initial tests have led to not reliable results since the obtained attenuator factors appeared very high.

It was necessary to increase particles concentration to get better results and lower attenuators. The samples were tested with various increasing concentration (8; 20; 50; 100; 150 ppm). In *Appendix: Table 2* are reported the DLS results – size and zeta measurements – of different samples concentrations (50, 100 and 150 ppm).

Meanwhile the CNC samples (1,2,3,4) and the 7, diluted with MQ, resulted stable with concentrations higher than 100 ppm; the CNF samples, 5 and 6, still presented too high Pdl and ZP outside the stability interval.

Therefore, the dilution of CNF samples 5 and 6 with SDS and NovaChem were performed.

In all cases, with the three diluent solutions, the best concentration for analyzing nanocellulose samples resulted being 150 ppm.

Even to assess the quality of Zeta potential measurements, the Transfer standard, -40 ± 5.8 mV, was tested.

2.3.2. Nanoparticles Tracking Analysis (NTA)

The Nanoparticle Tracking Analysis is a visualization technique that can measure size, zeta potential and concentration of suspended nanoparticles (21).

A laser light illuminates dispersed particles, which due to light scattering, appear as individual points moving under Brownian motion. Particles' visibility is enhanced by a black background posed behind them.

The images are acquired by a light sensitive camera, placed at a 90° angle to the irradiating plane, in this way all the particles with size in the range 10-1000 nm can be detected (22). A schematic representation of NTA working principle is reported in *Figure 12*.

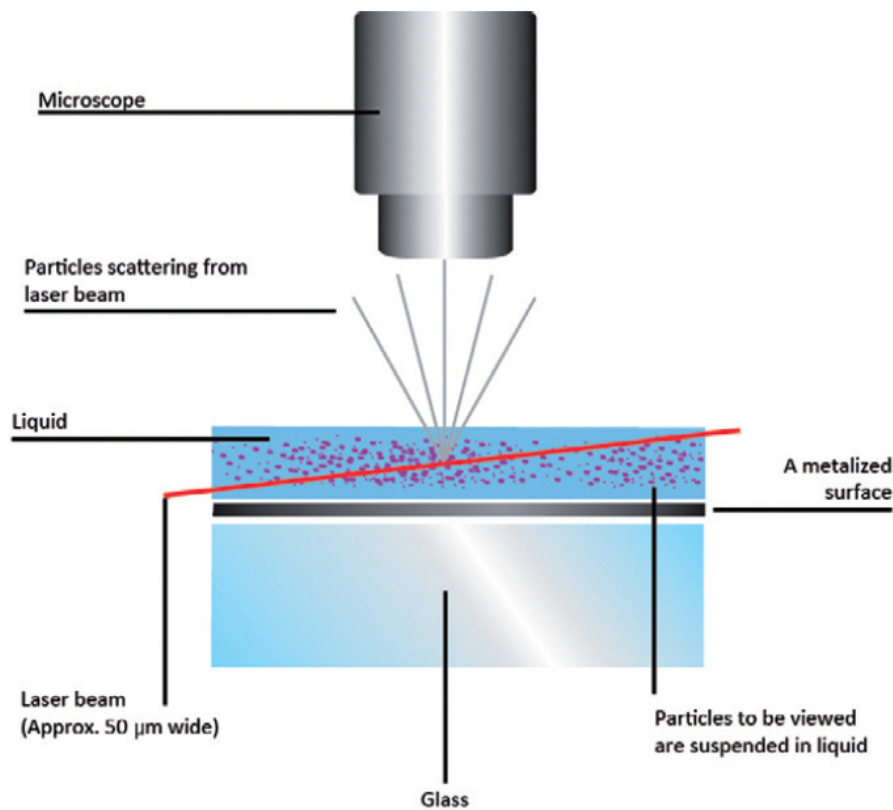


Figure 12: Schematic representation of NTA (14)

The recorded video of moving particles is then processed through the Particle Metrix Zetaview software, which is able to define, particle-to-particle, the sizing, and the concentration (particle/ml).

As for the DLS, also in NTA the diameter is calculated from the rate of particles movement through the Stokes-Einstein equation (*Equation 1*).

Together with size, the software is able to measure the particles concentration in the sample, which is the number of particles and the zetapotential. Furthermore, with this technique is it possible to monitor the real-time events, such as aggregation of particles.

The instrument used for the analysis of NC samples is the Zetaview TWIN by Particle Metrix, shown in *Figure 13*.



Figure 13: Zetaview TWIN (by Particle Metrix) (23)

Testing phase

The NTA Zetaview TWIN instrument is composed by a central chamber in which the sample is injected using a 1ml disposable syringe. The solution flows through the cell and the particles, hit by the laser beam, are detected by the camera.

It was necessary before and after each measurement, to rinse the system with MQ to remove particles and residues.



Cell calibration is performed following the guidelines given by the NTA Software, so a 250000 times diluted solution of PS 100 nm beads was injected in the chamber, as described in the *Paragraph 2.2.2*.

All the experiments were carried out with controlled temperature, which was set to 25°C. Samples size measurement was executed once the result of the daily performance measurement was categorized by the software as “*very good*”.

After each injection, and analysis, the cell was rinsed with MQ at least three times, until the displayed window showed a pure black screen without any visible particle.

Once the calibration of the instrument was done, the measurements were carried out injecting in the cell samples solution with a concentration of 0.75 ppm.

It is worth to highlight which are the experiment parameters set for the video recording. Most important parameters' categories to be set for the analysis are:

- Experiment: which includes position, measurement mode (zeta/size), cycles and recording quality;
- Options: which includes exporting settings and temperature control;
- Camera controls: which include sensitivity, frame rate and shutter speed;
- Post acquisition parameters;
- Dilution factor.

The results are given as pdf documents for each measurement – three consequent measures for each sample.

For all the samples, position, temperature, dilution factor and post-acquisition parameters were set, as reported in *Table 6*.



Table 6: SOP setting

Experiment	Positions	11
	Measurement mode	size
	Cycles	2
	Recording quality	Med.
Option	Autosave .txt	
	Autosave .pdf	
	Multiple acquisition	3
	Temperature (°C)	25
Post acquisition	As default	

Along the experiment different Camera Control setting were used for different samples; in detail, the sensitivity of detection was changed.

The sensitivity refers to the level of camera detection; higher sensitivity camera can detect weaker signal coming from smaller particles.

Therefore, sensitivity was set and adjusted analyzing the real-time images of the particles.

For nanocellulose's size and concentration determination, the following Camera Control setting were used. For the CNC samples – 1, 2, 3, 4 – and CNF sample 7, the Camera Control settings were set as follow (Table 7).

Table 7 : Camera control setting samples 1,2,3,4,7

Camera control	Sensitivity	75
	Frame Rate	30
	Shutter	100

Instead, for the CNF samples 5 and 6 another sensitivity value was set, since the images obtained with higher sensitivity resulted blurred and not suitable for the analysis (Table 8).



Table 8: Camera control setting samples 5,6

Camera control	Sensitivity	65
	Frame Rate	30
	Shutter	100

Size measurement analysis was carried out by taking into consideration the frequency distribution graphs (Diameter (nm) vs Concentration (particles/ml)) and the mean, median and mode values provided by the NTA software. In the following paragraph, results given by the NTA software were analyzed.

2.3.3. Dispersion test

Prior the use and application of nanocellulose in many industrial and commercial field, it is necessary to assess the behavior of the particles when released in the environment, especially in aqueous compartments. It is fundamental to determine the fate and transport of these nanoparticles in aqueous streams, as they represent the major means of transport and diffusion of these nanomaterials.

The parameter that can be used to define the fate of nanoparticles in aqueous media is the dispersion stability (24).

The experiment, which assesses the behavior and the dispersion stability of nanocellulose particles in mediums that can mimic the environmental waters, was developed starting from the OECD test n°318 (24). This test guidelines, titled “*Dispersion stability of nanomaterials in simulated environmental media*”, provide a simple procedure to determinate the dispersion stability of nanoparticles in various aqueous conditions, aimed to represent natural waters conditions (8).

Further modifications of these test guidelines were performed to adapt these indications to nanocellulose particles.

The primary objective of the OECD test n°318 is to evaluate the capacity of a nanomaterial to form a colloidal dispersion and maintain its stability under environmentally relevant conditions. The dispersion stability was determined over 6 hours experiment. Different

parameters, such as pH, presence of NOM, anions and cations, were chosen to determine the behavior of nanoparticles in different mediums.

In an aqueous dispersion, the nanoparticles undergo a Brownian motion, i.e. a random movement, which lead to particle-particle collisions. Consequently, the particles may aggregate and sediment. When the sedimentation increases due to collisions and becomes dominant the system results unstable. Many factors affect this process, such as size, density and shape of particles. Also, environmental conditions are influent on particles' fate. The agglomeration is prevented and slowed down by the energy barrier that is due to particle-particle interaction. The main contributors to energy barrier are the Van der Waals, the electrostatic and the steric forces. In aqueous media, these interactions are controlled by the hydrochemistry and particles' surface chemistry.

Test process

The test is structured as a dispersion-agglomeration-settling procedure conducted in 50 ml vials. Phase separation, driven by particle agglomeration and settling (*Figure 14*), is evaluated by measuring particle concentration in the upper portion of the supernatant, top 0-1 cm of the dispersion.

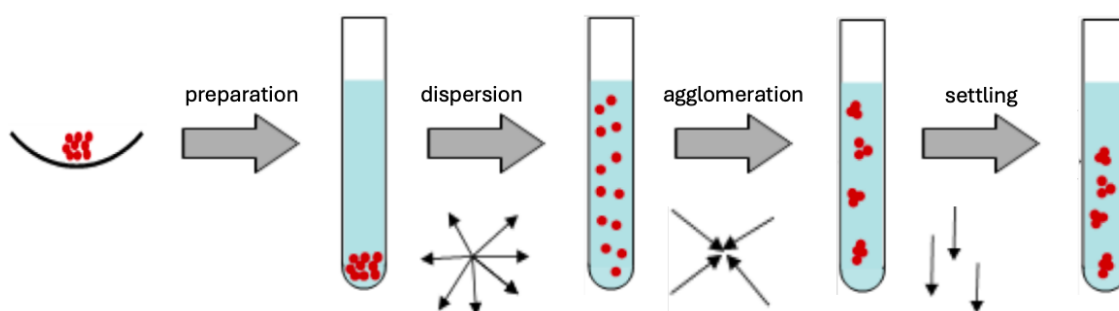


Figure 14: Sample preparation, dispersion, agglomeration and settling of particles (8)

The test can be executed in two steps: at first a screening analysis is done, then, for a more precise definition of the dispersion stability, an extended test is performed (*Figure 15*).

In both cases, the dispersion stability is evaluated through the determination of variation of nanoparticles' concentration in the upper layer of the dispersion. If the concentration does not vary along the test duration the dispersion is considered as stable, while it is unstable if the concentration of particles in the upper layer decreases along the test duration.

In the screening test, the aliquots of supernatant are taken at the beginning (at time $t_0 = 0$ hour) – setting the concentration correspondents to the 100% – and at the end of the experiment (at time t_{end} , usually 6 hours). In between the two withdrawals, the dispersion is left undisturbed to aggregate and settle. The aliquots, which were of 1 ml, were taken 1-1.5 cm below the free surface of the dispersions.

The suspension can be defined with “*high dispersion stability*” if the nanomaterial concentration in the upper layer is correspondent to $\geq 90\%$ of the initial one; while it is defined with “*low dispersion stability*” if the concentration of the nanomaterial is $\leq 10\%$ of the initial one. For concentration values in between the two extremes (so in the range 10-90%), the extended version of the test, which consists in sampling of the aliquots from the top layer each hour, is performed.

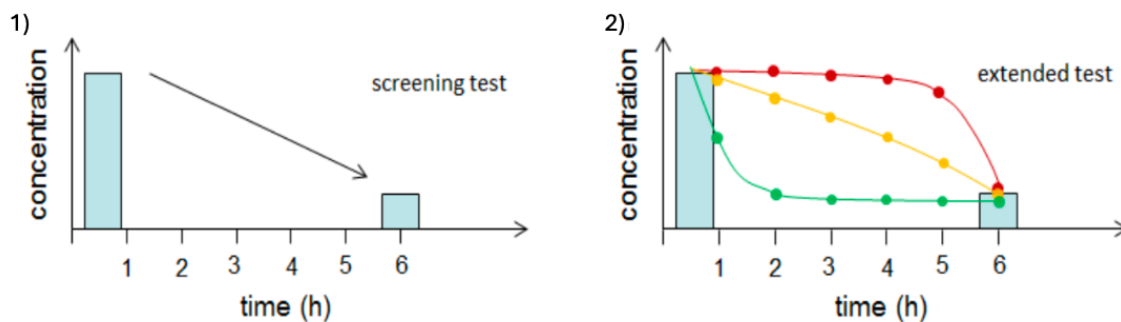


Figure 15: Schematic representation of dispersion stability test - screening test (1) and extended test (2) (8)

Analyzed sampled were prepared using different electrolytes concentrations and in presence or absence of NOM. The concentration of nanomaterial inside the taken aliquots throughout the experiment were measured different methods – including TOC measurements and the Py-GC-MS.

Test medium parameters selection

The test mediums, used to determine the dispersion stability of a suspension, was chosen to represent relevant natural condition. Particularly, the choice of individual parameters and their ranges should be based on the effectiveness of parameter’s influence on dispersion stability,



and on the magnitude of the parameter itself in natural waters. The chosen test media should be representative of a broad range of natural surface waters (10).

The parameters influents on nanocellulose behavior in water include the subsequent:

- Ionic strength, which is the measure of the ions present in the solution. It is dependent on the molar concentration of the i -th ion c_i and its valence z_i , therefore it is directly proportional to the thickness of the Electric Double Layer (EDL).

$$IS = 0.5 \sum_{i=1}^n c_i z_i^2$$

Equation 8: Ionic Strength

As the electrolyte concentration and ion valence increase, the distance from the particle surface at which the potential dissipates decreases. Among the various forces at play, electrostatic interactions significantly influence the stability of the dispersion. For particles with like-charged surfaces, low electrolyte concentrations enhance stability, while higher concentrations lead to agglomeration and sedimentation.

- The pH, which has effect on surface charge. Particles dispersions, which are electrostatically stabilized, are more stable at pH of point of zero charge.
- The Dissolved Organic Carbon (DOC) is the fraction of NOM that is dissolved in water. Generally, the 50-70% portion of NOM is DOC.
- The concentration of particles is a very important parameter since it defines the number of collisions. The optimal range of particles, to determine the dispersion stability of nanoparticles suspension, is found, according to TG (24), to be $0.5 \cdot 10^{12}$ - $5 \cdot 10^{12}$ particles/L.
- Physical and chemical characteristics of the nanomaterial have strong influence on the attractive/repulsive forces that act on the particles; particularly, the presence of certain functional groups on the surfaces, slow down or accelerate the aggregation process. Particles size and density influence the settling velocities and the velocity of Brownian motion, e.g. particles < 100 nm undergo rapid Brownian motion and have small settling velocities. In the same way, also density affects the settling of particles.



Methods to measure the concentration of NC in the taken aliquots

Particles' concentration can be measured with different methods and techniques. A relationship between the number of particles in the samples and the organic carbon concentration could be found.

To facilitate the detection of the organic carbon the highest number of NC particles, allowed by the TG, was put in the samples. In 40 ml sample the maximum number of particles that could be contained was around 2×10^{14} . On average, the carbon content in nanocellulose particles results approximately 44% (in mass) – without taking into consideration the carbon coming from the surface functional groups.

Considering the elementary structure of cellulose as $C_6H_{10}O_5$, molecular weight 162.14g/mol; the carbon weight percentage was calculated as the ratio between the carbon contribution and the total weight of the molecule, *Equation 9*.

$$C (w/w\%) = \frac{\text{mass of carbon atoms}}{\text{molecule total weight}} * 100 = \frac{72.06}{162.14} * 100 \approx 44.4\%$$

Equation 9: Carbon weight percentage of Nanocellulose

The particles were all approximated as spherical elements, the density of CNC particles was assumed as 1.6 g/cm^3 , while the one of CNF particles as 1.5 g/cm^3 (25).

In *Table 9*, the volumes, the masses of particles and the expected carbon concentration are reported for the samples which were selected for the dispersion stability test.



Table 9: Particles number and Carbon concentration of NC samples

Sample name	Particles in vial volume (40 ml) (Particles number)	Volume of particle (nm ³)	Mass of particle (g/particle)	Conc. of Nanocellulose (mg/L)	Conc. of Carbon (mg/L)
CNC 1	1.967×10 ¹¹	448920.5	7.18×10 ⁻¹³	3.532	1.554
CNC 2	1.960×10 ¹¹	796328.3	1.27×10 ⁻¹²	6.243	2.747
CNC 3	1.994×10 ¹¹	1022653.9	1.64×10 ⁻¹²	8.158	3.590
CNC 4	1.976×10 ¹¹	1767145.9	2.83×10 ⁻¹²	13.968	6.146
CNF 7	1.992×10 ¹¹	904778.7	1.36×10 ⁻¹²	10.771	2.973

The measurement of the nanoparticles' concentration inside the taken aliquots were carried out using different instruments and methods: the TOC (Total Organic Carbon) measurement and the PY-GCMS (Pyrolysis – Gas Chromatography – Mass Spectrometry).

TOC measurements

The TOC (Total Organic Carbon) measurement processes are analytical methods to quantify the amount of Carbon presents in a certain sample. The TOC can be assessed as the difference between the Total Carbon (TC) and the Total Inorganic Carbon (TIC), *Equation 10*.

$$TOC = TC - TIC$$

Equation 10: TOC definition

The TC represents the total amount of carbon inside the sample, both organic and inorganic forms, while the TIC represent the portion of inorganic carbon.

The carbon coming the NC particles can be distinguished from the one of the test mediums, since the first one is detected ad Organic Carbon, while the second one coming from the NaHCO₃ is detected as Inorganic carbon. Different situation was faced in presence of NOM, in this case the portion of Carbon coming from the NC could not be distinguished from the portion coming from the Natural Organic Matter, since both are detected as OC.

Two TOC measurements techniques were used to determine NC concentration in the samples. The first technique allows the TOC measurement of solid samples, so evaporation of the dispersions was necessary. The second one measures the carbon content of liquid samples, so nanocellulose solutions were directly injected in the instrument.

The instrument used to measure TOC in solid samples, was the TOC analyzer Primacs ATC100-IC-E produced by Skalar (*Figure 16*).



Figure 16: TOC analyzer Primacs ATC100-IC-E Skalar (source: <https://www.skalar.com/products/primacs-total-organic-carbon-total-nitrogen-analyzers>)

The analyzer, equipped with a 100 positions autosampler, takes each solid sample that goes through the combustion reactor. Inside the reactor, gasification process takes place at 1100°C; afterward, the produced gases go through scrubbers, which dry and cool down the effluents. The produced Carbon Dioxide is then measured. The differentiation between Organic Carbon (OC) and Inorganic Carbon (IC) is achieved placing the samples at different heights in the combustion reactor, so differentiation is temperature dependent (26).

To check whether this technology was suitable to measure NC concentration, as required by the set up experiment, three test mediums with NaHCO₃ and different electrolytes concentrations (0 mM Ca(NO₃)₂ and Mg(SO₄) (4:1 molar ratio); 1 mM Ca(NO₃)₂ and Mg(SO₄) (4:1 molar ratio); 10 mM Ca(NO₃)₂ and Mg(SO₄) (4:1 molar ratio)) were tested with this method. The purpose was to measure the amount of inorganic carbon (IC) present in the



background. Since this method necessitates solid samples, evaporation of the liquid dispersion was required.

At first, three steps evaporations of the test mediums were performed, adding each time 3.33 ml of dispersion, after 4 hours of exposition of the previous aliquots to 105°C.

The removal of inorganic carbon was carried out adding 1 ml of 2 M HCl solution to the dried sample, and left to dry overnight at 80°C. After this procedure, no carbon, both organic and inorganic, was expected to be found in the test mediums.

Then the samples were added in the autosampler, and the TOC measurement was performed. The calibration curve, *Figure 17*, was built using Glycine 0.5% as standard.

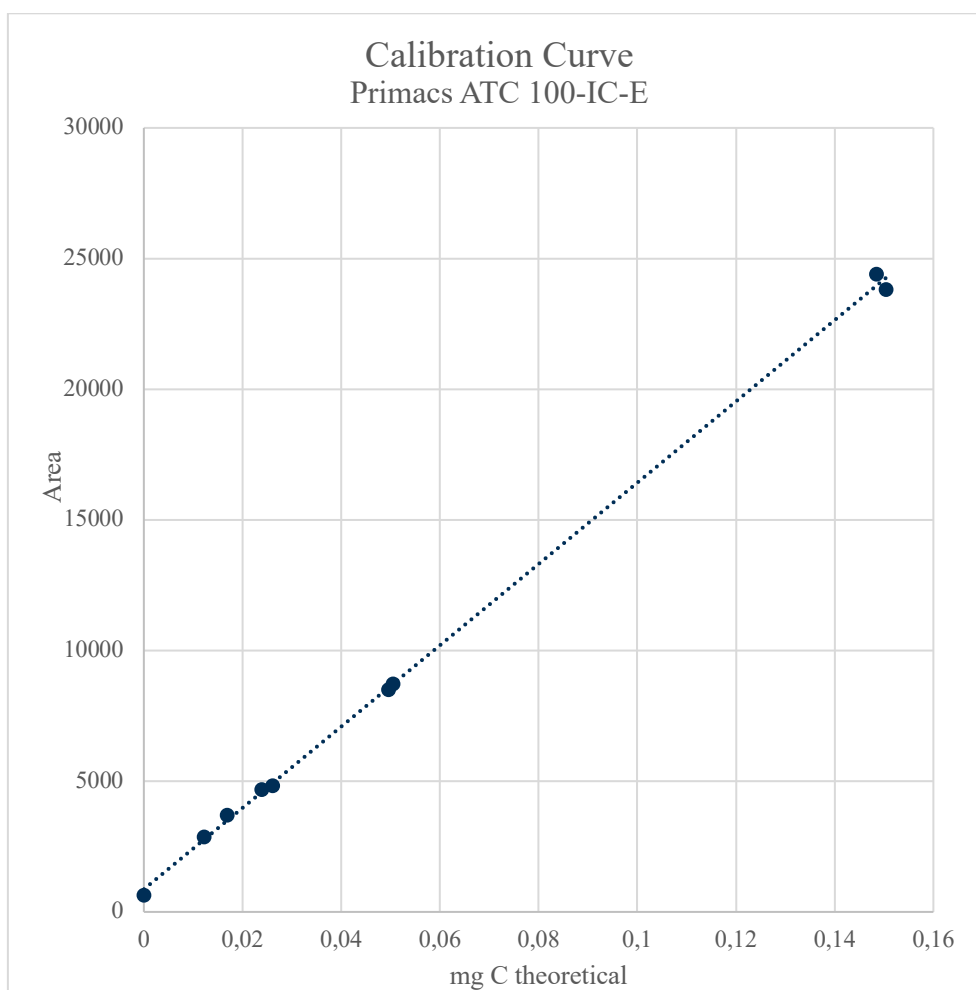


Figure 17: Calibration Curve for TOC measurement, built using Glycine 0.5%

The linear regression analysis of plotted data is performed. The goodness of the calibration is verified analyzing the correlation coefficient (R^2). Values close to 1 are index of a good fitting, so of a good calibration.

Table 10: Calibration curve - equation and correlation coefficient

Calibration curve	
Equation	$y = 155549x + 868.43$
R^2	0.9991

The R^2 , resulting from the calibration curve, reported in Table 10, is index of a good calibration. Therefore, TOC measurements obtained with this calibration curve – whose equation is reported in Table 10 – were considered reliable.

The calibration curve, used to assess the quality and the reliability of the test measurement, is applied to the samples to determine the carbon concentration.

The other method, used to determine the carbon content, is the TOC measurement of liquid samples. In this case the evaporation of the samples is not required since the instrument can measure the carbon content of liquid solutions.

The instrument used is the multi N/C3100 produced by Analytik Jena, Figure 18. With this technology is possible to measure many parameters such as TOC, TC, TIC and NPOC (Non Purgeable Organic Carbon).



Figure 18: Multi N/C3100 produced by Analytik Jena (27)

The general working principle of the instrument, reported in Figure 19, is briefly outlined. At first, the sample is inserted in the instrument using a needle. The suspension goes through a combustion furnace, where the present organic carbon is oxidized to CO₂ through combustion – an oxidizer such as UV radiation is used. The carbon content can be determined measuring the carbon dioxide presents in the effluent, or after its reduction to methane. Different sensor can be used for this purpose.

Prior TOC measurement, the IC is removed from the sample via acidification. Alternatively, the TOC can be defined as the difference between TC (Total Carbon) and the TIC; this is possible for samples which have expected TIC concentration lower than TOC one.

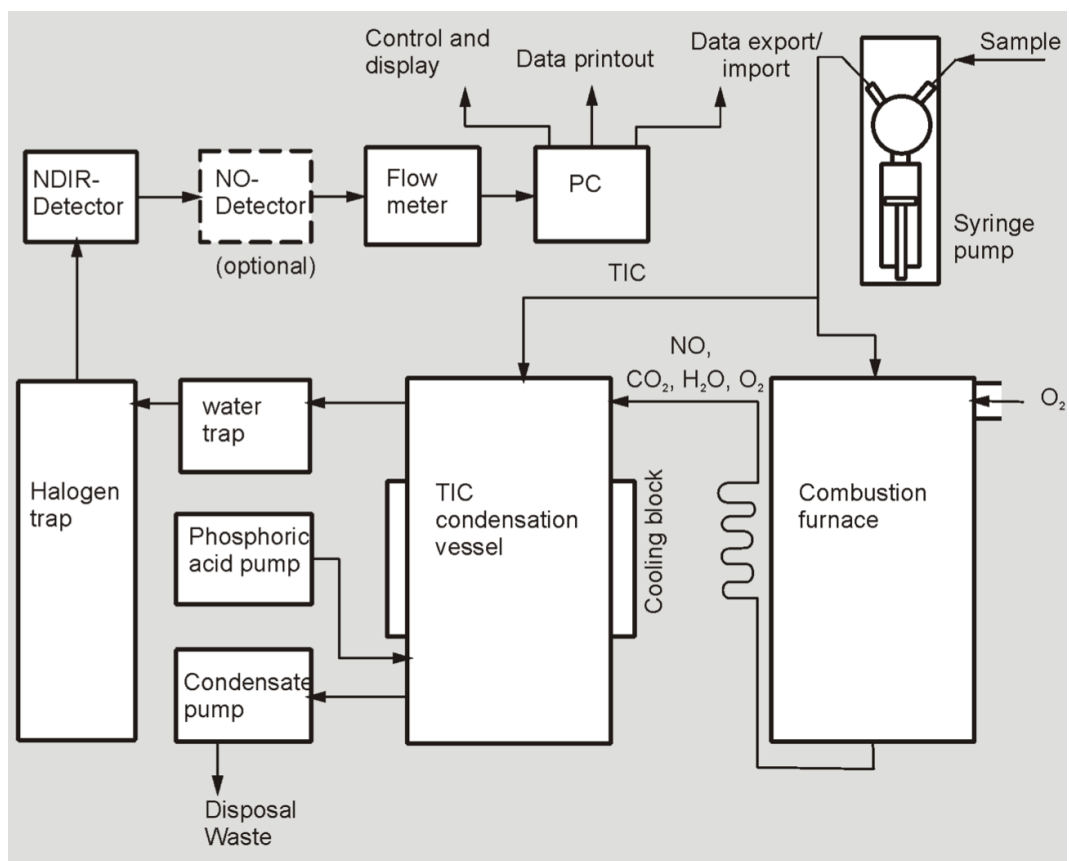


Figure 19: Working principle of the analyzer Analytik Jena, multi N/C3100 (27)



The sensor used to detect the CO₂, and so the TOC, is NIDR (Non-dispersive Infrared Absorption Detector) sensor. The gasses molecules, which are produced by combustion and oxidation, have distinct absorption bands in the infra-red spectrum. When the IR beam, emitted by the NIDR, goes through these molecules, they absorb radiation according to their molecular composition. The NIDR, which is equipped with a radiation detector, sensible to Carbon Dioxide emitted radiations, therefore it can measure the concentration of this gas in the effluent (27).

To determine nanocellulose concentration in the samples, NPOC was measured. The sample was acidified injecting HCl (2 N) in the instrument, and the released carbon dioxide measured. The remaining carbon was measured via combustion.

Calibration was performed, according to the guidelines described in NBN EN 1484 and ISO 8245, with multiple TOC concentrations and constant sample volume, *Figure 20*. The concentrations range was chosen according to the expected carbon concentration in the sample.

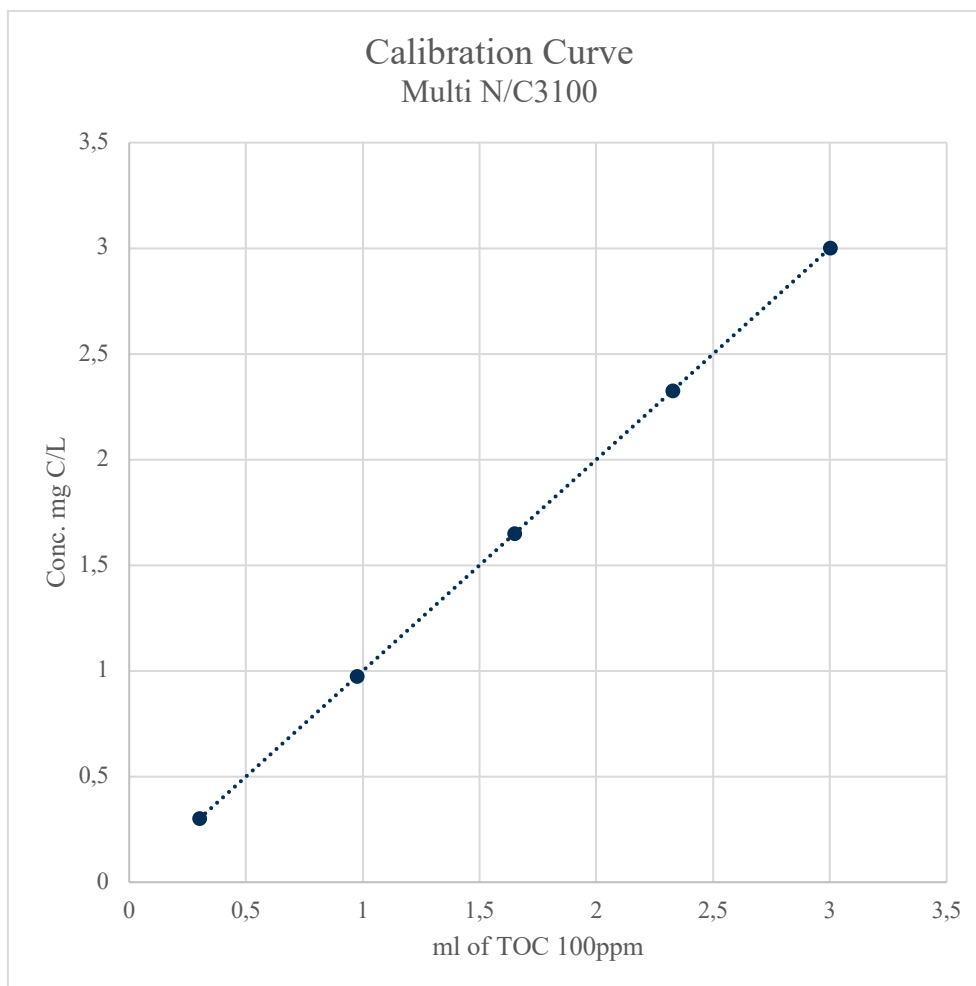


Figure 20: Calibration curve (Constant sample volume and varying TOC concentration) for Analytik Jena, multi N/C3100

To check the suitability of this method to determine the dispersion stability of the nanocellulose, many tests were performed.

In this case, to better mimic the experimental set up, 1 ml of prepared dispersion was taken and diluted to 10 ml with MQ. The final volume was injected in the instrument and the NPOC measured.

Firstly, CNC 2 dispersion in test medium with pH 7 and electrolytes ($\text{Ca}(\text{NO}_3)_2 + \text{Mg}(\text{SO}_4)$) concentration 1 mM (TM 2) was prepared. This preparation followed the guidelines of the OECD test n°318, which are reported in the *Paragraph 2.4.3*. As blank and reference, also MQ and the pure test medium (TM 2 without nanocellulose) were analyzed.

Following the results of the first tests, others TOC measurements of liquid samples were performed, with the aim of finding correlation between IC and OC content.

In the same test medium, the concentration of CNC 2 was increased, in order to get expected carbon concentration from 0.5 to 1.5 mg/L.

Pyrolysis – Gas Chromatography – Mass Spectrometry (Py-GC-MS)

The Pyrolysis – Gas Chromatography – Mass Spectrometry is an analytic technique that can be used for molecular characterization of polymeric samples.

The molecules are broken into volatile fragments in high temperature with pyrolizer and then separated with the Gas Chromatography, finally compounds are analyzed by Mass Spectrometry.

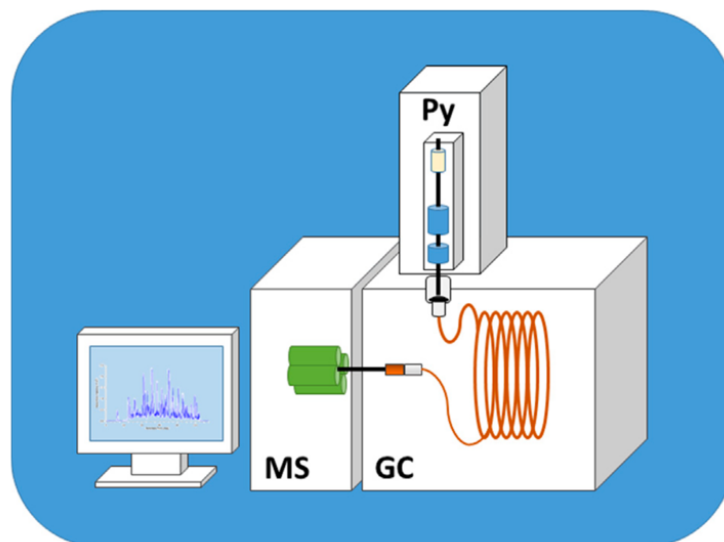


Figure 21: Py-GC-MS scheme (28)

Entering the chamber, the sample is heated in the pyrolizer (Py) with an inert gas, generally helium. Molecular bonds, from the weakest to the strongest are broken due to temperature increase. In this process different reactions take places, such as depolymerization, random excision and remotion of radical groups.

Many working modes of Py-GC-MS were defined to analyze different compounds. In pyrolizer, single shot and double shot working modes can be chosen depending on the samples. In GC, different split ratio, ramping temperature can be selected. And in MS, different scanning ranges, and ion selecting modes can be decided based on various analytical purpose. These



modalities vary according to the temperature ramping – temperature increase per minute – and duration.

In order to avoid samples' contamination with particles existing in air, filtrations were performed in the laminar flow cabinet which is a clean air and particle-free environment. Aliquots, taken from the same samples subjected to liquid TOC measurement, were at first diluted to 10 ml using MQ. Filtration of the samples, on glass fiber filters with pore size of 2.2 μm (Whatman QMA, diameter 25mm), was subsequently performed. The filters, which were expected to retain nanoparticles, were then folded and put in stainless steel pyrolysis cups.

As standard, 15 μL of polymethyl methacrylate (PMMA) 50 ppm were tested before and after the samples; also, as blank a clean filter was analyzed.

Afterward, the cups, filled with the used filters, were put in a 104°C oven for 20 minutes.

Thereafter, the injectors of the autosampler were cleaned and the cups put, leaving an empty space between each other.

The following setting were imposed to analyze NC samples, *Table 11*.

Table 11: Py-GC-MS setting

Pyrolizer	EGA/PY-3030 D
Carrier gas	Helium
Oven temperature	590°C
Interface temperature	300°C
Pyrolysis time	18 s
Gas chromatogram	Agilent 7890B
Split ratio	100:1
Temperature Column Flow	320°C
30 m	30mx250pm x 0.25 pm
Flow	1 mL/min
Mass spectrometer	Agilent 5977B
Mode	Full scan
Scan rate	2.9 scan/s
Scan range	40-550 amu



The results of these measurements are reported in Total Ion Chromatograms (TIC) which represent the total abundance of ions in the same scan over time. In the X-axis the retention time is represented while in the Y-axis the signal strength, so the ion abundance is shown. The peaks in the chromatograms represent polymers or groups of compounds. The baseline, when low and stable, is sign of a non-contaminated samples and absence of issues in the instrument's column. The baseline and the background are removed from the sample signal comparing it with the sample of a blank. The used blank was pure MQ water, while the background was checked testing a clean filter.

The retention time is characteristic of each ion or polymer, thanks to the correspondence of peaks to a certain retention time it is possible to define the polymers and compounds that characterize the analyzed sample (29).

To understand which were the influences on the results given by the filter and the MQ, a clean glass fiber filter (pores 2.2 μm) and 5 ml of pure MQ samples were tested with Py-GC-MS.

2.3.4. Attachment efficiency determination

Another parameter that can be used to assess the behavior of nanoparticles in different test mediums, such as the natural waters is the collision or attachment efficiency (α_a), which describes how efficiently the particles adhere to each other or to a different surface. This parameter can be expressed as the ratio between the successful attachments and the total number of collisions, *Equation 11*.

$$\alpha_a = \frac{\text{rate of successful attachments}}{\text{rate of collisions}}$$

Equation 11: Definition of the attachment efficiency

The collision efficiency is dependent on nanoparticles' surface chemistry and physical proprieties, chemistry of the solution and generally on the environmental proprieties of the medium in which the particles are dispersed.

This parameter can be experimentally determined monitoring the aggregation rate of the particles, so the growth of particles over time, *Figure 22*. The method that was used to measure the size of the aggregated particles is the Dynamic Light Scattering (DLS).

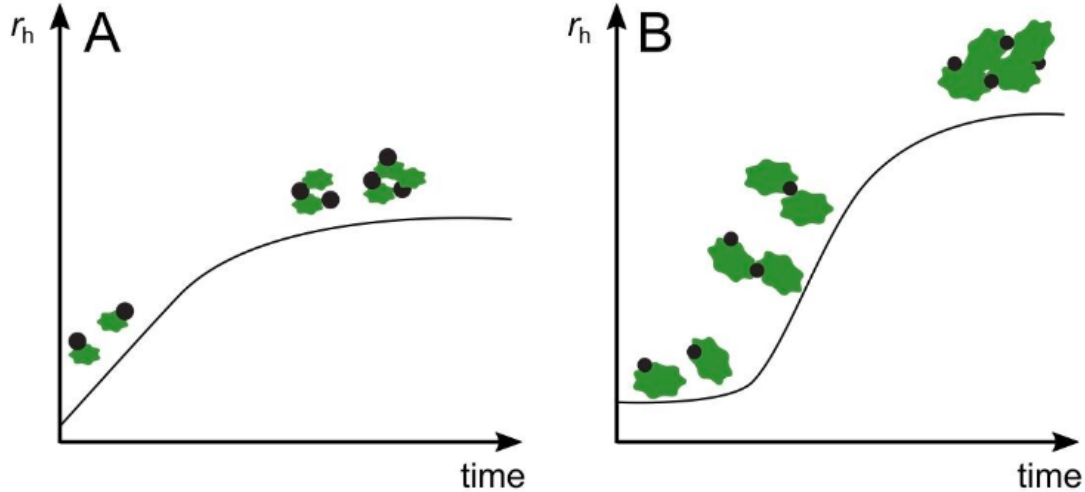


Figure 22: Growing Hydrodynamic diameter of particles over time due to collisions and particles' attachment (30)

The attachment efficiency can be defined from the slope of the change of the hydrodynamic diameters throughout the experimental timespan. α_a is also known as the inverse of the stability ratio W , Equation 12 (31) (32).

$$W = \frac{1}{\alpha_a}$$

Equation 12: Stability ratio

The attachment efficiency was determined as the ratio between the hydrodynamic radius variation in normal conditions and in “fast” aggregation conditions, as shown in Equation 13 (32).

$$\alpha_a = \frac{\frac{1}{N_0} \left(\frac{da_h(t)}{dt} \right)_{t \rightarrow 0}}{\frac{1}{N_{0, fav}} \left(\frac{da_h(t)}{dt} \right)_{t \rightarrow 0, fav}}$$

Equation 13: Attachment efficiency

Where N_0 is initial particle number concentration and a_h is the hydrodynamic radius. The α_a with this method can be obtained also for particles that have shape different from spherical.



The aggregation of particles is defined as “*fast*” when the concentration of salts in the solution is above the Critical Coagulation Concentration (CCC), in these conditions, which can be defined as favorable, the particles aggregate almost immediately (31) (33). The concentration interval in which the particles aggregation switch from “*slow*” to “*fast*” is narrow. With this electrolyte concentration it is possible to determine the fast aggregation rate, as the variation of the hydrodynamic diameter over the particles number.

The attachment efficiency, which represent the probability of efficient and irreversible collisions, ranges from 0 to 1 (33).

In practice, the experiment was carried out over six hours, the aliquots (1 ml) were taken each hour and immediately analyzed with the DLS instrument, set up in size mode.

Before the first sample is taken, the dispersions were sonicated for 10 minutes, into a sonicator bath. After the first measurements, the solutions containing particles were not moved anymore, in order to not interfere with the collision and so with the results of the experiment.

To determine the fast aggregation the three measurements performed by the instrument, at the initial time (t_0), in one single run were analyzed, outliers were taken out from the analysis. To obtain more trustable results, all the samples were tested in duplicates.

2.4. Nanocellulose suspensions preparation

The nanocellulose samples are described in the *Paragraph 2.1*. Different preparations were necessary to perform the characterization of the particles size using the DLS and NTA, since distinct concentrations and diluents were required by the two methods.

Whereas, regarding the dispersion test, nanocellulose dispersions were prepared according to the number of particles required by the OECD test n°318.

2.4.1. Samples preparation for DLS

In order to obtain good results with the DLS method, the concentration of particles in the solution must be chosen carefully. Too high concentration of particles would lead to multiple scattering, interparticle interaction and optical density. All these phenomena would give unreliable and incorrect measurements. Contrary, too low particles concentration would lead

to insufficient scattered intensity, noise dominance and low accuracy for ZP determination – not measurable electrophoresis mobility.

Pure NC samples had to be diluted to obtain reliable size and Zeta potential analyses.

To obtain the best possible results were used different diluents and stabilizers, which are described in the *Paragraph 2.2.1*.

Many dilutions of the samples were performed to find the nanocellulose concentration that could give the best results. To do so preliminary DLS tests were performed using non-filtered diluents.

At first, samples with concentration from 4 to 10 ppm were tested; but the number of particles was not high enough to be detected by the instrument. Consequently, samples with increasing concentrations (50,100,150 ppm) were tested. Finally, the optimal concentration of particles to test the samples was found to be 150 ppm, results of this first testing phase are reported in *Appendix: Table 2*.

Once, the best concentration was found, the diluent solutions were filtered with a 0.1 μm PVDF membrane. The purpose of the filtration was to remove all the particles that could be dispersed inside the solvents, and which could have interfered with the results of the test.

As blank test, the filtered solvents were tested with DLS to ensure the absence of interfering particles; as expected, no particles were detected in these solutions. As shown in *Appendix: Table 3*.

2.4.2. Samples preparation for NTA

The samples, after being characterized with the DLS, were analyzed with NTA, for each of them the diameter and the concentration (particles/L) were measured.

To perform the Nanoparticle Tracking Analysis, and obtain the best possible result, different sample concentrations were tested. The particle concentration necessary to perform good NTA was lower than the one necessary for DLS.

Indeed, with this method, a too concentrated sample would give an image that is not enough clear and suitable for a precise analysis and size determination; moreover, in too concentrated samples the particles would not move freely, with Brownian motion, inside the cell.

At first nanocellulose samples with 150 ppm concentration, were diluted 100 times (to 1.5 ppm) and injected in the cell, but the number of detected particles resulted too high for the analysis. Further dilution to 0.75 ppm – corresponding to 200 times dilution from starting sample – was actuated. With this concentration the NTA software was able to give a correct number of detected particles and a clear image of the suspension, which resulted more suitable for the measurements.

2.4.3. Samples selection and preparation for the dispersion test

The dispersion test was set up to determine the stability of nanocellulose in environmental water. According to the resulting of the characterization phase, it was not possible to test all the nanomaterials. Sample preparation occurred following the guidelines of the OECD test n°318 (24).

Samples selection

From the tested material set of five samples was selected. The assortment was based on the availability of information provided by suppliers and results of samples characterization. Other parameters, used for the selection of the samples, were the surface functional group and the aspect ratio. Samples that showed different characteristics were chosen, in doing so a broader range of behaviors could be analyzed.

From the provided set, the CNC samples 5 and 6 were taken out due to the lack of provided information and the impossibility of obtaining reliable size measurements with the DLS method.

The samples that resulted suitable for the determination of the dispersion stability were the CNC samples 1,2,3,4 and the CNF sample 7.

The selected samples presented different nanocellulose types, aspect ratio and surface functional groups.

Samples preparation

To assess the dispersion stability of nanocellulose materials, samples solutions were prepared in a 50 ml vials. OECD test guidelines (TG) were followed to guarantee the repeatability of the experiment.

The test mediums, which were used for the experiment were representative of different natural water conditions; electrolytes concentration and pH vary in different samples.

Stock solution of NaHCO_3 , $\text{Ca}(\text{NO}_3)_2$ and MgSO_4 were prepared, the chemicals used for these preparations are reported in the *Paragraph 2.2.3*.

The stock solutions are detailed below.

Nanoparticles stock dispersion

According to the OECD TG (24), the particle concentration in the final volume, which was 40 ml, has to be in the range $0.5 \times 10^{12} - 5 \times 10^{12}$ particles/ml.

The nanocellulose stock dispersions were prepared diluting the original samples, with MQ, to a concentration of 20 ppm. The particle concentration of the original sample was obtained with the Nanoparticles tracking Analysis. The volumes of nanoparticle stock dispersion that were taken to obtain the optimal particles concentration are reported in *Appendix: Table 4*.

The taken nanocellulose dispersion was put in the vials and MQ was added to reach 20 ml volume.

NOM and NaHCO_3 stock solution

Since the aim of the experiment was to assess the behavior of nanocellulose in test mediums that could mimic different environmental waters, sources of organic and inorganic carbon were used.

The Suwannee River NOM (2R101N) stock solution was prepared in accordance with OECD TG, the concentration of Dissolved Organic Carbon to be added to the vials had to be 10 g/L DOC. Given the well-defined characteristics of 2R101N, a stock solution with a concentration of 0.5 g NOM/L was prepared using MQ.

The volume of this NOM stock solution that was added to each vial, to reach the required DOC concentration in the final volume, was 0.95 ml.

The Sodium Bicarbonate (NaHCO_3) 0.1 M stock solution was prepared with MQ. The volume of this dispersion to be added to each vial was 2 ml, in order to obtain a concentration of 5 mM in the final volume.

$\text{Ca}(\text{NO}_3)_2$ and MgSO_4 stock solution

To adjust the ionic strength of the solutions and evaluate different aqueous conditions, a solution of Calcium Nitrate and Magnesium Sulfate with a 4:1 molar ratio was added.

The above-mentioned solution was chosen according to Monikh, et al., 2018 (34) and it is representative of the European stream waters.

The two stock solutions, with 80 mM concentration, were prepared.

Three distinct conditions were analyzed, adding different volumes of salts solutions to the samples, obtaining concentrations of 0 mM $\text{Ca}(\text{NO}_3)_2$ and $\text{Mg}(\text{SO}_4)$ (4:1 molar ratio) or 1 mM $\text{Ca}(\text{NO}_3)_2$ and $\text{Mg}(\text{SO}_4)$ (4:1 molar ratio) or 10 mM $\text{Ca}(\text{NO}_3)_2$ and $\text{Mg}(\text{SO}_4)$ (4:1 molar ratio).

According to the concentration of electrolytes, three test mediums could be defined.

Table 12: $\text{Ca}(\text{NO}_3)_2$ and $\text{Mg}(\text{SO}_4)$ for ionic strength adjustments

Test medium	Volume of 80 mM stock solution to be taken				Concentration in the final volume (40 ml)
	$\text{Ca}(\text{NO}_3)_2$		$\text{Mg}(\text{SO}_4)$		$\text{Ca}(\text{NO}_3)_2 + \text{Mg}(\text{SO}_4)$ (4:1 molar ratio)
-	(ml)	(μl)	(ml)	(μl)	(mM)
TM 1	0	0	0	0	0
TM 2	0.4	400	0.1	100	1
TM 3	4	4000	1	1000	10

Afterward, MQ was added to reach 35 ml volume inside the vial.

NaOH and HNO_3 stock solution

The pH adjustment of dispersions was performed using stock solution of NaOH and HNO_3 , which respectively are a strong base and acid.

HNO_3 , with 66-69% purity was diluted 5 times, reaching approximately a 3M concentration, while a NaOH 0.1 M solution was prepared.

Once the desired pH was reached, MQ was added to accomplish the final volume of 40 ml.



2.4.4. Samples preparation to determine the attachment efficiency

The behavior of nanocellulose particle in environmental waters was assessed with the determination of the attachment efficiency. This parameter could be used in the implementation of the Full Multi (9), which is a model able to predict the transport of the nanoparticles in natural streams.

To determine the attachment efficiency the samples were prepared with similar methodology to the one used for the dispersion test.

The attachment efficiency of the particles was determined measuring the variation of their hydrodynamic diameter over time, to do that the DLS method was chosen. To secure reliable measurements with this technique, it was necessary to increase the NC concentration inside the samples, to an optimal value of 150 ppm – as was stated for NC characterization.

Also in this case, the samples suitable for the analysis were the CNC samples 1,2,3,4 and the CNF sample 7.

Samples were prepared with the three different test mediums (TM 1, TM 2 and TM 3) with a pH 7 in presence and absence of NOM; totally thirty samples were tested.

In *Appendix: Table 6- Appendix: Table 7*, the compositions of samples are reported.

2.5. The Full Multi

To determine the behaviors of NC particles in generic rivers the Full Multi open-source framework was used.

The Full multi has been developed to model the transport of nanoparticles in environmental waters (9). This model, based on a generic modular unit cell, can predict the transport of nanoparticles between the different compartments of a generic water body; in addition, it can predict particles interactions, such as homo- and hetero- aggregation and biofouling.

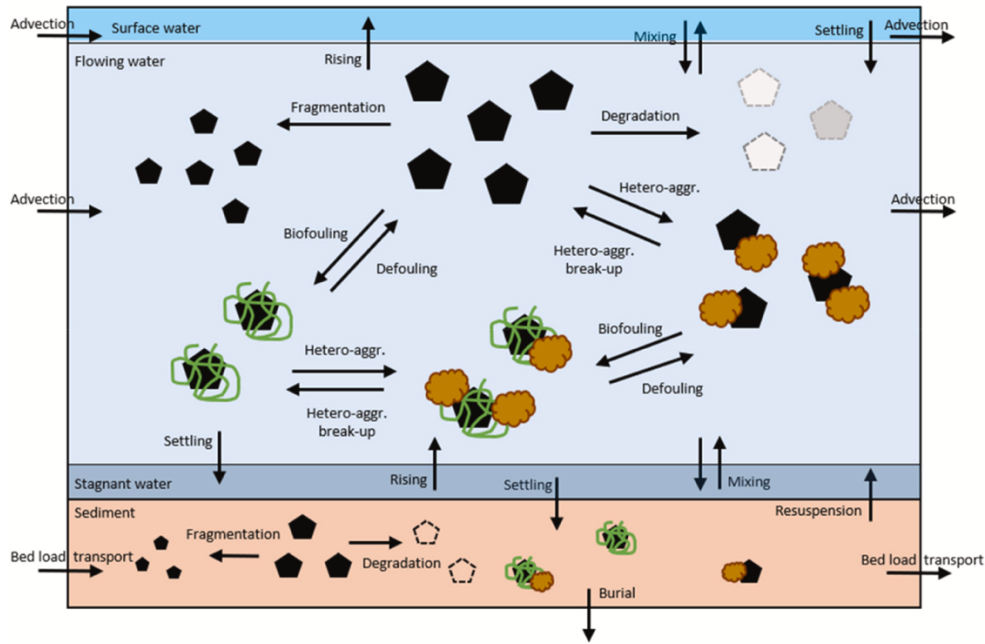


Figure 23: Schematic representation of the Full Multi model unit cell (9)

The Full multi is a multimedia mass-balance model, whose each unit is a well-mixed environmental compartments, the fate of the particles is governed by first-order kinetics. Other relevant processes are also modelled such as the biofouling and the fragmentation. Using the standard parametrization, for each compartment, twenty mass balance equations are developed considering five size classes and four speciation states. The speciation states which are implemented in the model are pristine, heteroaggregated, biofouled, and biofouled and heteroaggregated (9).

The unit cells, which are connected by a unidirectional flow, can be divided horizontally in four different compartments. From the top to the bottom: the surface water, the flowing water, the stagnant water and the sediment, as shown in Figure 24.

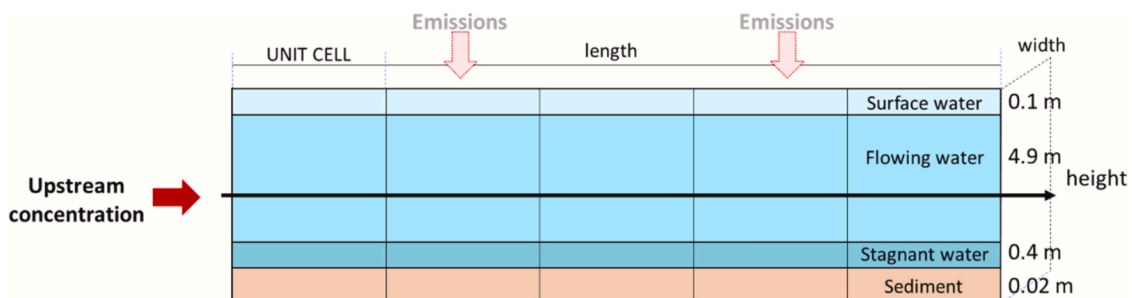




Figure 24: Schematic representation of the unit cells and their horizontal layering with default heights (9)

As default, the heights of the compartments are, from top to bottom, 0.1 m, 4.9 m, 0.4 m and 0.02 m respectively; overall, the elementary units are 5.42 meters high (8).

The transport processes, which are of greatest interest in this study, are the advective transport of nanoparticles, vertical mixing of the bulk water, the horizontal transport in the sediment bed, burial into deep sediments and resuspension (9). These processes are modelled through a first-order kinetic constant which relies on the depth of the compartment and particles' velocity. Stokes-Einstein equation is used to calculate the velocity of the particles, assuming them all as spheres.

For the purpose of this study, only homoaggregation was considered and some default parameters were chosen – all the river compartment and aggregation states were selected, also the degradation half-life, the timescale for fragmentation and the time for the biofilm coverage were left as default.

The sizes and the attachment efficiencies determined in the previous experimental phases were used as input of the Full Multi model, with the aim of modelling the transport and the fate of this kind of particles in environmental water bodies.

The particles characteristics that were inserted as input are the size of the NC particles, including their length and width, the density and the attachment efficiency. Even though the model was developed for spherical particles, it could be used also for fibers.

2.5.1. Framework and configuration and parametrization

The unit cells of the generic river, configured by Prado et al. (9), are connected by a uni-directional flow in surface and stagnant water, while bedload transport was imposed for sediments. The parametrized river, composed by 20 identical unit cells, was 1000 km long; vertical layering was the same reported in *Figure 24*. The flow velocity, in the top layers, was set to 1.3 m/s. The river's parametrization was based on the modelling of Rhine River, by Praetorius et al. (35).

Particles' size classes were selected according to the characterization. In *Appendix: Table 8*, the particles' size, density and other parameter necessary for the modelling are reported.



3. Results

3.1. Cellulose characterization

The DLS and NTA results can be reported subdividing the samples in four groups, according to their CNC/CNF content and their behaviors.

3.1.1. DLS results

Prior the measurements, the instrument was checked with two standards, which aimed to define its reliability and the goodness of the measurements.

Regarding the size measurements, 92 nm PS beads with a concentration of 5 ppm and a blank were tested. As expected, due to the absence of particles, the MQ, i.e. the blank, gave no results in particle size determination.

The standard solution, which was tested each time before the NC size measurement, was PS with 92 nm beads with a 5 ppm concentration, gave the following results.

Table 13: Size measurement for 92 nm PS standard.

Sample Name	Size measurement		
	Z-Ave (d. nm)	PdI	Attenuator
92 nm PS 5 ppm	99.53	0.023	7

In *Table 13* is reported the Z-average (nm) for the 92 nm PS standard – defined on 21 tests, therefore 63 total measurements, with a standard deviation of 1.61. It is possible to define the percentage error that affects the DLS measurements in size mode, as shown in the *Equation 14*.

$$\text{Percentage Error [\%]} = \frac{|\text{Measured Value} - \text{True Value}|}{|\text{True Value}|} * 100$$

Equation 14: Percentage error definition

The resulting percentage error, which affect size measurement, is 8.19%.

The Zeta Potential Transfer Standard -40 ± 4.8 mV was also tested. In *Table 14*, the achieved ZP and standard deviation values are reported.



Table 14: Zeta measurement of Zeta Potential Transfer Standard -40 ± 4.8 mV.

Name	Zeta measurement		
	ZP (mV)	Std deviation	pH
Std - 40 mV \pm 5.8 mV	-38.17	6.76	7-8

The percentage error, which affected the ZP measurements, could be defined as for the Polystyrene standard (*Equation 14*).

The zeta potential measurements were affected by a percentage error of 4.58%.

According to the results of the tests of the standards, it was possible to ascertain the reliability and trustability of the instrument.

Samples 1,2 – CNC 3.98 %

The CNC samples 1 and 2 gave good results starting from lower nanocellulose concentration (50-100 ppm), but to have a more precise comparison with the other samples, they were tested also at 150 ppm concentration. The DLS measurements – size and ZP – for all the three solutions are reported in the following table. It can be noticed that the standard deviation for the sample 2, when diluted with filtered SDS, had a high value. It means that the Zeta Potential Distribution (*Appendix: Figure 1*) and the ZP values given for this dispersion, are not completely reliable, for this reason the Z-average (d. nm) of the solution diluted with SDS was not taken into consideration in the final size determination. Given that, it was possible to define that the CNC sample 1 and 2 present characteristic size dimensions of $152 \text{ nm} \pm 12.5 \text{ nm}$ and $118 \text{ nm} \pm 9.7 \text{ nm}$; both results could be considered reliable.

Samples 3,4 – CNC 1.00 %

The CNC samples 3 and 4 gave reliable results, with low PdI and high stability, when diluted with filtered MQ and NovaChem; while the results obtained with SDS as solvent could not be trusted, since the PdI was 1 and the solution resulted unstable.

The results for all the diluents are reported in *Table 15*.

Table 15, in red are highlighted values of PdI > 0.7 and in yellow are highlighted ZP values in the instability range ($- 30 \text{ mV} : + 30 \text{ mV}$).

Taking this into account, the size determination of the samples 3 and 4, could be performed by taking into consideration the values of Z-average obtained with filtered MQ and filtered NovaChem, removing from the study the values obtained with the filtered SDS solution, which were not trustable. The size dimension of the CNC sample 3 is $125 \text{ nm} \pm 10.2 \text{ nm}$, while the one of the CNC sample 4 is $150 \text{ nm} \pm 12.3 \text{ nm}$.

Samples 5,6 – CNC 1.99 %

Unlike other tested samples, CNF samples 5 and 6, were found to be not stable when diluted with the three solvents.

Table 15 shows the results for these samples diluted with filtered MQ, filtered SDS, filtered NovaChem, MQ and NovaChem – values of $\text{PdI} > 0.7$ are highlighted in red and in values in the instability range ($-30 \text{ mV} : +30 \text{ mV}$) are highlighted in yellow ZP. Even though the sample 5 showed low PdI and attenuator values when diluted with NovaChem, the size dimension could not be considered trustable because of high uncertainty in sample's stability determination, indeed the Standard Deviation of the Zeta potential resulted very high, as shown in *Appendix: Figure 2*.

It is worth to notice that the samples 5 and 6 were made of CNF particles, so the shape of the analyzed nanoparticles could not be assumed as spherical, instead these are therefore elongated and amorphous fibers. In addition, those materials were obtained with a mechanical and non-chemical pre-treatment which is the fibrillation; this difference in the preparation phase led to less stable dispersions.

As consequence of these considerations, it was not possible to obtain reliable dimension measurements for the CNF samples 5 and 6 using the DLS method.

Sample 7 – CNC 2.09 %

The sample 7, even being made of amorphous CNF particles, appeared stable when diluted with MQ, SDS and NovaChem therefore size measurement was reliable. Differently from the CNF sample 5 and 6, to this one also chemical modification are applied as pre-treatment. Pre-treatment such as high-pressure surface modification were executed on this sample.

In the following table are reported all the results for the sample 7 (*Table 15*).



The resulting characteristic dimension of the CNF sample 7, obtained as the mean of the Z-averages obtained diluting the CNF with the three diluents, was $107 \text{ nm} \pm 8.8 \text{ nm}$.

Table 15: Size and Zeta measurement for NC samples 1 diluted with filtered MQ, filtered SDS and filtered NovaChem.

Name	Sample		Diluent	Size measurement			Zeta measurement		
	%wt	Conc. (ppm)		Z-Ave (d. nm)	PdI	Attenuator	ZP (mV)	Std deviation	pH
1 CNC	3.98%	150	Filt. MQ	150.4	0.272	7	-45.1	6.1	5/6
			Filt. SDS	155.6	0.278	7	-40.4	20.3	5/6
			Filt. Novachem	150.6	0.288	7	-42.7	25.3	6
2 CNC	3.98%	150	Filt. MQ	121.9	0.137	7	-49.8	13.5	5/6
			Filt. SDS	116.5	0.137	7	-49.4	40.7	5/6
			Filt. Novachem	114.1	0.154	7	-46.5	24.2	6
3 CNC	1.00%	150	Filt. MQ	109.9	0.222	8	44.6	150.3	5/6
			Filt. SDS	12718.7	1	8	-14.8	3.0	5/6
			Filt. Novachem	142.1	0.334	8	32.6	5.2	6
4 CNC	1.00%	150	Filt. MQ	151.1	0.200	7	-49.6	9.8	5/6
			Filt. SDS	150.9	0.217	7	-0.1	114.3	5/6
			Filt. Novachem	146.7	0.220	7	-41.0	51.0	6
5 CNF	1.99%	150	Filt. MQ	793.4	0.726	7	-24.2	3.4	5/6
			Filt. SDS	1.04×10 ⁴	0.700	7	-18.3	4.2	5/6
			Filt. Novachem	2568.3	1	7	-32.6	39.3	6
			MQ	631.7	0.642	7	-25.00	22.00	5
			Novachem	166.7	0.494	8	-59.40	22.0	7
6 CNF	1.99%	150	Filt. MQ	817.9	0.723	6	-23.5	3.5	5/6
			Filt. SDS	1.11×10 ⁴	1	6	-18.4	9.2	5/6
			Filt. Novachem	2584.7	1	6	-14.3	31.6	6
			MQ	863.2	0.751	6	-24.2	3.99	5
7 CNF	2.09%	150	Filt. MQ	104.1	0.273	9	-37.3	41.0	5/6
			Filt. SDS	103.5	0.359	9	-47.8	23.0	5/6
			Filt. Novachem	114.2	0.352	8	-58.4	16.2	6



DLS results

According to the DLS results, the different NC particles were characterized by different dimensions. Even though this method was able to determine only the hydrodynamic diameter of the particles it is possible to outline the characteristic size of NC.

Hydrodynamic diameters of CNC particles were found to be ranging from 118 to 152 nm, smaller values were found for the CNF sample; this might be due to the different and more elongated shape of the particles. It is worth to remark that due to their instability it was not possible to determine the hydrodynamic diameter for two of the CNF samples with the DLS technique.

3.1.2. NTA Results

The results of NTA, as the ones of DLS, can be reported in four groups, according to the CNC/CNF contents and behavior of the samples. To determine the size measurement of particles the frequency distribution graphs (Particles/ml vs Diameter) were analyzed.

Samples 1,2 – CNC 3.98%

The frequency distributions obtained for the CNC samples 1 and 2, show a relevant first peak. The first peak is defined by the diameter (nm) that is detected with the highest frequency, and it is expressed as the corresponding particle concentration (particle/ml).

In *Figure 25* the frequency distributions for both samples are reported; it can be noticed that the particles in sample 1 most frequently showed a diameter of 89.6 nm, while those of sample 2 of 111.0 nm.

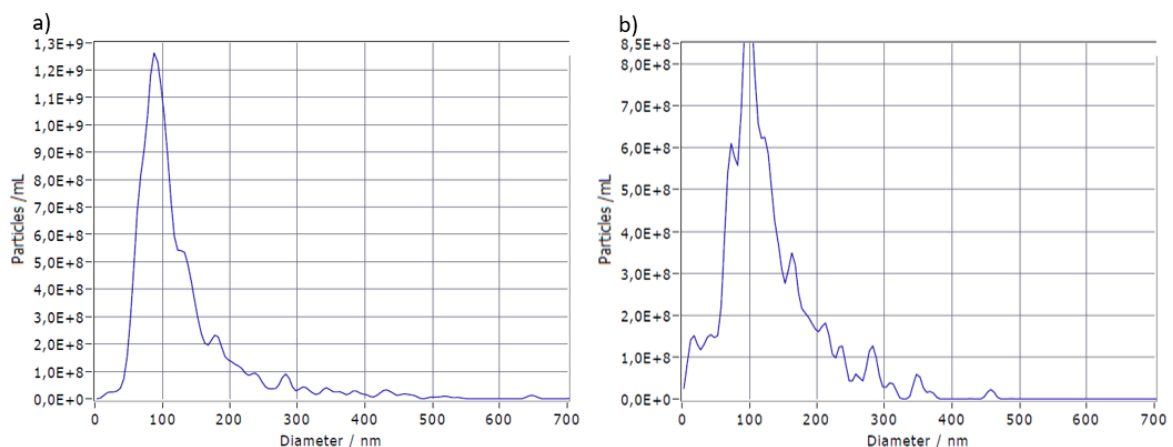


Figure 25: Diameter (nm) vs Particles concentration (Fig. a) sample CNC 1 measurement 2, Fig. b) sample CNC 2 measurement 1)

The median values, for these samples, were respectively 101.0 nm and 116.6 nm. To sum up, it was possible to define a size range for each sample.

The diameter of the CNC particles in sample 1 was between 85 and 105 nm, while for 2 was in the range 110-120 nm.

In *Figure 26* are displayed the particles detected by the camera; the concentrations in the non-diluted samples (150 ppm) were 3.93×10^{12} particles/ml in sample 1 and 3.27×10^{12} particles/ml in sample 2.

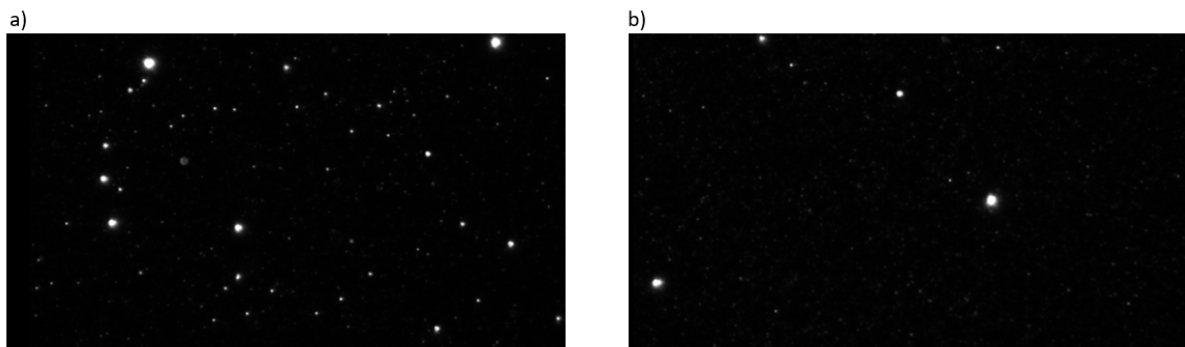


Figure 26: Particles detected by the camera (Fig. a) Sample CNC 1 measurement 3, Fig. b) Sample CNC 2 measurement 3)

Samples 3,4 – CNC 1.00%

Unlike other samples, the frequency distributions of 3 and 4 do not show a well-defined first peak (*Figure 27*).

Size range can be defined considering the quantiles (X Values), in particular X10 and X90. The quantile X10 describes the diameter value for which 10% of the particles have smaller diameter and 90% a larger diameter. The same concept applies for X90, that describes the diameter value for which 90% of population has smaller diameter (36).

For the sample 3, X10 and X90 values are, respectively, 144.3 nm and 413.4 nm; while for CNC 4 are 77.2 nm and 328.1 nm.

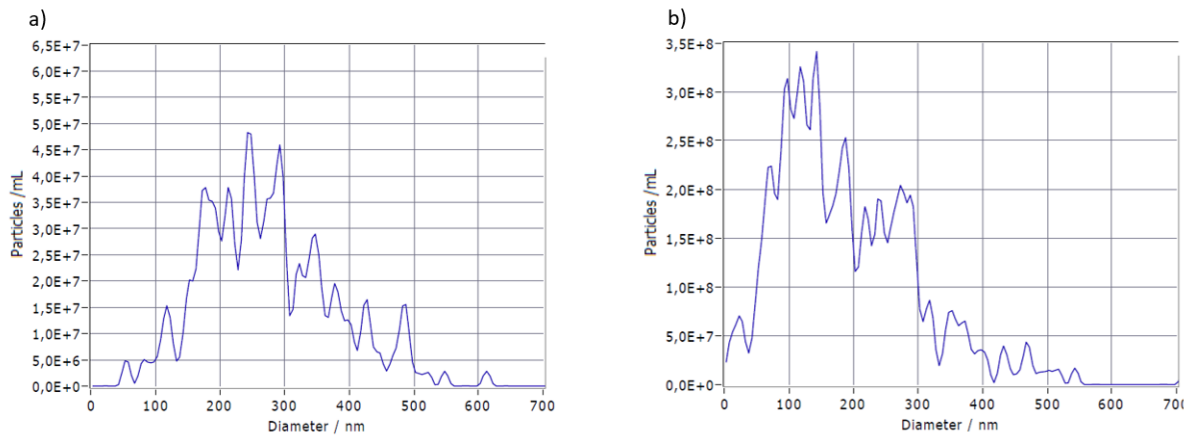


Figure 27: Diameter (nm) vs Particles concentration (Fig. a) sample CNC 3 measurement 2, Fig. b) sample CNC 4 measurement 1)

In both cases, it is possible to define a diameter range which results as 140-415 nm for sample 3 and 75-330 nm for sample 4.

Anyway, the ranges of diameter obtained with this method are broad; the NTA is unable to give narrower and more precise size intervals for these samples. In Figure 28, are reported the images detected by the camera.

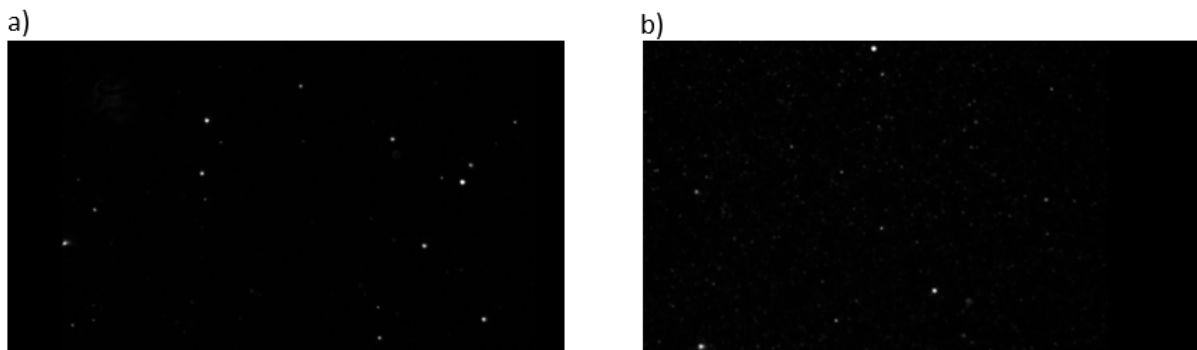


Figure 28: Particles detected by the camera (Fig. a) Sample CNC 3 measurement 3, Fig. b) Sample CNC 4 measurement 2)

The particles concentrations, in the non-diluted samples (150 ppm concentration), are respectively 3.60×10^{11} particles/ml and 2.60×10^{12} particles/ml, for samples 3 and 4.

Samples 5,6 – CNF 1.99%

To properly analyze the CNF samples 5 and 6, it was necessary to use lower sensitivity. The use of higher sensitivity (value of 75, as set for other samples) led to not clear and blurred

images, as shown in *Figure 29*. For those images the software was not able to give good results. So, for the samples 5 and 6 the sensitivity was set to 65.



Figure 29: Particles detected by the camera (sample CNF 5 sensitivity 75, measurement 3)

Samples 5 and 6's distributions show two main peaks (*Figure 30*); in both cases, the diameters that recur with higher frequency are close. It is possible to deduce that the two principal dimensions of those fibrils are similar, and so equally detected by the NTA.

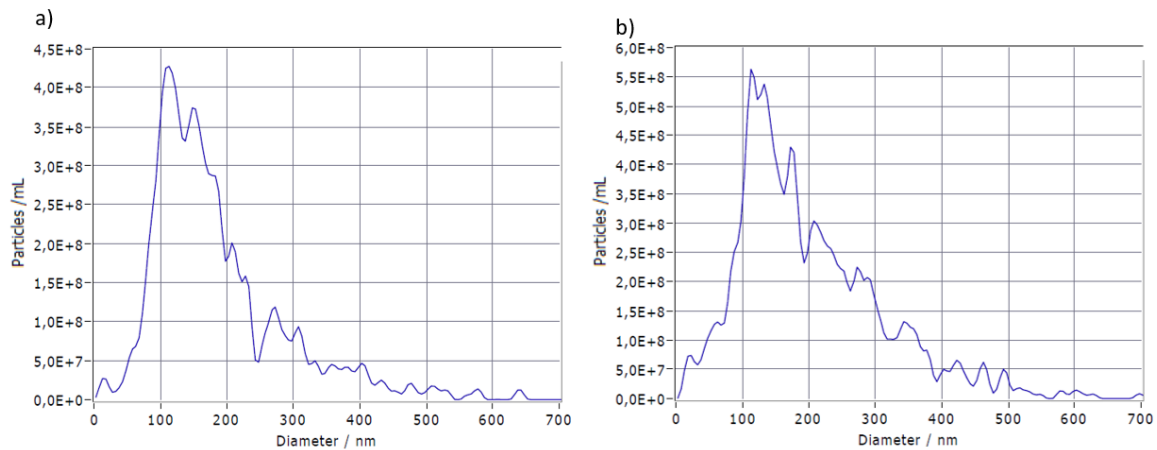


Figure 30: Diameter(nm) vs Particles concentration (Fig. a) sample CNF 5 measurement 3, Fig. b) sample CNF 6 measurement 2)

The first and second peak diameters, and so the main dimensions of particles are, respectively, 147.0 nm and 128.2 nm for the 5 and 150.3 nm and 206.3 nm for sample 6.

For these samples, it is possible to assume that the characteristic size is in the ranges 130-150 nm and 150-210 nm, respectively.

The particles concentration of non-diluted CNF sample 5, with 150 mass concentration, was 2.13×10^{12} particles/ml, while it resulted slightly higher for sample 6, precisely 3.80×10^{12} particles/ml. In *Figure 31* the images analyzed by NTA software are shown.

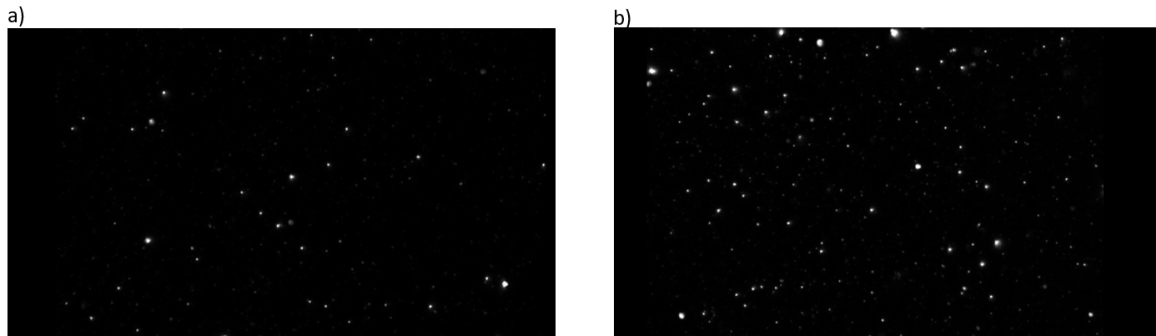


Figure 31: Particles detected by the camera (Fig. a) Sample CNF 5 measurement 3, Fig. b) Sample CNF 6 measurement 3)

Sample 7 – CNF 2,09%

The CNF sample 7, like the CNC samples 1 and 2, shows a clear first peak. The mode of this distribution is 111.7 nm, the median is 129.4 nm (*Figure 32*).

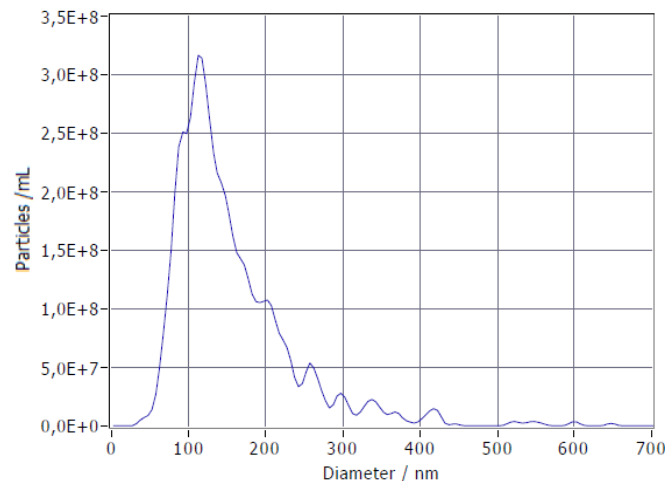


Figure 32: Diameter (nm) vs Particle concentration: sample CNF 7, measurement 3

Given the NTA results, it is possible to determine the diameter of particles of the CNF samples 7, which is in the range 100-130 nm; the concentration of particles in the original sample (150 ppm) is 1.29×10^{12} particles/ml. In *Figure 33*, is displayed the image analyzed by NTA software.



Figure 33: Particles detected by the camera: sample CNF 7, measurement 3

NTA measurements

Using the NTA, which was able to determine the particles' sizes through a visualization technique, wider dimension ranges were detected for the NC samples.

Even though it was not possible to define the size of all the CNC samples, their particles were found to have sizes ranging from 85 to 120 nm, while CNF particles showed dimensions between 100 and 210 nm. The range found for CNF particles resulted wider because of the shape of the particles, which are fibers.

3.2. Dispersion test – NC concentration measurement

As stated in the previous paragraph, different methods were used to determine Nanocellulose concentrations in the 1 ml aliquots taken from the dispersions, with the aim of determining the dispersion stability of nanomaterials.

Measurements, carried out using the TOC analyzer Primacs ATC100-IC-E, led to the results which are detailed below (*Table 16*). The test mediums were analyzed to detect the background carbon; even though, the inorganic carbon was removed using 1 ml of HCl (2 M), some unexpected Organic Carbon was found in the solutions.

Table 16: Expected and Measured value of IC and OC for the test mediums (TM 1, TM 2 and TM 3);
ph7

Sample Name	IC		OC	
	Expected Concentration (mg/L)	Measured Concentration (mg/L)	Expected Concentration (mg/L)	Measured Concentration (mg/L)
TM 1	0	-*	-	0.563
TM 2	0	-*	-	0.538
TM 3	0	-*	-	0.456

* Values of IC were not measured

The presence of Organic Carbon in the test mediums could be due to contaminations caused by impurities in the used MQ, and in the stock solutions that were prepared for the TMs formulation.

In addition, the Organic Carbon, which was expected in the samples containing nanocellulose materials (*Table 17*), was less than the OC measured in the test mediums due to impurities. Due to that, the background OC could not be distinguished from the nanocellulose's Organic Carbon. Furthermore, the concentration of organic carbon expected in the samples, was way below the detection limit obtained with the calibration curve, which was built with Glycine 0.5%.

Table 17: Expected IC and OC for nanocellulose materials, with particles concentration in the range required by the OECD TG

Sample name	IC	OC
	Expected Concentration (mg/L)	Expected Concentration (mg/L)
CNC 1	60	1.554
CNC 2	60	2.747
CNC 3	60	3.590
CNC 4	60	6.146
CNF 7	60	2.973

Due to these considerations, the TOC measurement of solid samples with the Primacs ATC100-IC-E, could not be considered suitable for the determination of the dispersion stability of nanocellulose materials.

Instead, lower limit of carbon concentration could be detected by the liquid TOC analyzer, multi N/C 3100. The OC concentration that could be measured with this method was 0.3 mg of carbon per liter. Liquid samples of nanocellulose material and test medium – taking 1 ml from the dispersion and diluting it to 10 ml with MQ – were tested. The results are reported in *Table 18*.

The organic carbon measured for the CNC 2 sample diluted in MQ and the pure test medium (TM2) corresponded to the expected ones, while the OC measured for the dispersion of NC in test medium resulted more than twice the expected value.

The obtained data resulted inconsistent; contamination in the stock dispersions used for sample preparation could explain this data inconsistency.

Table 18: Expected and Measured IC and OC concentration in test medium, CNC 2 dispersion and CNC 2 with TM dispersion

Sample name	IC		OC*	
	Expected Concentration (mg/L)	Measured Concentration (mg/L)	Expected Concentration (mg/L)	Measured Concentration (mg/L)
TM 2 (no cellulose)	60	50	0	< 0.3
CNC 2 + MQ	0	< 0.5	0.275	0.3
CNC 2 + TM 2	60	49	0.275	0.67

*The NPOC (Non-Purgeable Organic Carbon) is measured with this instrument

To assess the influence of the impurities and OC concentrations on the measurements other test were carried out, particularly to check if a correlation between the OC and the IC was present. Samples which presented increasing Organic Carbon concentrations were tested. In *Table 19* the expected and measured values of OC and IC are reported; it is worth to notice, that even in this second test, the OC is measured as NPOC (Non-Purgeable Organic Carbon).



Table 19: Expected and Measured IC and OC concentration in test medium, CNC 2 dispersion and CNC 2 with TM dispersion; samples with increasing expected OC content

Sample Name	IC		OC	
	Expect. (mg/L)	Measured (mg/L)	Expect. (mg/L)	Measured (mg/L)
Test medium (no cellulose)	60	47	0	<0.3
CNC 2 (0.5 mg OC/L)+ MQ	-	<0.5	0.5	<0.3
CNC 2 (1 mg OC/L)+MQ	-	0.58	1.0	<0.3
CNC 2 (1.5 mg OC/L) + MQ	-	0.60	1.5	0.36
CNC 2 (0.5 mg OC/L)+TM2	60	48	0.5	4.7
CNC 2 (1 mg OC/L)+TM2	60	47	1.0	2.2
CNC 2 (1.5 mg OC/L)+TM2	60	49	1.5	1.0

*The NPOC (Non-Purgeable Organic Carbon) is measured with this instrument

Organic and Inorganic carbon measurements, obtained with liquid samples TOC analyzer, differ from the expected ones. Indeed, an increasing concentration of OC was not detected by the instrument. Reason of that could have been the presence of impurities in the test mediums or in the NC stock dispersion; but more surely, it was due to the low concentration of OC that was expected in the samples. However, because the number of particles in the OECD dispersion test is fixed, it was not possible to increase the OC concentration.

Since both TOC instruments did not give acceptable results, a different technique was used to determine the carbon concentration in the samples. The Py-GC-MS, which can be used to characterize polymers and determine their quantity inside the samples, and so the NC concentration.

To define the background of the Py-GC-MS measurements, a clean glass fiber filter and pure MQ were tested; the TICs (Total Ion Chromatogram) are reported in *Figure 34*.

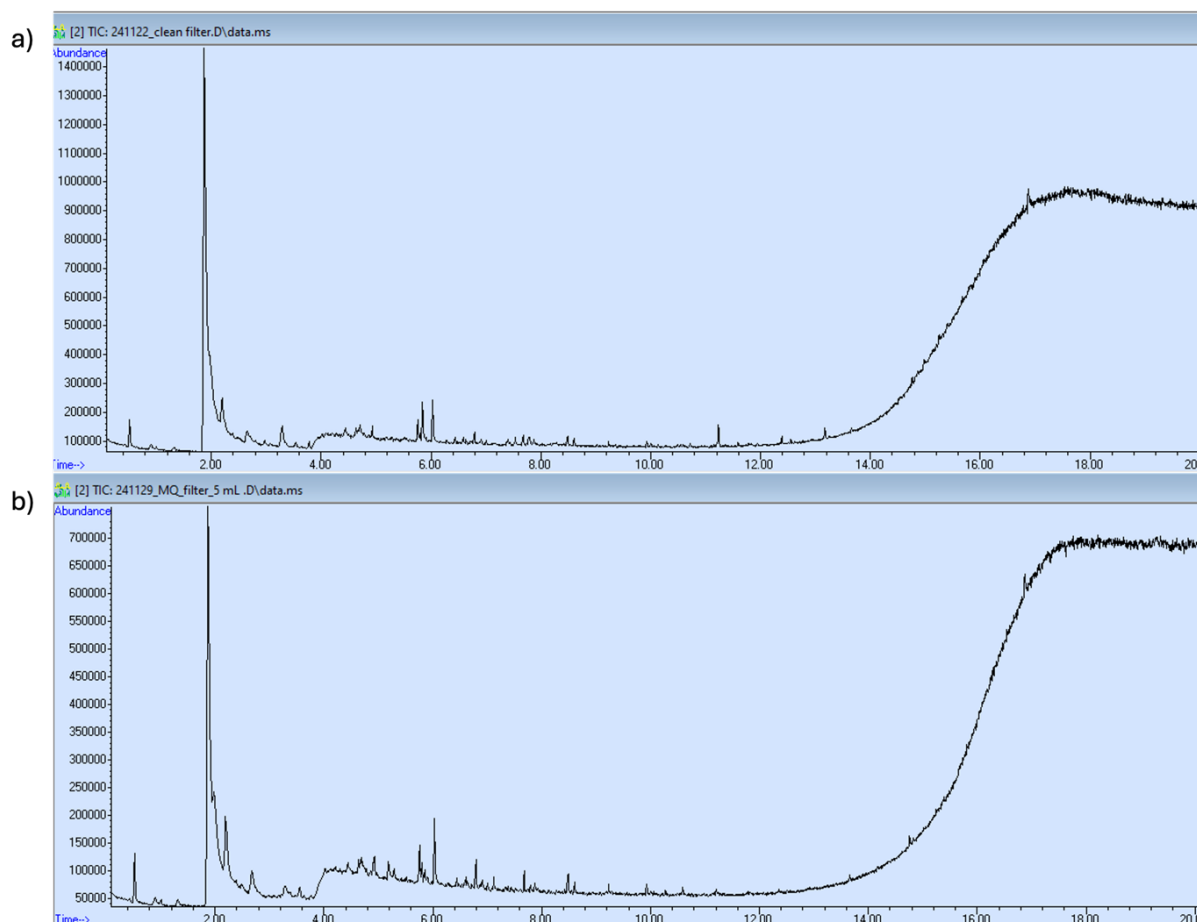


Figure 34: Background characterization with Py-GC-MS. a) TIC of Clean glass fiber filter (pores 2.2 μm) b) TIC of pure MQ

In the Total Ion Chromatograms just small peaks were observed from the filter and the MQ, meaning that no noticeable interferences are present.

Pure test medium (TM 2), NC dispersion in water and NC dispersion in the test medium were tested with this technique. As expected, the pure TM 2 gave TIC similar and comparable to the one of the MQ, since it did not contain nanocellulose particles (*Appendix: Figure 3*).

Overlaying the two TICs, the one of the pure TM 2 and the one of MQ it is possible to see that just marginal differences were present.

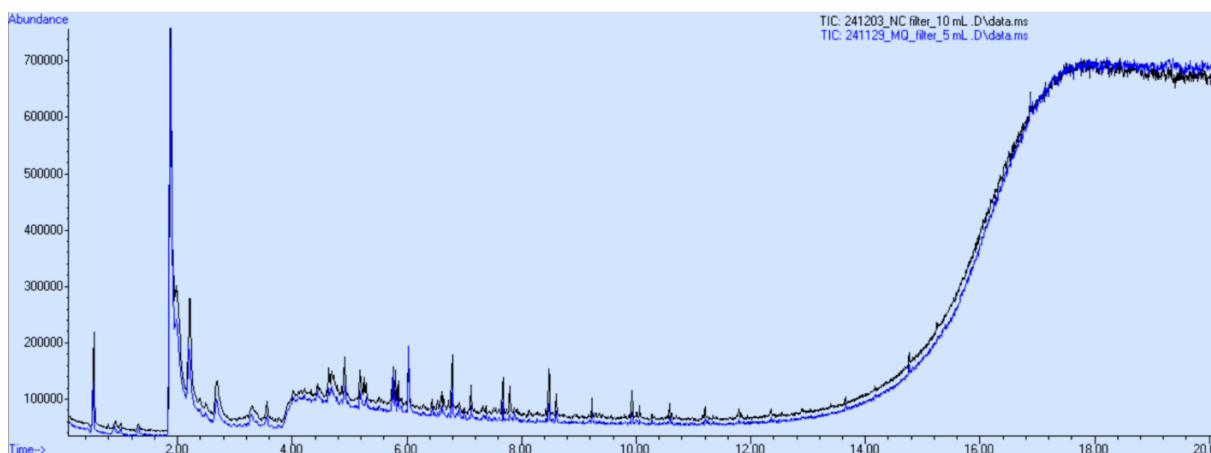


Figure 35: TICs Overlaying (in blue MQ, in black TM 2)

Afterward, in the same way, a dispersion with NC (CNC 2) and MQ was tested (*Appendix: Figure 4*). As in the previous TOC experiment, the concentration of the nanoparticles in the dispersion is the one required by the OECD test guidelines.

Even though the presence of nanocellulose, the TICs are similar, *Figure 36*. No peaks due to NC particles were detected. As for TOC measurements, also in this case, the low carbon concentration did not allow reliable measurements.

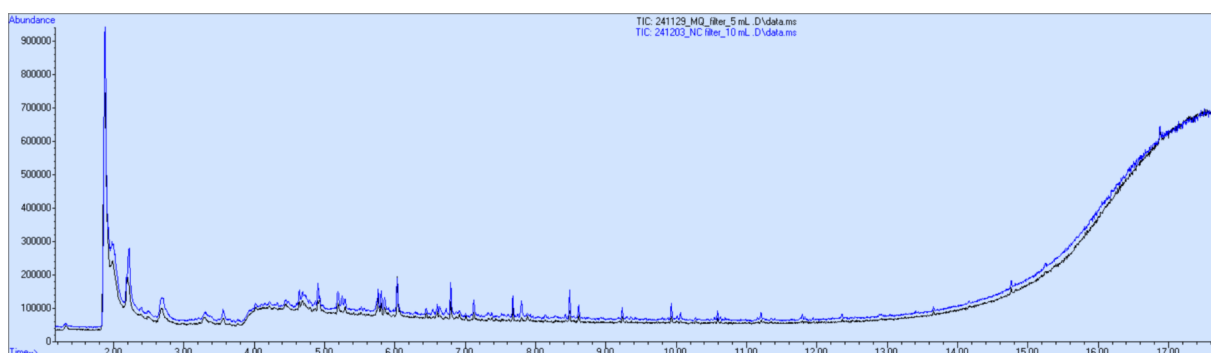


Figure 36: TICs Overlaying (in blue MQ, in black CNC 2 dispersion)

Finally, the sample containing NC and TM was tested. The TIC of this sample showed two big peaks, which, according to the software F-search, corresponded to PP and nylon-6,6. These two polymers could be associated to contaminations in the preparation process, since the wipe paper used to clean lab table was made of PP and nylon-6,6 is commonly used in clothes.

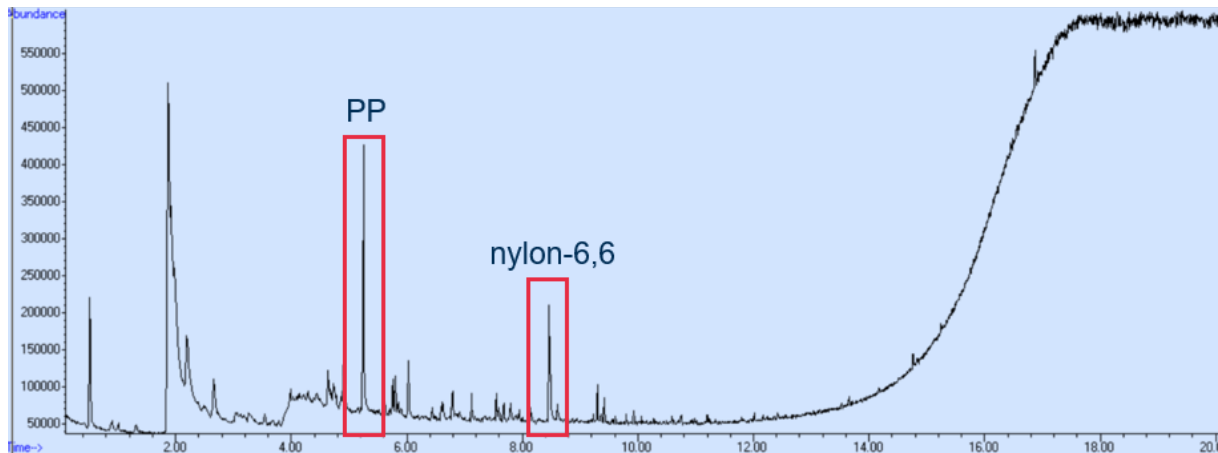


Figure 37: TIC of Nanocellulose (CNC 2) and test medium dispersion, Peaks showing contaminations of PP and Nylon-6,6

Beside these considerations, the overlaying of TICs (pure TM2 and NC dispersion in TM2) was performed to check whether other differences in the graphs were present.

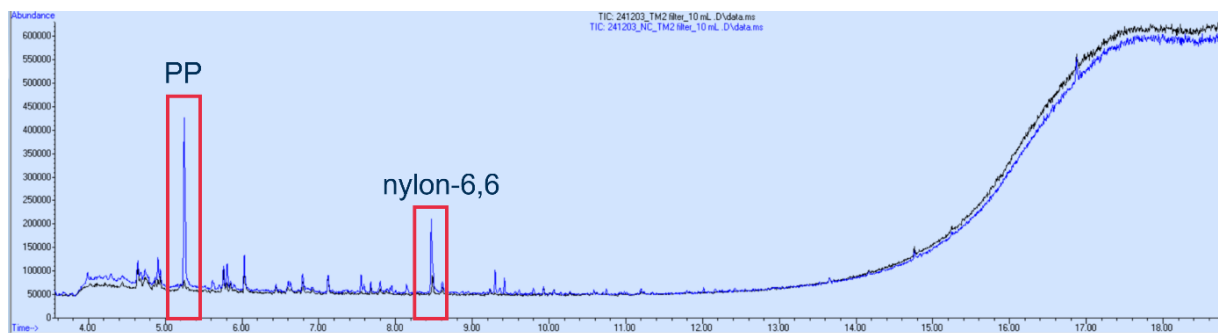


Figure 38: TICs Overlaying (in blue Nanocellulose and Test medium dispersion, in black pure test medium)

Apart the two peaks coming from contaminations, no differences in the graphs are shown. This indicates that was not possible to distinguish nanocellulose in the test medium. Reasons of that could be the low nanocellulose concentration and the losses of particles during the filtration process, due too big filter's pores size. To ensure that the particles were not lost during the filtering process, another test with an anodisc filter with pores size 20 nm was performed.

In this second test, the aliquots taken from the dispersion test samples were not diluted to 10 ml with MQ, but were directly filtered. The collected filters were dried in the oven with 105 °C

for 20 min. The filters, before being put in the pyrolysis cups, were grinded into powder. Then samples powder was transferred to the cups as much as possible.

Despite these precautions, again, it was not feasible to distinguish the NC from the test medium, *Figure 39*.

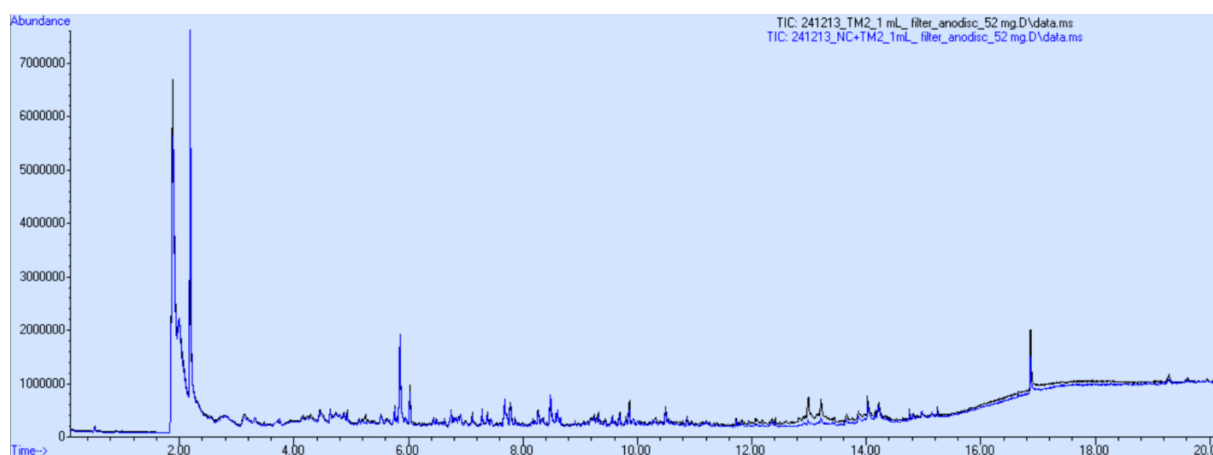


Figure 39: TICs Overlaying (in blue Nanocellulose and Test medium dispersion, in black pure test medium)

In this way it was proved that even Py-GC-MS was not able to distinguish the nanocellulose from the test medium, so it was not possible to perform the dispersion experiment using this technique. As for the TOC measurements, the too low nanocellulose concentration prevented its measurement even with the Py-GC-MS.

Since it was not possible to carry out the Dispersion test following the OECD test guidelines, another parameter useful to determine the behavior of NC in environmental streams was determined.

3.3. Attachment efficiency determination

The attachment efficiency could be experimentally determined for homoaggregation of NC particles computing the ratio between the aggregation rate and the aggregation rate at favorable conditions, the “fast” aggregation. For nanocellulose, it was possible to determine the fast aggregation rate monitoring the growth of particles over time when dispersed in the test medium with highest electrolytes concentration (TM 3), since this salt concentration was found

to be above the CCC. For all the different test mediums the fast aggregation rate was determined.

Further tests, with different NC concentrations were performed to verify that the number of particles was not influencing the attachment efficiency. As expected, the concentration did not influence the results, and in addition, being the attachment efficiency calculated as the ratio of the growth rate between “*slow*” and “*fast*” aggregation conditions of solution containing the same amount of nanocellulose sample it was possible to not include the number of particles (N_0) in the equation.

The fast aggregation was determined as the variation of the hydrodynamic diameter of particles dispersed in the test medium with highest electrolytes concentration in the shortest time span detectable in each run of the instrument.

In order to determine the hydrodynamic diameter of NC particles dispersed in different TMs the DLS was used. This method was chosen because of the goodness of the results obtained in the characterization phase and the repeatability of the measurements in a relatively short time, which guaranteed the possibility to perform the analysis in duplicates. Due to the use of the DLS, nanocellulose concentration was increased to assure its detectability and reliable size determination by the instrument.

Table 20: Fast aggregation rate for samples CNC 1,2,3,4 and CNF 7

Sample Name	Fast aggregation rate nm/s
CNC 1	0.55000
CNC 2	0.47595
CNC 3	0.00365
CNC 4	0.38935
CNF 7	1.32515

Consequently, the aggregation rate of particles dispersed in the test mediums 1 and 2 were computed.

Similar values of attachment efficiencies for the TM 1 and 2, without NOM, were expected for almost all the particles. Reason of that is the similar behavior of NC when immersed in test

mediums with low electrolytes concentrations. Differences in the behaviors were mostly found when in presence of NOM.

The samples CNC 1, 2 and 3 showed constant size values in time with all the different test mediums. In absence of NOM the nanoparticles had the same size that was measured in the characterization phase; while, in presence of NOM the particles' dimensions increased of few nanometers over time. The NOM, when present in the test mediums, can form a film around the nanoparticles, *Figure 40* (37) (38). The interference of NOM with particles is strictly related to their surface functional groups. Due to that, similar behaviors were shown by nanoparticles that were characterized by the same surface functional groups.

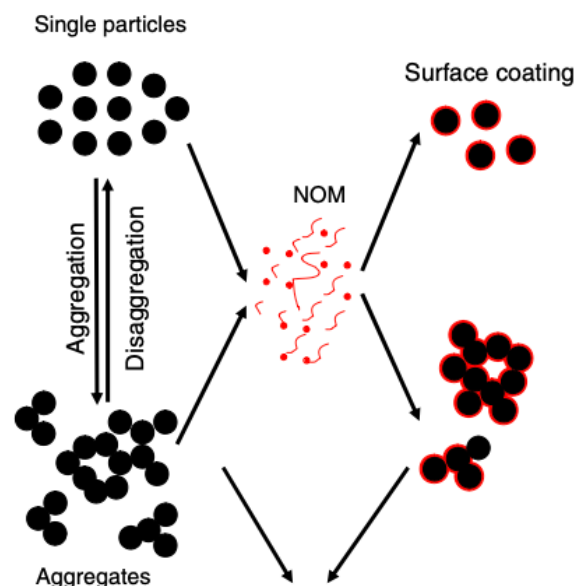


Figure 40: NOM coating of particles (37)

Different behavior was noticed for the sample CNC 3, whose particles' size grew with higher electrolytes concentration, 1 mM, corresponding to the electrolytes concentration present in TM 2. Even in this case the presence of NOM enhanced particles growth. Similar behavior was shown by the CNF sample 7.

It is noticeable that in all the cases, even after the growth of particles, due to the presence of NOM, the dimensions remained constant along the experiment time. It meant that the size variation, for all the samples, in all the test mediums, was very small.

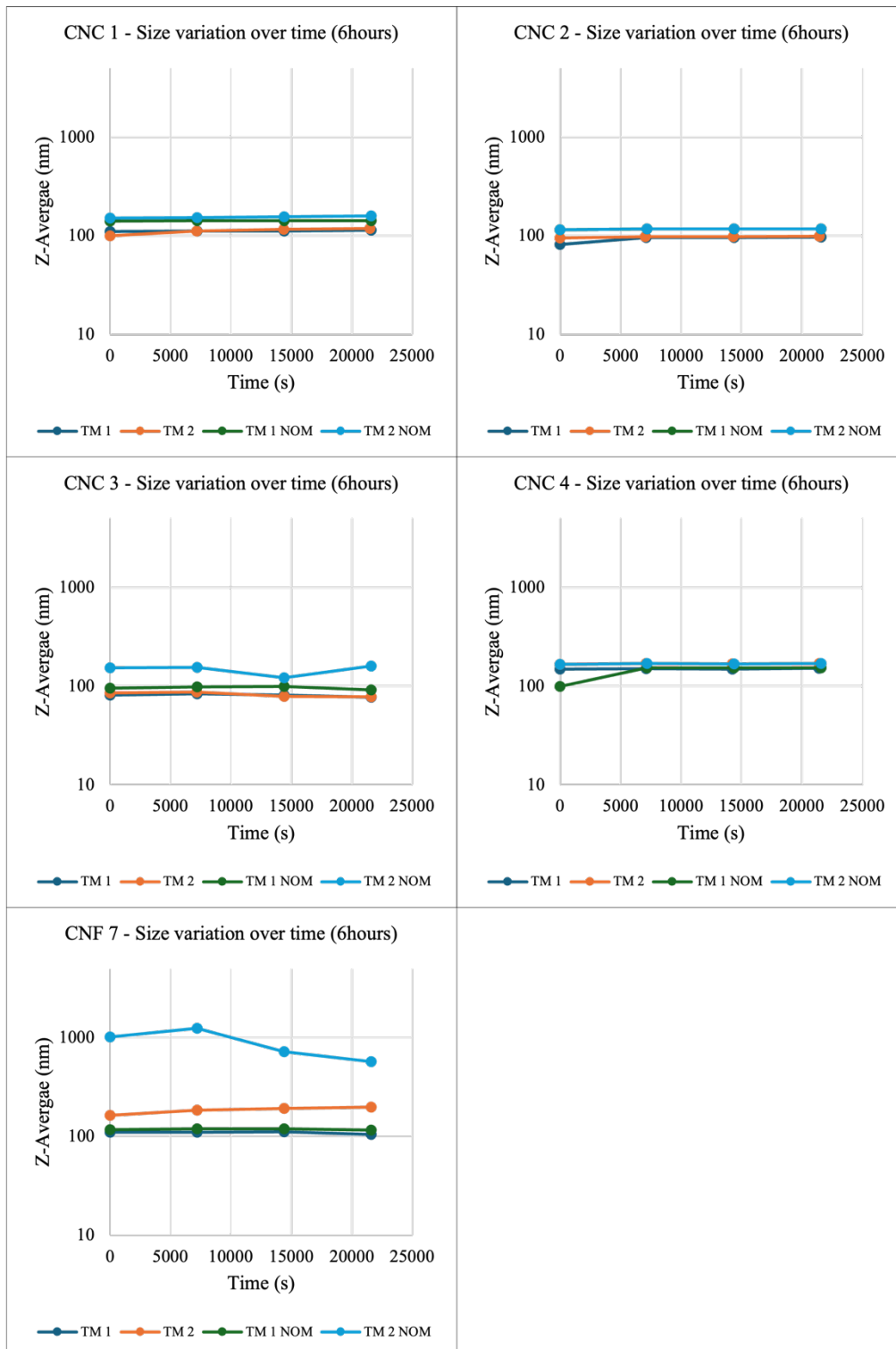


Figure 41: Size variation of particles in different test mediums (TM1 and TM2) in absence and presence of NOM



Finally, the attachment efficiency was determined for all the samples, in all the test mediums as the ratio between the attachment rate in “normal” and “fast” aggregation conditions. As expected, small value of α_a characterize the homoaggregation of these nanoparticles.

Table 21: Attachment efficiency for the samples CNC 1,2,3,4 and CNF 7 in different test mediums

Sample Name	Test Medium	Attachment efficiency (α_a)
CNC 1	TM 1	0.0437
	TM 2	0.0358
	TM 1 NOM	0.0213
	TM 2 NOM	0.0202
CNC 2	TM 1	0.0403
	TM 2	0.0416
	TM 1 NOM	0.0235
	TM 2 NOM	0.0305
CNC 3	TM 1	0.1649
	TM 2	0.2999
	TM 1 NOM	0.1043
	TM 2 NOM	0.2670
CNC 4	TM 1	0.0192
	TM 2	0.0453
	TM 1 NOM	0.0161
	TM 2 NOM	0.0145
CNF 7	TM 1	0.0138
	TM 2	0.0155
	TM 1 NOM	0.0208
	TM 2 NOM	0.8133

Since the samples CNC 1 and 2 presented similar characteristics, in terms of size and functional groups, also their behavior in water resulted similar. Both presented values of aggregation



efficiency around 0.4 when dispersed in test medium that did not contain OC; lower values of α_a were shown when the NOM was present in the dispersion.

Other behavior was shown by the sample CNC 3, which was the only one with a positively charged surface. Due to surface positivity the attachment efficiency of particles, despite the measurements, has to be considered close to one; since, in environmental waters, positively charged particles have more probability of a non-reversible attachment after collision respect to negatively charged particles.

The CNC sample 4 showed, as expected, higher attachment efficiency when dispersed in test mediums with higher electrolytes concentration. The same result was obtained for the CNF sample 7. The attachment efficiency determined for the CNF sample 7 in the test medium TM 2 in presence of NOM, which resulted 0.8133, was removed from the results' set since this value could not be reliable. Even tough different values of α_a could have been expected for this sample, being the only CNF material, the attachment efficiency obtained for sample 7 in TM 2 NOM was expected to be lower or similar to the values obtained in the other TMs, since smaller values of α_a were found when in presence of NOM. This is because the NOM can act as particles stabilizer, so in TM which contained NOM, the surface groups of particles were modified and the dispersions got more stable (39) (40).

Due to these reasons this outlier was removed from the results' set.

3.4. Full Multi model results

The Full Multi model was adapted to the purpose of the study, in fact, homoaggregation was monitored instead of heteroaggregation. All the nanomaterials were tested in mediums with varying electrolytes concentration and in presence and absence of NOM.

As results heatmaps of the transport and fate processes half-lifetimes (t_{half}) of nanoparticles in the simulated generic river system are given (*Figure 42* - *Figure 43*), together with the concentration of the nanoparticle in various compartments and in different states (pristine, biofouled, heteroaggregated and biofouled & heteroaggregated) (9).

Distributions representing particles' concentrations after 365 days of modelling (*Figure 44* - *Figure 47*) are reported for each compartment along the length of the river. Particularly, in surface, flowing and stagnant waters the concentrations are reported as number of particles per cubic meter (N_0/m^3), while for the sediment compartment, they are reported as number of



particle per gram of sediment (N_0/g). The distribution of particles in each compartment is determined from a particles inflow of 100 particles per minutes. Physical characteristics of nanoparticles had high influence on the distributions, so on their fate in the river, particularly, distributions were highly influenced by size and density of the particles.

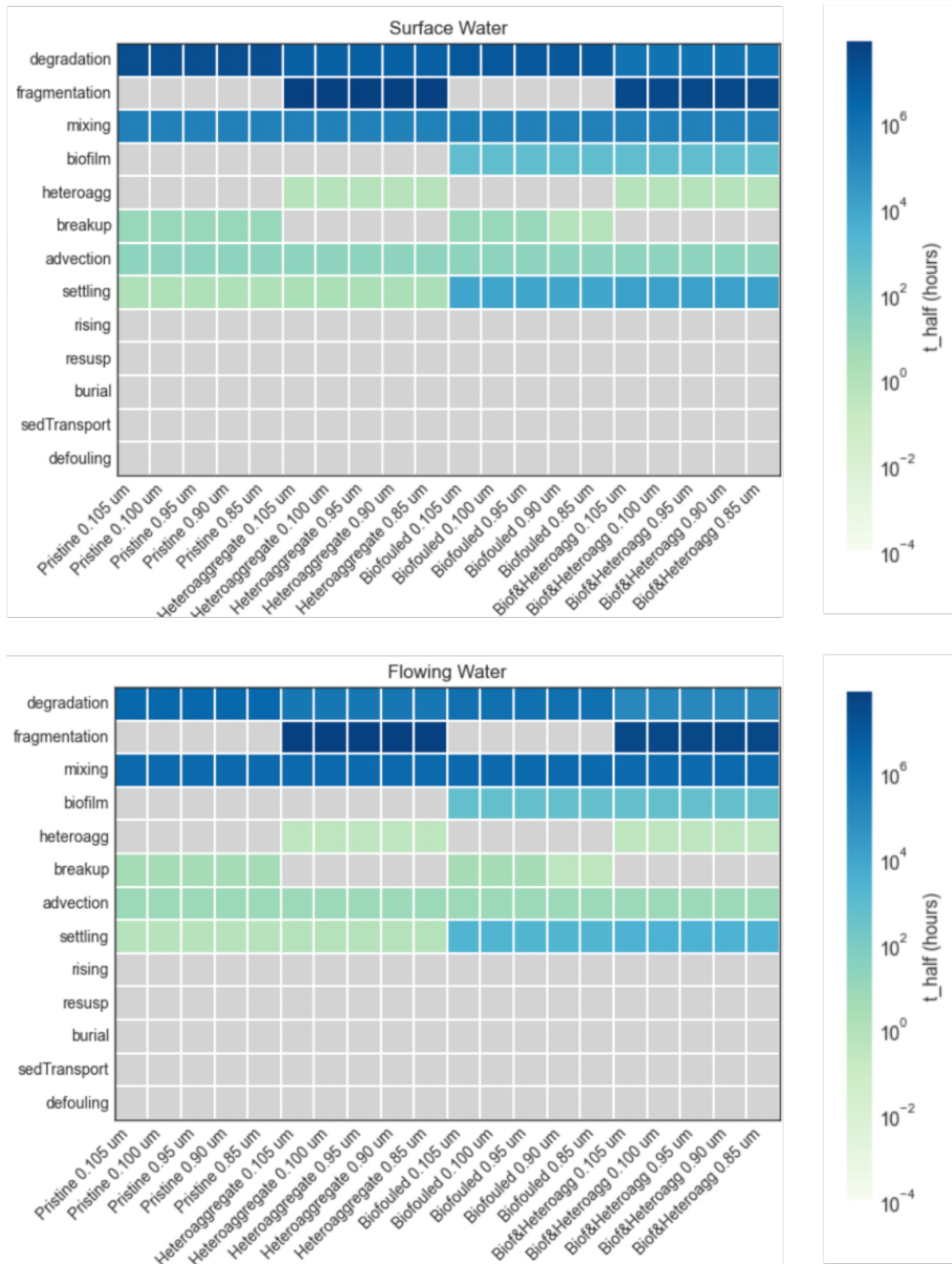


Figure 42: Heatmap of the transport and fate processes half-lifetimes (t_{half}) of CNC I particles in the simulated generic river system, in the two upper layers (surface and flowing water) (9).

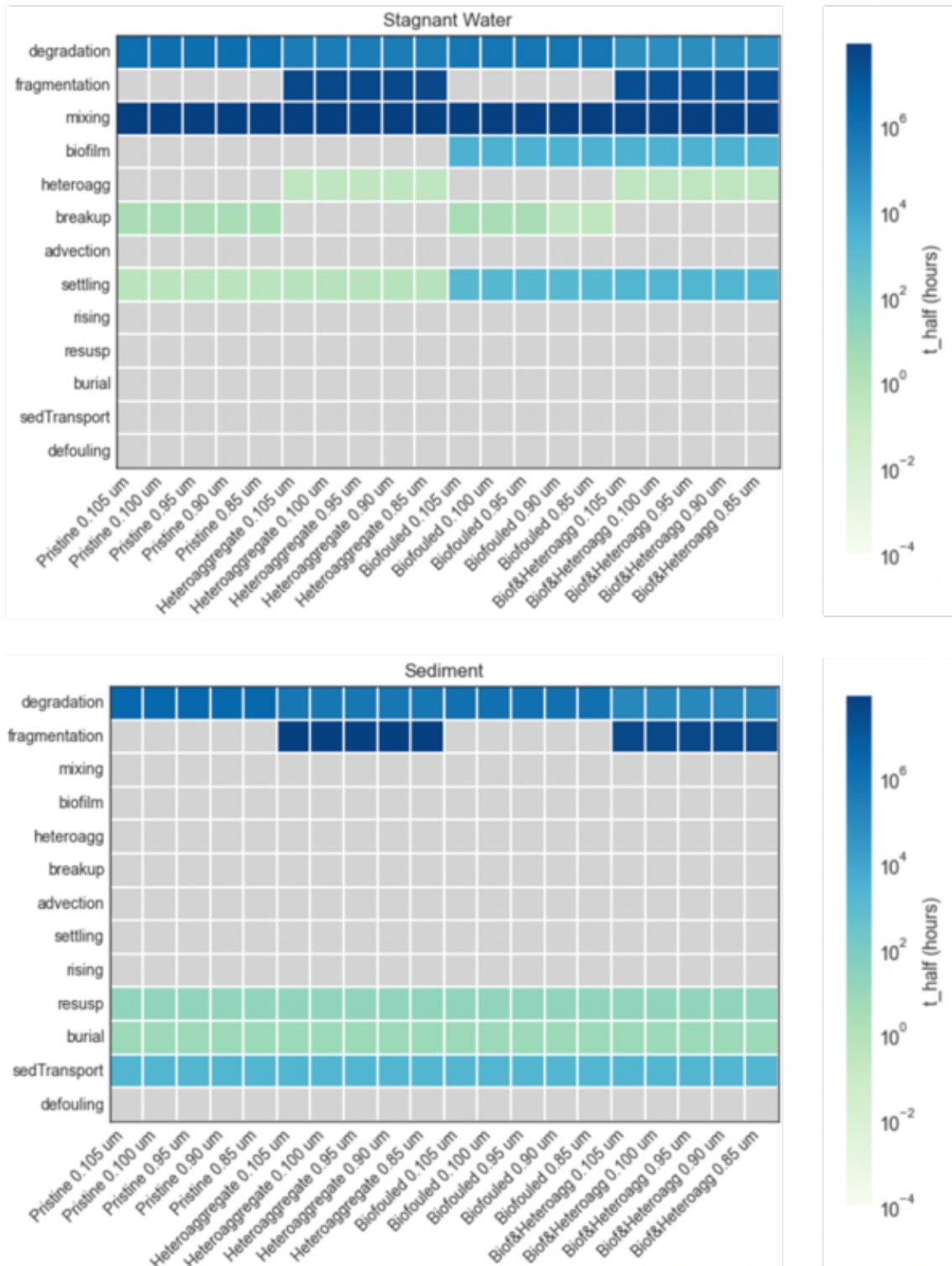


Figure 43: Heatmap of the transport and fate processes half-lifetimes (t_{half}) of CNC I particles in the simulated generic river system, in the two lower layers (stagnant water and sediment) (9).

After 365 days, CNC 1 and 2 particles in the two top layers belonged to the two biggest size classes, which were respectively 0.100 μm - 0.105 μm and 0.1175 μm - 0.120 μm .

It is worth to notice, that not many particles were found as biofilm-covered in the top layers of the river, this could be due to sedimentation of these particles and their tendency to be transferred to the bottom layers. Whereas the particles belonging to the smaller classes were mostly found in the sediment layer, for these samples, particles never belonged to the smallest classes, which were 0.085 μm for CNC 1 and 0.110 for CNC 2. Generally, particles' concentration raised along the river course, for all the states and the compartments.

Particles concentration and form varied in the different test mediums, mostly influenced by the presence of NOM. The particles of the sample CNC 1 were found to be mostly in flowing and stagnant water, respectively $\approx 54\%$ and $\approx 44\%$ of the particles were in these compartments. Particles' distribution for this sample was not dependent on the test medium. Meanwhile, it was not the same for the "state" of the particles, in the TMs, which did not contain the NOM, 51-57 % were aggregated, while 42-47% were free; although, in the test mediums with NOM more particles were found to be aggregated (up to 70% of the total).

1 CNC particles after 365 days in TM 1

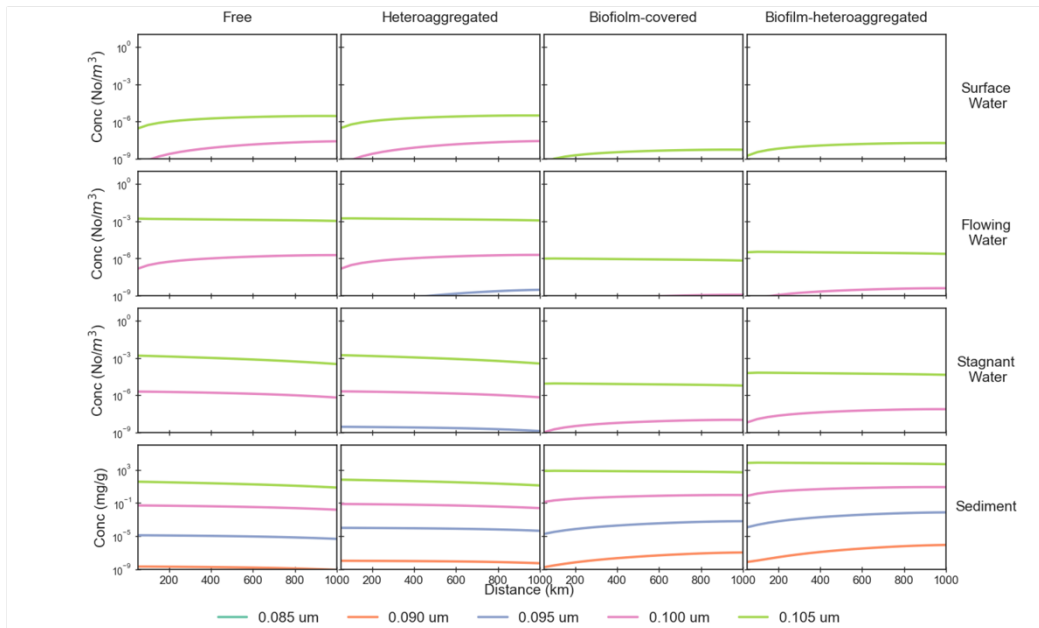


Figure 44: Fate of CNC 1 particles after 365 days in different TM1. In these distributions sample's concentrations are shown in the different compartments and states.

1 CNC particles after 365 days in TM 1 NOM

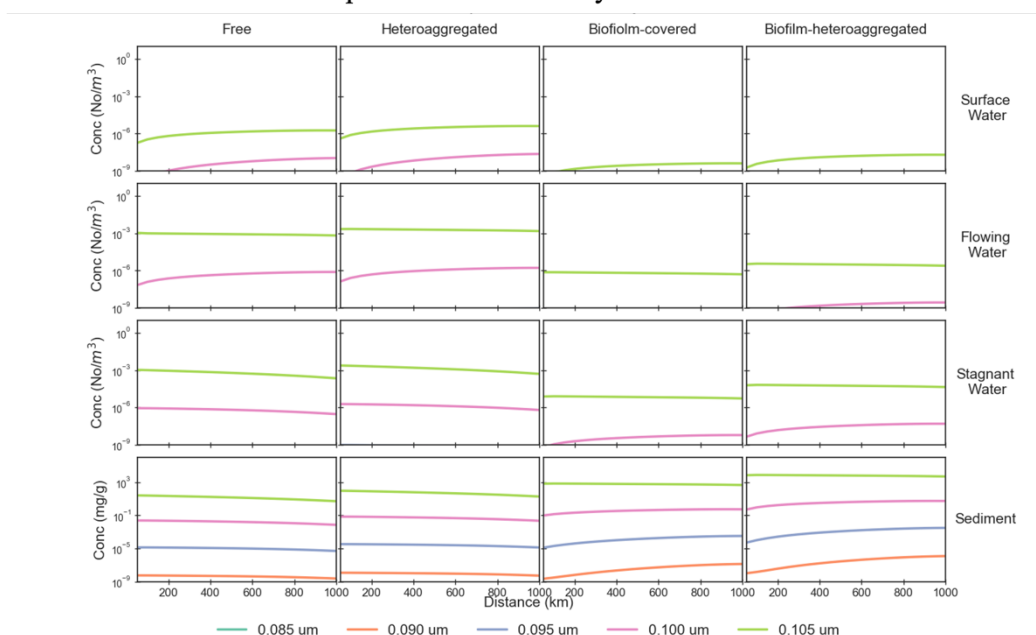


Figure 45: Fate of CNC 1 particles after 365 days in different TM1 NOM. In these distributions sample's concentrations are shown in the different compartments and states.

1 CNC particles after 365 days in TM 2

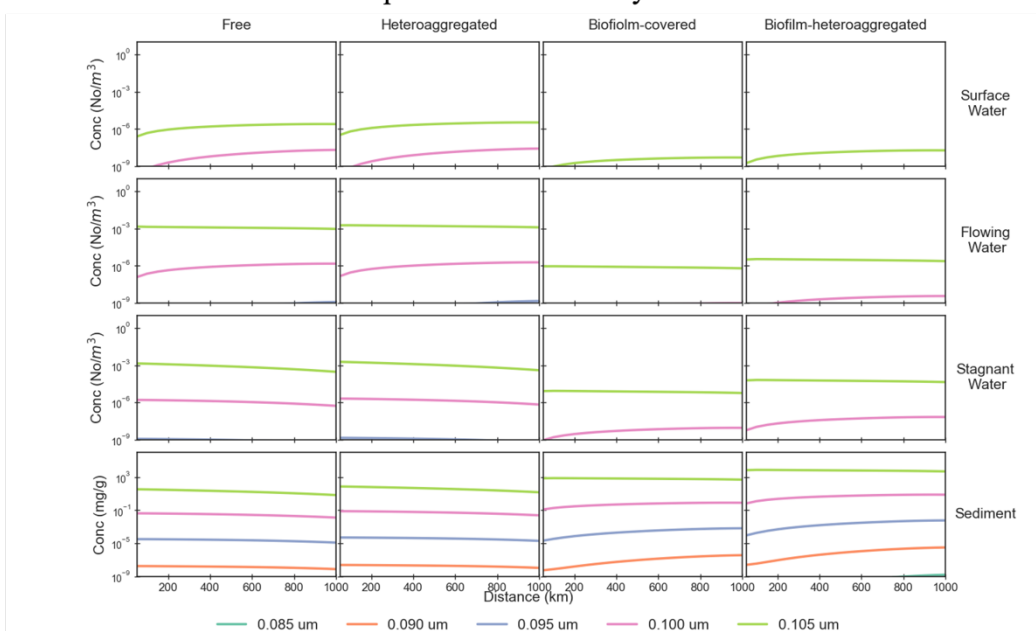


Figure 46: Fate of CNC 1 particles after 365 days in different TM2. In these distributions sample's concentrations are shown in the different compartments and states.

1 CNC particles after 365 days in TM 2 NOM

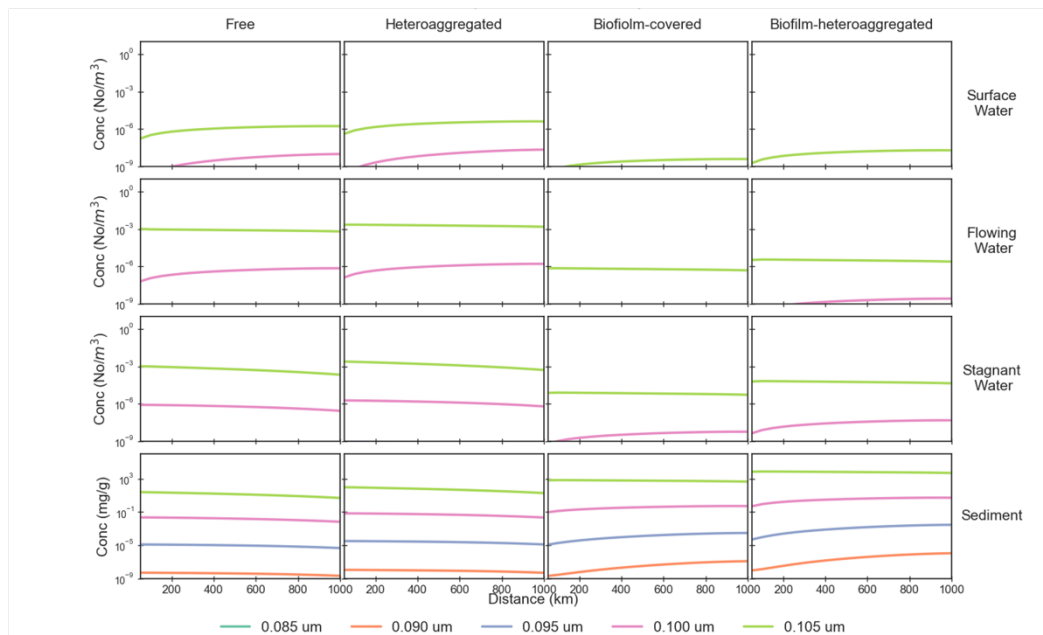


Figure 47: Fate of CNC 1 particles after 365 days in different TM2 NOM. In these distributions sample's concentrations are shown in the different compartments and states.

Different concentration's distributions were found for the sample CNC 2, in this case in particles were mostly dispersed as aggregated (up to 90%), less than 10% of the particles were free. Most of the particles of this sample were found in the flowing and stagnant water compartments, respectively 56-57% and 41-43%.

Despite the sample CNC 3 was the only one which presented positively charged surface, its behavior could be comparable to the one of the sample CNC 2, just slightly different shares of concentrations were shown. In this case, most of the particles, 52% were found to be in the stagnant water while 47% was in the flowing water.

Particles of the CNC 4 were mostly aggregated 74-89%, in all the TMs, the remaining were free. For this samples the particles were almost equally distributed between the flowing water and the stagnant water compartments, 47-48% and 51-52% respectively. The only CNF sample analyzed, the 7, had in all the test mediums a higher percentage of aggregated particles, \approx 57-64%, the remaining were "free". Similarly to the samples CNC 1 and 2, the CNF 7 particles were mostly found in the flowing water compartment, while \approx 40% of particles were in the stagnant water compartment.

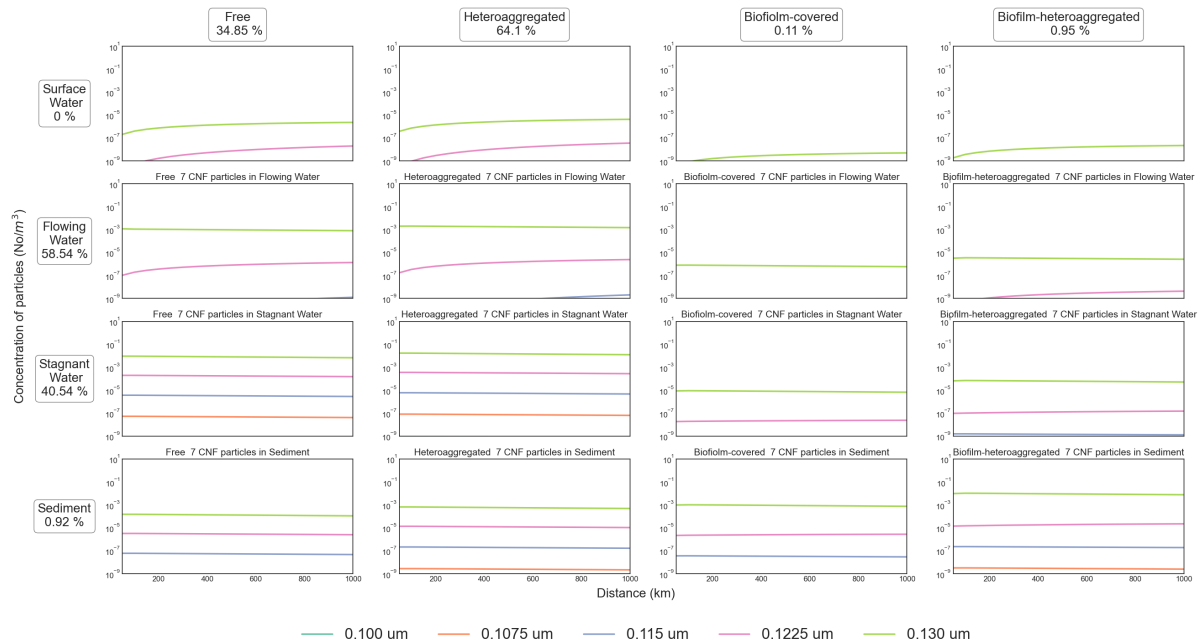


Figure 48: 7 CNF particles fate in generic river over time (inflow = 100 particles/min)

The heatmaps of the transport and fate process half-life time could be used to compare the different processes which are competing in the natural environment. Those processes were comparable between each other since were all described as first order kinetics. The parameter used for this comparison was the half-life time, which outline the time in which the initial particles' concentration is half its initial value when particles are submitted to a certain process. The half-life time for a first order kinetic process is inversely proportional to the process rate constant ($k_{process}$) that is expressed in s^{-1} and varies process to process.

$$t_{half-life} = \frac{\ln 2}{k_{process}}$$

Equation 15: Half-life time (s) definition

In the heatmap the half-life time of each process can vary from seconds, light green, to days, dark blue. Instead, cells are shown in grey when the process is not involved (9).

All the NC samples showed similar behaviors to the one of CNC 1, showed in Figure 42. In the three top layers similar processes took places, even characterized by similar half-life times. In the top layer, superficial water, the processes that affect more quickly the NC particles were settling, advection and breakup. Bigger particles were also subjected to biofilm formation and fragmentation. Slower processes also took place in this compartment such as degradation and



mixing, whose t_{half} is in the hours scale. Same processes took place in the second top layer, flowing water, with similar velocities. On the other side, in the stagnant water compartment advection process did not take place.

Meanwhile, in the sediment compartment burial, resuspension and sediment transportation happened, with quite small t_{half} . Overall, it can be said that in all the river compartments, degradation and fragmentation occurred with similar intensities and velocities.

4. Discussion

4.1. Particles characterization

The DLS and the NTA are the methods that were chosen to determine the dimension of nanocellulose particles. Those two technologies use the Brownian motion, to which particles are subjected, to determine their velocity. The determination of particles velocity in relation with the Stokes-Einstein equation (*Equation 1*), is used to characterize the nanoparticles.

The main difference between the two used techniques, DLS and NTA, is the working principle. While the DLS measures the fluctuation of scattered light, the NTA tracks the motion of each particle recording it on video. Therefore, the Dynamic Light Scattering determines the hydrodynamic diameter through a correlation function, while the NTA calculates particles size starting from their velocity.

In the process of NC particles characterization, the DLS method was found to be reliable for CNC samples, whereas it was not for all the CNF particles. The dimension range of the analyzed CNC turned out to be 115-155 nm.

Instead, the NTA gave narrow enough size ranges for all the samples, exception made for CNC samples 3 and 4. For those, the size ranges defined by this method are too broad, so the characterization of the suspended particles has not been precise enough.

Table 22: DLS vs NTA size determination for CNC/CNF particles

Sample		DLS	NTA
Name	% wt	Hydrodynamic diameter (nm)	Diameter (nm)
CNC 1	3.98%	152 ± 13.9	85-105
CNC 2	3.98%	118 ± 11.2	110-120
CNC 3	1.00%	125 ± 11.5	-
CNC 4	1.00%	150 ± 13.8	-
CNF 5	1.99%	-	130-150
CNF 6	1.99%	-	150-210
CNF 7	2.09%	107 ± 9.8	100-130

In *Table 22*, the obtained diameter ranges for all the samples are reported. All the CNC materials when diluted in MQ could be considered stable, while it was the same for the CNF samples. It is noticeable that the CNF materials that were pre-treated with only mechanical forces and no chemical modifications, resulted not stable when dispersed in different solvents; whereas the dispersions containing CNF particles which had undergone chemical pre-treatment resulted stable.

It is worth to notice that both NTA and DLS instruments can just determine the hydrodynamic diameter of the particles, which are considered as spheres; indeed, with this technique it was not possible to define the width and the length of NC. So, for this study the dimensions and aspect ratios that were used are the ones provided by the suppliers of the material, which were determined using the transmission electron microscopy (TEM).

Following these results, is it possible to say that a reliable characterization of these material was obtained, since size ranges given by the two technologies are comparable between each other and with Safety Data Sheets (SDS) data. As such, samples selection was based on the result of this first characterization phase; the unstable materials were taken out from the analysis.

4.2. Attachment efficiency

Overall, the attachment efficiency of NC particles, so the effectiveness of adhesion of particles of the same type after a collision resulted being in the range 0.1-0.4 for particles with negatively charged surface, while it resulted higher for particles with positively charged surface.

Such low α_a is index of a poor particle aggregation, instead of aggregating and flocculating, most of the particles remained suspended and did not change their state during the experiment. Different behavior was shown by the particles when dispersed in solutions which contained NOM. The presence of natural organic matter led to the formation of a thin film around the particles, modifying their surface chemistry. These modifications, together with the film formation, resulted in lowering the attractive potential between the particles, so the colloidal solutions resulted more stable in these test mediums (39). In presence of NOM, instead of flocculation and sedimentation, the NC particles underwent a stabilization process, thus the particles remained in suspension in the top layer of the vials.



Meanwhile, in test mediums which contained carbon derived from an inorganic source, the particles' size did not change along the experimental time and resulted the same measured in the characterization phase; aggregation occurred only in presence of high electrolytes concentration.

4.3. Fate and transport of NC particles – Full multi model

The Full Multi framework provided a reliable simulation of nanocellulose particles' fate and transport in a generic river system. These processes were determined for five cellulose nanomaterials, which presented different characteristics in term of size and aspect ratio. Despite the different characterization of the NC materials, similarity in their behaviors were found.

In general, particles were primarily observed in two states—aggregated and free—within the two middle layers of the river, specifically in the flowing and stagnant water compartments. The behavior of nanoparticles was largely influenced by the presence of NOM. The mechanisms that involved more the nanocellulose particles are settling, breakup and advection; those processes occurred with a faster rate than other processes (e.g. degradation). Meanwhile, processes such as degradation and fragmentation occurred with a slower rate. Finally, it is worth to notice that despite NC particles were characterized by different sizes and aspect ratios, their fates and transport mechanisms in environmental waters resulted similar.

5. Conclusion

Starting from the '40s massive plastic production and use begun. Thanks to its properties, such as high durability and cost-effectiveness, plastic was found to be a perfect material for many applications (41). The huge use of plastic, in many application and industrial sector, has led to spread of the plastic itself and its debris in the environment.

Emerging pollutants, characterized by long-lasting nature and low degradability, such as micro and nano plastics represent a big concern for human and ecosystems' health (42). Issues related to these contaminants are due to their dimensions (MPs 1 μm – 5mm and NPs 1nm-1 μm) and their production's source. MPs and NPs can have impacts on the human and animal health because of their accumulation in the organisms, and their ability to act as carrier for other toxic compounds and pollutants. These compounds can be very impactful both on terrestrial and aquatic ecosystems (41). MPs and NPs can be characterized as primary and secondary plastics, according to their provenience. In details, MPs and NPs are defined as primary when these polymers are manufactured for a direct/indirect use as raw materials (e.g. in cosmetics, scrubs and facial cleanser); while they are defined as secondary when are derived from larger plastic fragments, that due to external factors, degrade and form small debris.

The substitution of petroleum-based polymers with natural and biodegradable materials is a big step in reducing negative impacts on the environment.

Nanocellulose, thanks to its physical properties (e.g. high strength, light weight and flexibility) can be use as replace for plastics in many applications, such as cosmetic, packaging and biomedical industries. Moreover, NC is extracted from sustainable and renewable sources, and unlike micro and nano plastics, it is non-toxic and biocompatible, so it result not harmful on human health (43) (44) (45).

Nanocellulose, which can be extracted from plant, bacteria and other renewable and sustainable sources, can be found in form of nanofibers and crystalline nanoparticles. However, before applying NC in commercial market, its attitude after emission to the environment has to be studied and predicted. The assessment of fate and behavior of NC in aqueous stream results necessary because of the ability of these particles to act as carriers of other pollutants. Indeed nanocellulose, due to its highly modifiable surface can easily absorb and transport other contaminants (46).



Therefore, in this study, the stability of NC samples was assessed through the application of the Full Multi model, which is able to predict the fate and transport of NC in different water environments.

Nanocellulose particles, extracted from different sources, are characterized by dimensions ranging from 100 to 200 nanometers, and show similar behaviors when dispersed in solutions aimed at mimicking natural waters.

Even though it was not possible to determine the dispersion stability of these materials, it was possible to define their attachment efficiencies of homoaggregation, so the effectiveness of collisions.

The attachment efficiencies of NC particles, when dispersed in different test mediums, which were selected to mimic the European waters, were in the range 0.1-0.4. The results demonstrate that not many aggregates are formed in natural waters, especially when the electrolytes' concentration is small. The presence of NOM in the mediums led to a lowering of the attachment efficiency, so even smaller number of aggregates are formed in these conditions. Behaviors of NC particles were determined using the Full Multi model; fate and transport of nanoparticles in a generic river were assessed. Both CNC and CNF particles are subjected to strong settling, advection and degradation; these processes take place in the upper layers of the simulated river with different time scales. It is worth to notice that, even though the degradation process is characterized by a high half time (t_{half}) – in the order of years – it occurs in all the layer of the generic river.

In a previous research, conducted by Domercq et al. (9), the behaviors plastic particles (e.g. polyethylene PE, polypropylene PP and other plastics) was assessed in the same generic river used in the present study, comparison between the two cases is then possible.

The main differences between the plastic polymers and nanocellulose are encountered in the processes acting in the layers of the simulated river and their half-time.

In the top layers of the river, the fates of the two kinds of polymers, are similar: slow processes of degradation, fragmentation take places together with faster processes such as biofilm formation and advection. Even though, in both cases the same interactions happens, their time scales are slightly different. Half times were found shorter for nanocellulose particles respect to plastic particles (PE, PA, PVC).



Same analysis can be performed for the lower layers of the river, in which processes such as resuspension and burial takes place with higher half time for the plastic polymers.

Is it worth to notice that, in all the river compartments, nanocellulose particles degrade quicker than plastic particles with comparable dimensions ($\approx 10^2$ years of difference). Furthermore, due to this result, the substitution of petroleum-based polymers with NC particles with comparable physicals and chemical properties, in many fields and applications.

Future steps can be performed to assess in a more precise way the fate of nanocellulose particles and the possibility of using them in many applications. The parametrization of different aquatic systems through the Full Multi model and the variation of test mediums to represent many environmental conditions can be performed to obtain more data about the transport and fate of these particles.

The mixing of different NC particles, of different provenience and types, can be base for the use of these materials in other applications beside those already studied. So, the determination of heteroaggregation and stability can be performed with the same method used in this study.

The assessment of the fate of biodegradable polymers, such as nanocellulose, is a necessary step to seek for the development of more sustainable materials and technologies.



6. Acknowledgement

Part of this master thesis has been done under SSbD4Chem project that has received funding from the European Union's Horizon Europe research and innovation programme under grant agreement n° 101138475.

The use of the Full Multi model in this thesis has been possible thanks to the cooperation with Prof. Dr. A. Praetorius (University of Amsterdam, Faculty of Science Institute for Biodiversity and Ecosystem Dynamics) and the whole working group, which are authors and developers of the used framework.

7. Bibliography

1. *A review of nanocellulose as a new material towards*. Dhali, Kingshuk , et al. s.l. : Science Direct, 2024, *Science of the Total Environment*, pp. 1-24.
2. *Role of nanocellulose in industrial and pharmaceutical sectors - A review*. Pradeep, H.K. , et al. s.l. : Science Direct, 2022, *International Journal of Biological Macromolecules*, pp. 1038-1047.
3. *Nanocelluloses as skin biocompatible materials for skincare, cosmetics, and*. Meftahi, Amin , et al. s.l. : Science Diect, 2022, *Carbohydrate Polymers*, pp. 1-21.
4. Helmenstine, Anne Marie. *ThoughtCo*. [Online] 2019. <https://www.thoughtco.com/what-is-cellulose-definition-4777807#:~:text=Chemical%20Structure%20and%20Properties.%20Cellulose%20forms>.
5. *Nanocellulose: Extraction and application*. Phanthong, Patchiya , et al. s.l. : Science Direct, 2018, *Carbon Resources Conversion*.
6. *Emerging technologies for the production of nanocellulose from lignocellulosic biomass*. Pradhan, Dileswar , Jaiswal, Amit K. and Jaiswal, Swarna . 2022.
7. *Recent advances in nanocellulose-based different*. Khalid, Muhammad Yasir , et al. s.l. : Science Direct, 2021, *Journal of Materials Research and Technology*.
8. *Test No. 318: Dispersion Stability of Nanomaterials in Simulated Environmental Media*. OECD. 2017, *OECD Guidelines for the Testing of Chemicals*.
9. *The Full Multi: An open-source framework for modelling the transport and fate of nano- and microplastics in aquatic systems*. Domercq, Prado, Praetorius, Antonia and MacLaod, Matthew. s.l. : Science Direct, 2022, *Environmental Modelling and Software*.
10. *Scientific Rationale for the Development of an OECD Test Guideline on Engineered Nanomaterial Stability*. Monikh, Fazel Abdolahpur , et al. s.l. : Science Direct, 2018, *NanoImpact*, pp. 42-50.
11. IHSS. *humicsubstances*. [Online] <https://humicsubstances.org/product/suwannee-river-nom-ro-isolation->.
12. SYSMEX. *Malvern Zetasizer Nano Series (Particle Size – Zetapotential – Molecular Weight)*.
13. Lòpez, Francisco José. *Zetasizer Nano: specification*. 2016.

14. *Dynamic light scattering: a practical guide and applications*. Stetefeld, Jörg, McKenna, Sean A. and R. Patel, Trushar R. s.l. : PMC, 2016.
15. Nobbmann, Ulf. Polydispersity – what does it mean for DLS and chromatography? *Malvern Panalytical*. [Online] 2017. <https://www.malvernpanalytical.com/en/learn/knowledge-center/insights/polydispersity-what-does-it-mean-for-dls-and-chromatography>.
16. Malvern. *Zeta Potential - an introduction 30 minutes*.
17. *A Review on Thermophysical Property Assessment of Metal Oxide-Based Nanofluids: Industrial Perspectives*. s.l. : ResearchGate.
18. *DLS and zeta potential – What they are and what they are not?* Bhattacharjee, Sourav. *Journal of Controlled Release*.
19. Masek, Joseph. *Pharmacology and Immunotherapy*. [Online] <https://en.immunopharm.cz/zetasizer-nano-zsp/>.
20. Batili, Hazal. *Synthesis and Electrophoretic Deposition of*. 2018.
21. *Count, size and visualize nanoparticles*. Mallow, Andrew. Salisbury : NanoSight Limited, 2011, *materialstoday*, Vol. 14.
22. *Introduction to Nanoparticle Tracking Analysis (NTA)*. Meerbusch : ParticleMetrix.
23. Particle Metrix. [Online] <https://particle-metrix.com/ev-isolation-yields-confirmed-via-f-nta/>.
24. OECD. *OECD Guidelines for the Testing of Chemical*. 2017.
25. *Crystallinity-Independent yet Modification-Dependent True Density of Nanocellulose*. Daicho, Kazuho, et al. 2020, *Biomacromolecules*.
26. Skalar. PRIMACSTTM Series - TOC/TN analyzers for solid samples . [Online] <https://www.skalar.com/products/primacs-total-organic-carbon-total-nitrogen-analyzers>.
27. Analytikjena. *Operating Manual - multi N/C 3100*.
28. *Pyrolysis gas chromatography-mass spectrometry in environmental analysis: Focus on organic matter and microplastics*. Picó, Yolanda and Barceló, Damià. s.l. : Science Direct, 2020, *Trends in Analytical Chemistry*.
29. Stauffer, Eric, Dolan, Julia A. and Newman, Reta . *Fire Debris Analysis*. 2008.
30. *Strategies for determining heteroaggregation attachment efficiencies of engineered nanoparticles in aquatic environments*. Praetorius, Antonia , et al. 2020, *Environmental Science Nano*.

31. *Relating Colloidal Stability of Fullerene (C60) Nanoparticles to Nanoparticle Charge and Electrokinetic Properties*. Chen, Kai Loon and Elimelech, Menachem . 2009, Environmental Science & Technology.
32. *Aggregation and Deposition of Engineered Nanomaterials in Aquatic Environments: Role of Physicochemical Interactions*. Petosa, Adamo R., et al. 2010, Environ. Sci. Technol.
33. *Aggregation Kinetics of Alginate-Coated Hematite Nanoparticles in Monovalent and Divalent Electrolytes*. Chen, Kai Loon , Mylon, Steven E. and Elimelech, Menachem . 2006, Environmental Science & Technology.
34. *Scientific Rationale for the Development of an OECD Test Guideline on Engineered Nanomaterial Stability*. Monikh, Fazel Abdolapur, et al. s.l. : Science Direct, 2018, NanoImpact, pp. 42-50.
35. *Development of Environmental Fate Models for Engineered Nanoparticles—A Case Study of TiO₂ Nanoparticles in the Rhine River*. Praetorius, Antonia, Scheringer, Martin and Hungerbühler, Konrad. 2012, Environmental Science & Technology.
36. *ZetaView® analysis support*. s.l. : NTA service.
37. *Nanoparticles: Structure, Properties, Preparation and Behaviour in Environmental Media*. Christian, Patsy, et al. 2008.
38. *Aggregation and Deposition of Engineered Nanomaterials in Aquatic Environments: Role of Physicochemical Interactions*. Petosa, Adamo R., et al. 2010, Environmental Science & Technology.
39. *Attachment efficiency of nanoparticle aggregation in aqueous dispersions: modeling and experimental validation*. Zhang, Wen, et al. 2012, Environ Sci Technol.
40. *Effect of source and seasonal variations of natural organic matters on the fate and transport of CeO₂ nanoparticles in the environment*. Li, Zhen , et al. 2017, Science of the total environment.
41. *Effects of microplastics on the terrestrial environment: A critical review*. Dissanayake, Pavani Dulanja, et al. s.l. : Science Direct, 2022, Environmental Reserch.
42. *A review on microplastics and nanoplastics in the environment: Their occurrence, exposure routes, toxic studies, and potential effects on human health*. Sangkham, Sarawut , et al. s.l. : Science Direct, 2022, Marine Pollution Bulletin.

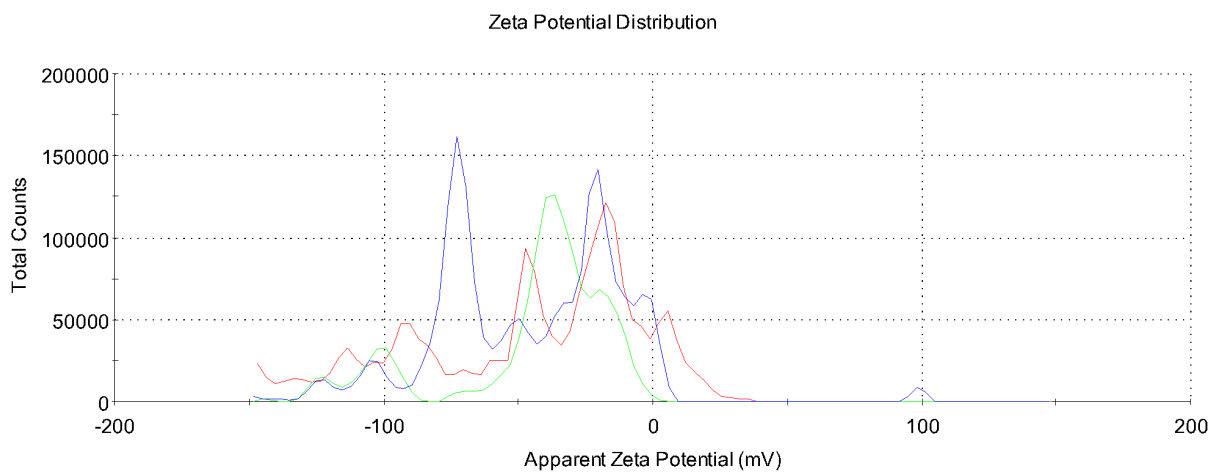


43. *Assessing cytotoxicity and biocompatibility of cellulose nanofibrils on alveolar macrophages.* Fujita, Katsuhide, et al. 2024, Springer Nature.
44. *Bioaccumulation, transfer, and impacts of microplastics in aquatic food chains.* McHale, Marykate E. and Sheehan, Kate L. . 2024, Journal of Environmental Exposure Assessment.
45. *Cellulose-based materials in environmental protection: A scientometric and visual analysis review.* Jing, Liandong, et al. s.l. : Science Direct, 2024, Science of The Total Environment.
46. *Nanocellulose-Based Materials for Water Pollutant Removal: A Review.* Abdelhamid, Hani Nasser. s.l. : Nereida Cordeiro, 2024, PubMed Central.
47. *Dimensions of Cellulose Nanocrystals from Cotton and Bacterial Cellulose: Comparison of Microscopy and Scattering Techniques.* Grachev, Vladimir , et al. 2024, Nanomaterials.
48. *Bacterial Nanocellulose toward Green Cosmetics: Recent.* Almeida, Tânia , et al. s.l. : MDPI, 2021, International Journal of Molecular Science.
49. *Settling Velocities of Environmentally Weathered Plastic Fibers from the Mekong River in Southeast Asia.* Brooks, Jenna M., et al. 2024, ACS ES&T Water virtual special.
50. *Effects of Particle Properties on the Settling and Rise Velocities of Microplastics in Freshwater under Laboratory Conditions.* Waldschläger, Kryss and Schüttrumpf, Holger. 2019, Environmental Science & Technology.

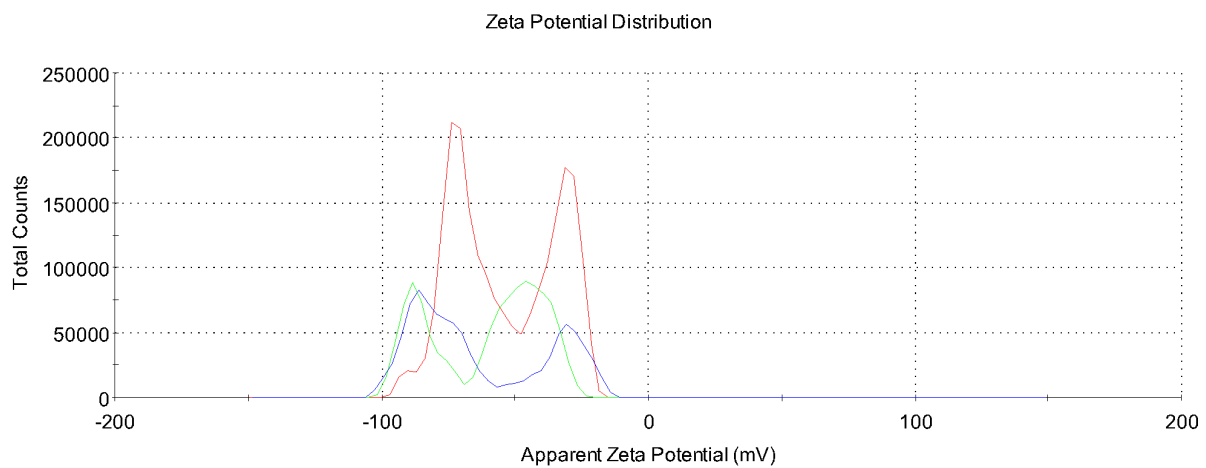
8. Appendix

Appendix: Table 1 Samples characteristic

Sample name	Sample composition	% wt
1	CNC	3.98%
	H ₂ O	95.54%
	1,2-hexanediol	0.24%
	4'hydroxyacetophenone	0.24%
2	CNC	3.98%
	H ₂ O	95.54%
	1,2-hexanediol	0.24%
	4'hydroxyacetophenone	0.24%
3	CNC	1.00%
	H ₂ O	98.80%
	1,2-hexanediol	0.10%
	4'hydroxyacetophenone	0.10%
4	CNC	1.00%
	H ₂ O	98.80%
	1,2-hexanediol	0.10%
	4'hydroxyacetophenone	0.10%
5	CNF	1.99%
	H ₂ O	97.61%
	1,2-hexanediol	0.20%
	4'hydroxyacetophenone	0.20%
6	CNF	1.99%
	H ₂ O	97.61%
	1,2-hexanediol	0.20%
	4'hydroxyacetophenone	0.20%
7	CNF	2.09%
	H ₂ O	97.49%
	1,2-hexanediol	0.21%
	4'hydroxyacetophenone	0.21%



Appendix: Figure 1: High standard deviation of the Zeta Potential Distribution for the sample CNC 2 (%wt 3.98%) diluted with SDS (conc. 150 ppm); Records 1,2 and 3.



Appendix: Figure 2: High standard deviation of the Zeta Potential Distribution for the sample CNF 5 (%wt 1.99%) diluted with NovaChem (conc. 150 ppm); Records 1,2 and 3.

Appendix: Table 2 – Nanocellulose size DLS results (PdI values > 0.7 are in red, Attenuator ≥ 10 are in yellow, ZP values in the stability range < -30mV or > +30 mV are in green)

Sample		Size measurement				Zeta measurement		
Name	Type	Concentration (ppm)	Z-Ave (d.nm)	PdI*	Attenuator**	ZP (mV) ***	Std deviation	pH
1	CNC	50	199.53	0.251	11	-37.17	7.94	5-6
		100	143.17	0.269	8	-40.03	5.41	5-6
		150	106.53	0.281	7	-31.43	7.53	5-6
2	CNC	50	124.80	0.147	8	-46.10	19.93	5-6
		100	121.60	0.140	7	-38.70	11.52	5-6
		150	121.50	0.144	7	-42.67	12.14	5-6
3	CNC	50	127.57	0.248	11	24.23	36.89	5-6
		100	140.47	0.246	9	29.60	9.71	5-6
		150	106.53	0.240	8	34.27	10.15	5-6
4	CNC	50	154.30	0.210	8	-32.47	8.04	5-6
		100	155.57	0.217	7	-23.25	41.50	5-6
		150	152.50	0.216	7	-43.80	10.44	5-6
5	CNF	50	2323.00	1.000	8	-21.13	6.51	5-6
		100	1045.43	0.796	7	-19.13	4.40	5-6
		150	631.73	0.642	7	-25.00	22.00	5-6
6	CNF	50	1156.10	0.851	7	-20.20	4.02	5-6
		100	1049.97	0.768	6	-21.27	3.56	5-6
		150	863.20	0.751	6	-24.17	3.99	5-6
7	CNF	50	150.97	0.338	10	-42.77	4.24	5-6
		100	108.67	0.275	9	-29.07	10.85	5-6
		150	98.20	0.324	9	-34.80	71.97	5-6

* RED: PdI values >0.7;

**YELLOW: attenuator values ≥ 10 ;

***GREEN: ZP values in the stability range < -30mV or > +30 mV



Appendix: Table 3 – Filtered solvent MQ, SDS and NovaChem no particles detected

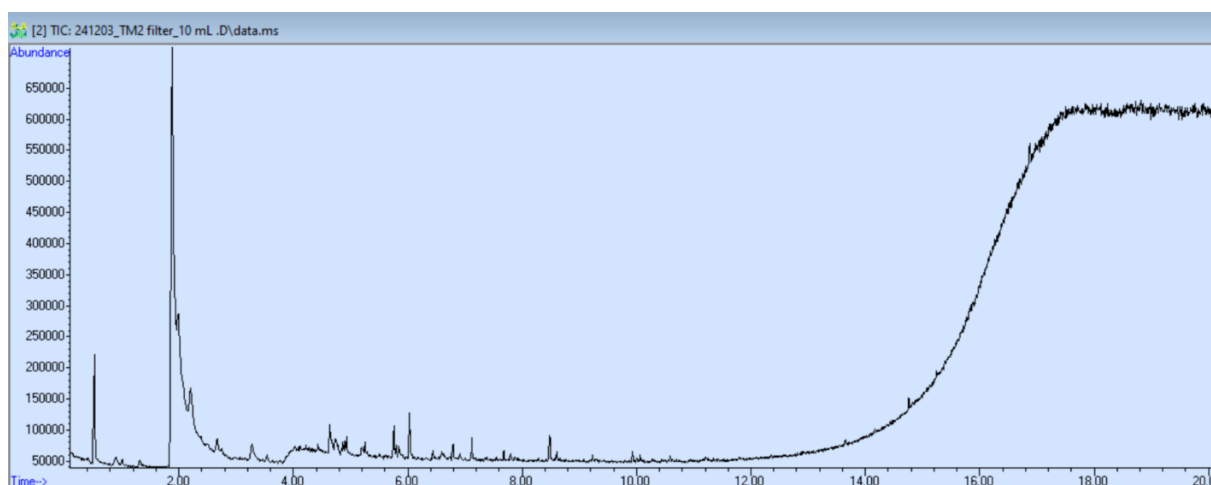
Sample Name	Z-Ave (d.nm)	PdI	Attenuator
Filtered MQ	969.07	0.557	11
Filtered SDS	373.07	0.343	11
Filtered NovaChem	235.67	0.341	11

Appendix: Table 4 – Volume of stock dispersion and particle number in the final test volume

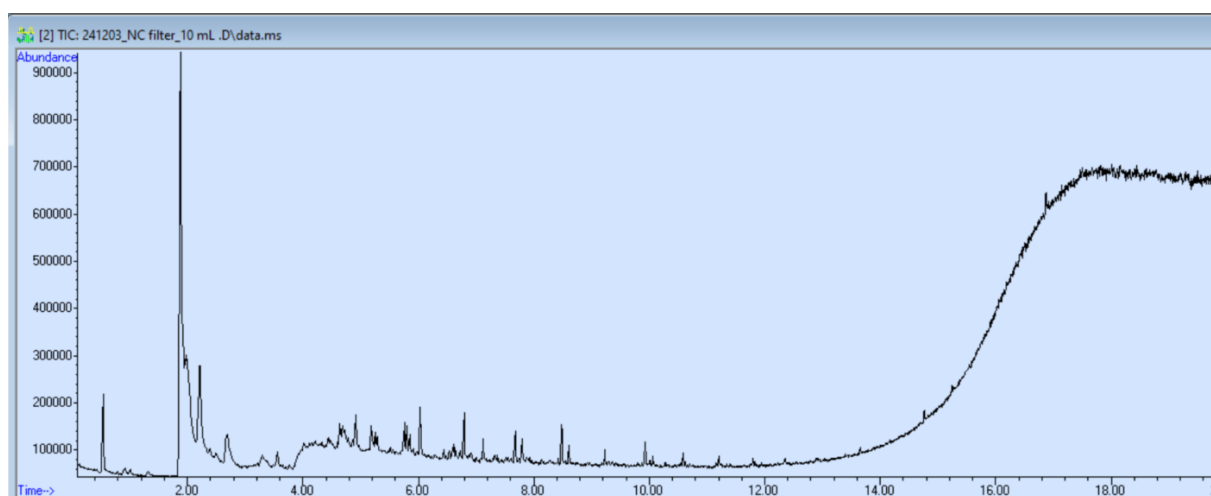
Sample name	Particle conc. in diluted sample (20 ppm)	Volume to be taken	Number of particles
	part/L	ml	-
CNC 1	5.24×10^{14}	0.21	1.101×10^{11}
CNC 2	4.36×10^{14}	0.25	1.088×10^{11}
CNC 3	4.8×10^{13}	2.29	1.099×10^{11}
CNC 4	3.47×10^{14}	0.32	1.109×10^{11}
CNF 5	2.84×10^{14}	0.39	1.105×10^{11}
CNF 6	5.07×10^{14}	0.22	1.114×10^{11}
CNF 7	1.72×10^{14}	0.64	1.103×10^{11}

Appendix: Table 5 – NTA results

Sample name	Mean size measur. (nm)	Mean volume (nm ³)	Quantiles			First peak		Second peak		Concentration (particles/ml)	
			Median (X50) (nm)	X10 (nm)	X90 (nm)	Diameter (nm)	% of particle	Diameter (nm)	% of particle	In diluted sample	In original sample
CNC 1	128.3	350.8	101.0	64.3	215.5	89.6	94.0	177.6	17.9	1.97×10^{10}	3.93×10^{12}
CNC 2	133.3	279.5	116.6	65.5	219.6	111.0	64.8	149.6	22.7	1.63×10^{10}	3.27×10^{12}
CNC 3	271.4	431.1	253.8	144.3	413.4	223.3	23.5	251.3	18.0	1.80×10^9	3.60×10^{12}
CNC 4	189.9	369.5	166.8	77.2	328.1	109.9	24.8	200.7	18.2	1.30×10^{10}	2.60×10^{12}
CNF 5	192.2	435.0	162.7	94.6	327.3	147.0	42.8	128.2	30.9	1.06×10^{10}	2.13×10^{12}
CNF 6	198.7	480.1	170.0	82.2	342.3	150.3	47.9	206.3	18.3	1.90×10^{10}	3.80×10^{12}
CNF 7	151.2	354.3	129.4	82.7	236.7	111.7	85.2	245.3	18.3	6.47×10^9	1.29×10^{12}



Appendix: Figure 3 – TIC of pure TM 2



Appendix: Figure 4 – TIC of NC (CNC 2)



Appendix: Table 6 – Stock dispersion preparation for DLS(attachment efficiency determination)

Sample name	stock dispersion	
	NC	MQ
	ml	ml
1 CNC	0.15	19.85
2 CNC	0.15	19.85
3 CNC	0.6	19.4
4 CNC	0.6	19.4
7 CNF	0.77	19.23



Appendix: Table 7 – Samples preparation for DLS (attachment efficiency determination)

Test medium	Stock dispersion	Carbon Source		Electrolytes solution			pH adjustment		
	Pure NC (ml)	NaHCO ₃ (ml)	NOM (0,5 g/l) (ml)	CaNO ₃ (ml)	MgSO ₄ (ml)	MQ (ml)	NaOH (ml)	HNO ₃ (ml)	MQ (ml)
TM1	20	2	-	0	0	13	-	0.02	4.98
TM2	20	2	-	0.4	0.1	12.5	-	0.02	4.98
TM3	20	2	-	4	1	8	-	0.02	4.98
TM1 NOM	20	-	0.95	0	0	14.05	0.1	-	4.9
TM2 NOM	20	-	0.95	0,4	0,1	13.55	0.1	-	4.9
TM3 NOM	20	-	0.95	4	1	9.05	0.1	-	4.9

Appendix: Table 8 - Inputs for Full Multi model (micropasticSizeClass)

Sample Name	Density kg/m ³	MP shape -	Diameter μm	Length A μm	Length B μm	Length C μm
CNC 1	1500	fiber	0.152	0.085 - 0.105	0.003	0
CNC 2	1500	fiber	0.118	0.110 - 0.120	0.008	0
CNC 3	1500	fiber	0.125	0.140 - 0.415	0.0125	0
CNC 4	1500	fiber	0.150	0.075 - 0.330	0.0115	0
CNF 7	1500	fiber	0.107	0.100 - 0.130	0.0035	0